

## 26. ALTERATION PROCESSES IN LAYER 2 BASALTS FROM DEEP SEA DRILLING PROJECT HOLE 504B, COSTA RICA RIFT<sup>1</sup>

J. Honnorez,<sup>2</sup> C. Laverne,<sup>3</sup> H.-W. Hubberten,<sup>4</sup> R. Emmermann,<sup>5</sup> and K. Muehlenbachs<sup>6</sup>

### ABSTRACT

Hole 504B, drilled into the 5.9 Ma crust of the southern flank of the Costa Rica Rift, tapped a hydrothermal system in its conductive stage. Three alteration zones were encountered along the 561.5 meters of basement drilled. The upper alteration zone, 274.5 to 584.5 meters below the seafloor (BSF), is characterized by the presence of color zonation in which red halos are located between dark gray inner rock portions and dark gray outer bands. The red halos are characterized by an abundance of iddingsite, and they have higher K<sub>2</sub>O contents and Fe<sup>3+</sup>/Fe<sup>T</sup> ratios, but lower SiO<sub>2</sub> contents, than the adjacent dark gray inner zones. The dark gray outer bands are characterized by the presence of celadonite-nontronite. Saponite is omnipresent in these three alteration bands. Phillipsite is the only zeolite that occurs in the upper alteration zone. The upper alteration zone is interpreted as being the result of low-temperature alteration, with large amounts of cold oxygenated seawater percolating through the upper ocean crust. In the upper alteration zone, the formation of red halos was both preceded and followed by formation of dark gray outer bands. Then followed formation of dark gray cores.

The lower alteration zone (584.5–835.5 m BSF) is characterized by the absence of color zonation, the downward-increasing abundance of pyrite and saponite, and the presence of quartz, talc, and calcite. The chemical changes (downhole MgO enrichment and concomitant CaO depletion) observed in the basalts of the lower alteration zone are thought to result from reactions of oceanic basalts with evolved seawater (i.e., solutions derived from seawater that has already reacted with ocean crust), which is thus depleted in oxygen, potassium, and radiogenic strontium. This alteration process, which was responsible for saponite formation in both the upper and lower alteration zones, was rock dominated, and it took place under suboxic to anoxic conditions during a second stage of alteration. Reaction temperatures could have progressively increased with depth.

There is also a zeolitic zone that essentially coincides with the lower part of the upper alteration zone (between 528.5 and 563 m BSF). The host rock adjacent to veins of zeolite exhibits a greenish discoloration due to the intensive replacement of the igneous minerals. The replacement minerals result in significant increases in the bulk rock K<sub>2</sub>O, MgO, CaO, CO<sub>2</sub>, and H<sub>2</sub>O<sup>+</sup> contents. The solutions circulating along the newly opened fissures had high Ca activity, and minerals probably precipitated in these fissures at 60°C or 110°C. These hydrothermal solutions circulated later than those responsible for the formation of the minerals that characterize the upper and lower alteration zones.

### INTRODUCTION

Hole 504B (in the Panama Basin) offers the opportunity to study one of the longest sections through ocean Layer 2 ever drilled during the Deep Sea Drilling Project. (During Leg 70, Hole 504B fell only 21.5 m short of the former record depth of 582 m of basement penetration, which was reached during Leg 37 at Hole 332B. During Leg 83, the record was far surpassed, with the hole reaching 1075 meters into the ocean crust, and it is still open for future drilling.) At Site 504, the upper ocean crust appears to be mainly made up of pillow lavas (which are interlayered with frequent and varied breccias) and a few massive flows (Fig. 1). The great structural heterogeneity of the crust is in contrast to its nearly uniform chemical composition. Bulk rock chemical analyses demonstrated that Hole 504B rocks are rather

primitive mid-ocean-ridge basalts. The basalts are depleted in light rare earth elements, except for Lithologic Units 5 and 36, which are 14 and 18 meters thick, respectively, and are slightly enriched. Perhaps the greatest advantage of Hole 504B is that students of seawater/crust interaction can compare the effects of different alteration processes because the processes affected rocks initially almost identical in composition (Natland et al., this volume). Therefore, differences in alteration effects can only be ascribed either to differences in the processes themselves or in the primary structure of the rocks.

The aging of the upper ocean crust at low temperature consists of a complex sequence of seawater/basalt reactions with effects that overlap through time and space (Alt and Honnorez, 1981). (We define low temperature as ranging from bottom water temperature up to, but not including, the crystallization temperature of unequivocally metamorphic minerals such as laumontite or chlorite [see Honnorez, 1981 for discussion].) Each stage of the submarine alteration corresponds to one process with its own rate and scale and differs from the others by its mechanism and the conditions under which it operates, mainly the water-rock ratio, the composition of the solutions, and temperature. The superimposed effects of the various alteration processes, including the igneous minerals affected, the secondary phases precipitated, and the elemental fluxes, are generally dif-

<sup>1</sup> Cann, J. R., Langseth, M. G., Honnorez, J., Von Herzen, R. P., White, S. M., et al., *Init. Repts. DSDP*, 69: Washington (U.S. Govt. Printing Office).

<sup>2</sup> Rosenstiel School of Marine and Atmospheric Science, University of Miami, Miami, Florida, U.S.A.

<sup>3</sup> Centre Scientifique Universitaire, Laboratoire de Géologie, B.P.5, 97490 St. Clotilde, La Réunion, France, D.O.M. Present address: Laboratoire de Géologie, Faculté des Sciences et Techniques, Route de la Soukra, 3038 SFAX, Tunisia.

<sup>4</sup> Institut für Petrographie und Geochemie der Universität Karlsruhe, Kaiserstrasse 13, D-75 Karlsruhe 1, Federal Republic of Germany. Present address: Universidad Autónoma de Nuevo Leon, Instituto de Geología, 67700 Linares, N.L., Mexico.

<sup>5</sup> University of Giessen, Senckenberg St. 3, 63 Giessen, Federal Republic of Germany.

<sup>6</sup> Department of Geology, University of Alberta, Edmonton, Alberta, Canada.

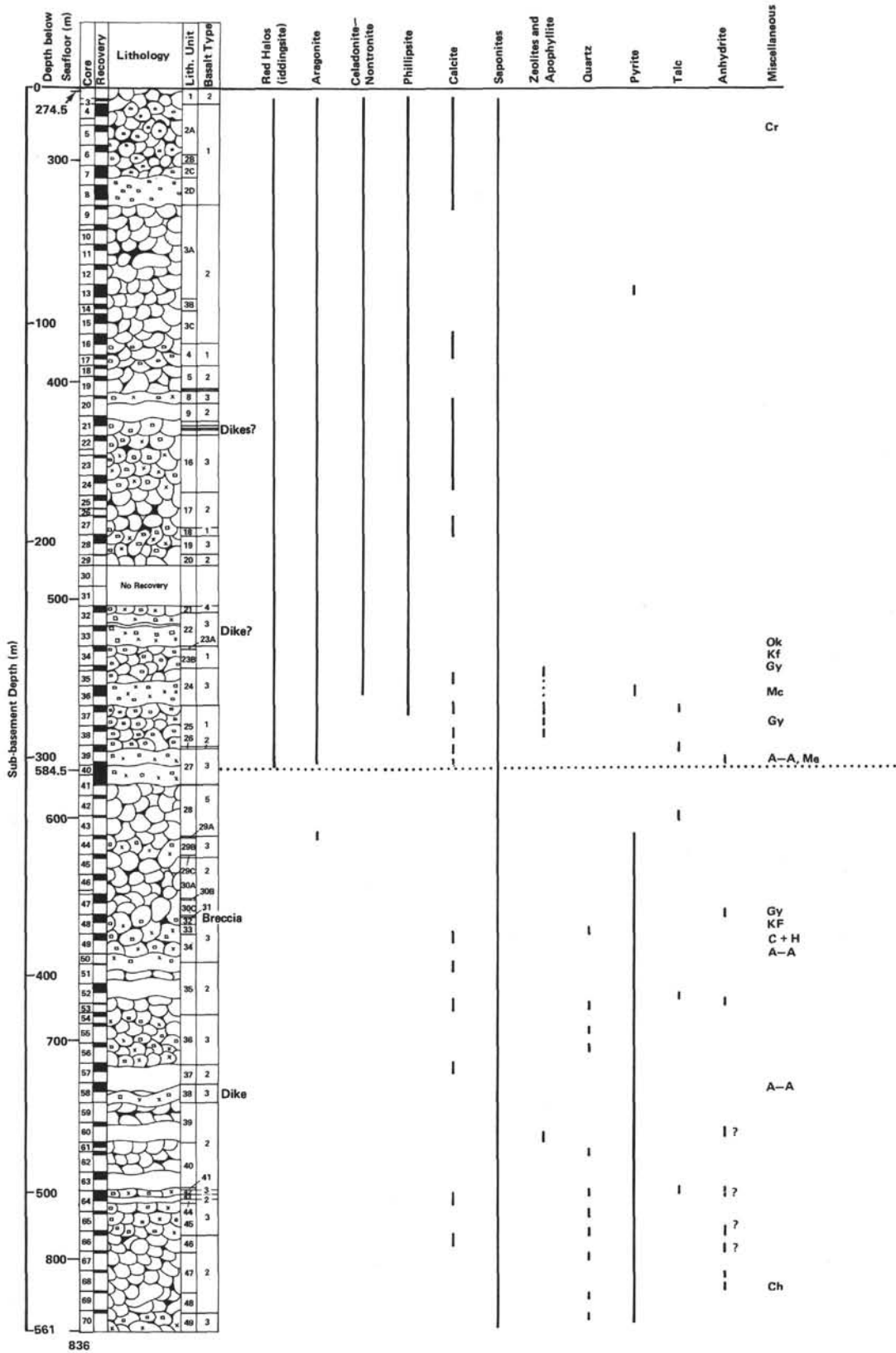


Figure 1. Downhole distribution of alteration minerals in Hole 504B. The rightmost column (entitled Miscellaneous) includes the following minerals: Ok okenite (Kurnosov et al., this volume); Kf K-feldspar (Kurnosov et al., this volume and J. Alt, pers. comm.); Gy gyrolite (Kurnosov et al., this volume and this chapter); Mc marcasite (this chapter); A-A aegirine-augite and Me melanite (Laverne, this volume); C chabazite and H heulandite (this chapter); Ch chlorite (this chapter).

ficult to decipher. Moreover, no clear depth trends have been observed in the cases studied to date (e.g., Bass, 1976; Böhlke et al., 1980; Alt and Honnorez, in press; Alt, in press). The most striking characteristic of the low temperature alteration in Hole 504B, on the other hand, is the change with depth in both alteration mineralogy and chemistry.

The basalts from Hole 504B are all more or less altered. Low temperature alteration was more pervasive in the hyaloclastites and pillow breccias than in the massive lava flows. However, none of the samples that we studied is completely altered; the igneous plagioclases are often completely fresh, and the clinopyroxenes are only exceptionally and partly replaced. Moreover, fresh glass was found in pillow rims down to about 798 meters below the seafloor (BSF) (Sample 504B-66-1, 120–122 cm; see Natland et al., this volume), that is, only 38 meters above the bottom of the hole.

In the following sections, we summarize first the downhole variation of alteration mineral parageneses. Then we describe the 31 alteration minerals that we identified and discuss their optical properties, chemical composition, and X-ray diffraction patterns. We illustrate the petrography of the different types of alteration by describing several representative examples of the variously colored halos throughout the hole. We then characterize the alteration phases as replacement or as fissure and void fillings. We discuss the effects of the alteration on bulk rock composition and oxygen isotope geochemistry. We conclude with a general discussion of the alteration processes in the crust at Site 504. This report is based almost entirely on our data. Other chapters in this volume provide additional data and discuss particular secondary minerals or the chemical and isotopic aspects of the alteration.

### DOWNHOLE DISTRIBUTION OF ALTERATION MINERALS

The frequency and occurrence of secondary minerals follow a definite pattern related to depth. We established tentative alteration zones for Hole 504B that were based on the presence of specific secondary minerals or mineral associations (Table 1 and Fig. 1). However, although we studied about 300 samples, our sampling only represents an average of one sample studied per core section, corresponding to a 30% recovery. Moreover, too few samples were studied by both electron microprobe and X-ray diffraction to permit a confident identification of all of the clay minerals.

The alteration minerals that either replace igneous phases or fill primary voids, vesicles, and cracks belong to three alteration zones.

The basement rocks from the uppermost 310 meters of Hole 504B (i.e., above 584.5 m BSF) are characterized in hand specimens by the presence of red halos. The halos are usually coupled with a dark gray outer band that runs parallel to veins or other exposed surfaces. The rocks from this upper alteration zone contain various combinations of the following secondary minerals: iddingsite (see below for definition), celadonite–nontronite

(a dark green clay mineral), celadonite (a bright green clay mineral), various saponites (pale green to dark olive green or brown clay minerals), phillipsite, and aragonite. Orange and blue green clay minerals also occur but are rare. Calcite is abundant; pyrite is exceptional. Olivine phenocrysts are usually completely replaced by various secondary mineral associations. Saponite is the major alteration product of olivine phenocrysts in the inner gray cores of samples from the upper alteration zone. On the other hand, iddingsite is generally abundant in the olivine pseudomorphs in the red halos, where it is often accompanied by saponites. Iddingsite is associated with celadonite in the part of the outer dark gray bands that is close to the red halos. Plagioclase and pyroxenes are generally fresh. Veins in the upper alteration zone are formed by various types of saponites, celadonite–nontronite, and iddingsite; more rarely, they are accompanied by phillipsite, aragonite, or calcite.

Rocks from the lower 251 meters of the hole (i.e., below 584.5 m BSF) do not display color zonation but are mottled or uniformly dark gray. This lower alteration zone is characterized by the presence of very pale green and dark olive green saponites and an abundance of pyrite. Talc, quartz, and calcite occur in veins with the saponites; aragonite was found only once. Olivine phenocrysts are replaced by fairly light-colored olive green saponites. Plagioclase and clinopyroxene are essentially unaltered. The presence of chlorite in the lower portion of the hole is indicated by X-ray diffraction, but it is rare as a discrete phase, more often forming a mixed-layer mineral with smectite.

We call the third alteration zone the zeolitic zone. It spans the interval from Core 35, Section 1 to Core 38, Section 2 (i.e., from 528.5 to 563 m BSF). It overlaps part of the upper alteration zone. It is made up of several veins of minerals found nowhere else in Hole 504B except in wall rocks near some of these veins (from Core 37, Section 1 to Core 37, Section 3; i.e., from 549.5 to 553 m BSF). When these veins occur in the upper alteration zone, they are characterized by the presence of zeolites other than phillipsite, namely analcime, natrolite, thomsonite, possibly mesolite, and an unidentified K-rich, Na-, Ca-zeolite. The zeolites are always accompanied by minor saponite, occasionally calcite, and exceptionally apophyllite (see the section on veins). In the wall rocks near these veins, both olivine and plagioclase are extensively replaced by some of the same minerals that form the veins. Petrographic evidence indicates that the zeolitic veins formed later than the alteration minerals characteristic of the upper portion of the hole (i.e., above 584.5 m BSF), including the thin veins that contain only phillipsite. In the rocks from the lower portion of the hole (i.e., below 584.5 m BSF), only one zeolitic vein was found (at about 657 m BSF). It is made up of heulandite and chabazite, which, as far as we know, do not occur anywhere else in Hole 504B.

Some of the veins are made up of Fe-rich saponite and have rims on the salband clinopyroxenes of either melanite + calcite or talc + aegirine–augite. Other veins contain anhydrite, calcite, gyrolite or quartz. We do not

Table 1. Main mineralogical and petrographic features of the alteration zones in Hole 504B.

Alteration Zone	Upper Alteration Zone	Lower Alteration Zone	Zeolitic Zone
BSF depth (m)	274.5 to 584.5	584.5 to 835.5	Overlaps both upper and lower alteration zones
Alteration halo: thickness; color	Up to 5 cm; red halos with frequent outer dark gray bands	Uniformly or mottled gray	Up to 1 cm; pale green discoloration
Vein composition	Iddingsitlike material Type 2 (colorless to very pale green) saponite Type 4 (dark green) celadonite-nontronite Greenish brown clay mineral Aragonite Phillipsite	Type 1a (olive green to pale green) Type 1b (dark olive green) Type 1c (olive brown) Calcite, pyrite, quartz Minor talc, mixed-layer smectite-chlorite	Anacite, thomsonite, natrolite, mesolite(?), K-rich zeolite Rare apophyllite, calcite Heulandite, chabazite Type 1a and 2 saponites
		Anhydrite + gyrolite + calcite; Fe-rich saponite, calcite ± talc ± melanite	
Vesicle and void fillings	Iddingsitlike material Type 4 (dark green) celadonite-nontronite Type 2 (colorless to very pale green) saponite Type 3 (orange) clay mineral Calcite	Type 1a, 1b, and 1c (pale green, dark olive green, olive brown) saponites Calcite Mixed-layer chlorite-saponite Rare chlorite	Rarely one of the above zeolites
Plagioclase	Generally unaltered, rarely partly replaced by Type 2 (very pale green) saponite	Often altered down to 441 m into Type 2 (very pale green) saponite Very rarely altered below 441 m	Partly or completely replaced by analcime, thomsonite, natrolite, apophyllite, saponite
Pyroxene	Unaltered	Unaltered	Unaltered
	Aegirine-augite reaction rims along veins		
Olivine (types of replacement)	Type 2 (colorless) saponite + iddingsite Type 1a (pale green) saponite Type 3 (orange) clay mineral Type 4 (dark green) celadonite-nontronite ± Type 1a or 2 saponite ± calcite Type 5 (bright green) celadonite + Type 2 (colorless) + Type 1a (pale green) saponite + iddingsite Type 6 (blue green) clay mineral + iddingsite	Type 1c (olive brown) saponite ± calcite Type 1a (medium olive green) saponite ± calcite Type 1b (dark olive green) + Type 1a (pale olive green) saponite + Ni, Fe-rich opaque needles	Various saponites and calcite; or some olivine replacements as for the alteration zone on which the veins are superimposed

know whether these veins are related to the zeolitic veins, to the other alteration products of the hole, or represent an altogether different alteration process.

## SECONDARY MINERALS

The clay minerals are the most common and abundant secondary minerals in the Hole 504B basalts. The other alteration products and minerals—iddingsite, Ca-carbonates, zeolites, anhydrite, quartz, and pyrite—occur in smaller quantities. Rare minerals include gyrolite, talc, aegirine-augite, and melanite. The identification of the secondary minerals is based on optical analysis, electron microprobe analysis, and X-ray diffraction analysis.

The electron microprobe analysis of the secondary minerals was difficult because of the minerals' high volatile content, mineral heterogeneity, small grain size, poor crystallinity, and imperfect polish. We did not use a defocused beam despite these problems, but a small count time (4 s) still allowed us to obtain satisfactory analyses with a high degree of uniformity and reproducibility.

### Clay Minerals

Clay minerals are present the entire length of Hole 504B. They commonly occur as fillings in miarolitic voids, vesicles, and cracks, and as replacements of glass, olivine, and plagioclase. X-ray diffraction data of clay minerals and their overall chemistry indicate that most of them are smectites.

The optical properties used to distinguish among the various types of clay minerals are absorption color, bi-

refringence, pleochroism, and anomalous interference color. For each type, the mode of occurrence, the relative abundance, and the size and habit of the clay particles were also noted. All of these features are summarized in Table 2.

The chemical composition of the clay minerals varies greatly (see Fig. 2 and Table 3), with variations in major-oxide content distinguishing different types. We distinguish six types, one of them having three subtypes, as described below. Variations in Mn, Cr, Ni, and Ti contents are not significant and were not used to make distinctions. Most varieties of clay minerals are Al poor, except for Types 1a and 6, which average 8.7 and 14.2%  $Al_2O_3$ , respectively. In the descriptions below,  $H_2O$  is calculated to be the difference between the totals of the analyses (Table 3) and 100%.

### Type 1a (olive green to pale green)

The distinction between the chemical and optical (mainly absorption color) properties of Types 1a and 2 is not always clear. Nevertheless, Type 1a clay minerals are characterized by a relatively high MgO content (19 to 26%).  $H_2O$  content ranges from 8.5 to 14%. The low  $SiO_2$  content of one of the Type 1a clay minerals (which was 38.4 to 42.7% in three analyses) and its high  $Al_2O_3$  content (7.6 to 9.4%) cannot be explained; the same clay minerals are very rich in  $H_2O$  (16 to 18%). Most of the calculated formulas for Type 1a clay minerals are similar to ideal saponite. Numerous X-ray diffractograms indicate that Type 1a is a trioctahedral smectite with a (060) peak ranging from 1,535 to 1,540 Å. Type 1a is identified as a saponite.

Table 2. Main characteristics of clay minerals from Hole 504B.

Type	Form	Pleochroism	Color with Crossed Polars	Mode of Occurrence	Abundance	Dominant Chemical Features
1a (olive green to pale green)	Fibers or slabs	Very variable	Gray to red (first order)	Replacement of olivine Replacement of plagioclase Vein	Very common	High MgO Low FeO*
1b (dark olive green)				Replacement of olivine Vein	Common	High FeO* Medium MgO
1c (olive brown)				Replacement of olivine Vein and vesicle fillings	Common	Medium FeO* High MgO
2 (colorless to very pale green)		Nonexistent or slight	Gray to indigo	Replacement of olivine	Common	High MgO and SiO <sub>2</sub> Very low FeO*
3 (orange)	Small grains or fibers	Nonexistent	Abnormal dark orange	Replacement of olivine	Rare Common	High CaO Low CaO
4 (dark green)	Small grains or short slabs	Nonexistent	Abnormal very dark green	Relacement of olivine Vein, vesicle, and void filling	Common to rare	Middle K <sub>2</sub> O High FeO Low Mg
5 (bright green)	Large slabs with perfect cleavage	Medium	White to yellow first order superimposed to bright green	Replacement of olivine	Very rare	High K <sub>2</sub> O Very high FeO* Low Mg
6 (blue green)	Needles or slabs	Strong	Abnormal bluish gray	Replacement of olivine	Rare	High Al <sub>2</sub> O <sub>3</sub> Low SiO <sub>2</sub>

Note: FeO\* is total iron expressed as FeO.

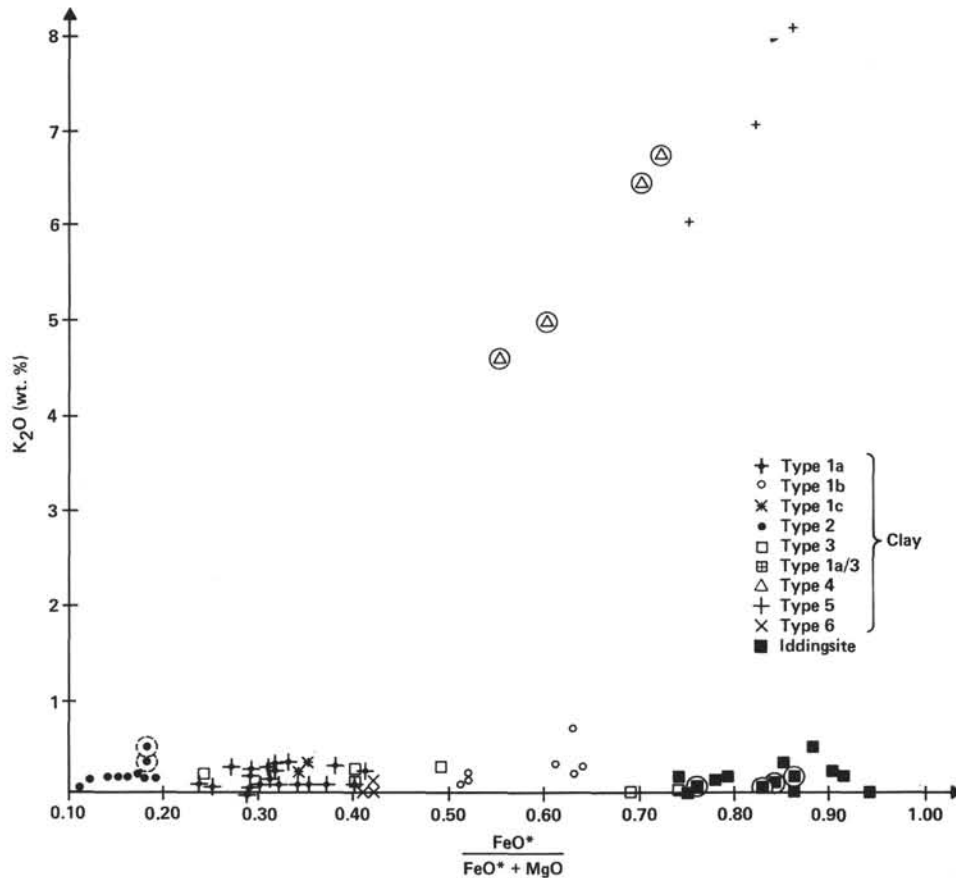


Figure 2. K<sub>2</sub>O contents versus FeO\*/FeO\* + MgO ratio of clay minerals and iddingsites that replace olivine and fill vesicles and voids. Circled symbols denote minerals that fill vesicles and voids.

Table 3A. Representative microprobe analyses of clay minerals from Hole 504B: mineral color and location.

Analyses 1-20: Type 1a (olive green to pale green) clay mineral—		Analyses 29-31: Type 1c (olive brown) clay mineral—	
1	Pale olive green clay mineral replacing olivine in red halo (associated with Analyses 30, 31, 44, 45, 46 in Table 3 and Analyses 1, 2 in Table 4); Sample 504B-33-1, 69-73 cm	29, 30	Olive brown clay mineral replacing olivine (no other secondary mineral associated); Sample 504B-40-3, 56-58 cm
2, 3	Pale olive green clay mineral replacing olivine in red halo (associated with Analyses 3, 4 in Table 4); Sample 504B-33-1, 69-73 cm	31	Olive brown clay mineral at the rim of a vesicle (associated with calcite at the center of the vesicle); Sample 504B-56-1, 2-4 cm
4, 5	Very pale olive green clay mineral replacing olivine (no other secondary mineral associated); Sample 504B-33-1, 69-73 cm	Analyses 32-35: Type 2 (colorless to very pale green) clay mineral—	
6, 7	Pale olive green clay mineral replacing olivine (no other secondary mineral associated); Sample 504B-33-2, 48-52 cm	32, 33	Colorless clay mineral replacing olivine in red halo (associated with Analyses 1, 44, 45, 46 in Table 3 and Analyses 1, 2 in Table 4); Sample 504B-33-1, 69-73 cm
8, 9	Medium olive green clay mineral replacing olivine (no other secondary mineral associated); Sample 504B-39-2, 144-147 cm	34, 35	Colorless clay mineral replacing olivine in red halo (associated with Analyses 5, 6, 7 in Table 4); Sample 504B-33-2, 48-52 cm
10, 11	Medium olive green clay mineral replacing olivine, located around fresh olivine relic (no other secondary mineral associated); Sample 504B-41-1, 118-120 cm	Analyses 36-39: Type 3 (orange) clay mineral—	
12, 13	Medium olive green clay mineral replacing olivine, located between two fresh olivine relics (same olivine phenocryst as in Analyses 10, 11); Sample 504B-41-1, 118-120 cm	36, 37	Orange clay mineral replacing olivine in red halo (no other secondary mineral associated); Sample 504B-33-1, 69-73 cm
14, 15	Medium olive green clay mineral replacing the rim on olivine phenocryst (associated with Ni, Fe-rich opaques, Analyses 21, 22 in Table 3); Sample 504B-63-4, 7-10 cm	38, 39	Mixture of orange clay mineral and calcium carbonate replacing olivine in red halo (no other secondary mineral associated); Sample 504B-38-2, 129-131 cm
16, 17	Pale olive green clay mineral replacing the rim of an olivine phenocryst (associated with Analyses 23, 24 in Table 3); Sample 504B-63-4, 90-91 cm	Analyses 40-43: Type 4 (dark green) clay mineral—	
18, 19	Pale olive green clay mineral replacing the rim of an olivine phenocryst (associated with Analyses 25, 26, in Table 3); Sample 504B-63-4, 90-91 cm	40, 41	Dark green clay mineral at the center of a vesicle in red halo (associated with Analyses 10, 11 in Table 4, at the rim); Sample 504B-33-1, 69-73 cm
20	Very pale green clay mineral partly replacing a plagioclase phenocryst; Sample 504B-33-2, 48-52 cm	42, 43	Dark green clay mineral in a vein (no other secondary mineral associated); Sample 504B-33-2, 48-52 cm
Analyses 21-28: Type 1b (dark olive green) clay mineral—		Analyses 44-46: Type 5 (bright green) clay mineral—	
21, 22	Dark olive green clay mineral replacing the core of an olivine phenocryst (associated with Analyses 14, 15 in Table 3); Sample 504B-63-4, 7-10 cm	44-46	Bright green clay mineral replacing olivine in red halo (associated with Analyses 1, 32, 33 in Table 3, and Analyses 1, 2 in Table 4); Sample 504B-33-1, 69-73 cm
23, 24	Dark olive green clay mineral partly replacing the core of an olivine phenocryst (associated with Analyses 16, 17 in Table 3); Sample 504B-63-4, 90-91 cm	Analyses 47-49: Type 6 (blue green) clay mineral—	
25, 26	Dark olive green clay mineral completely replacing the core of an olivine phenocryst (associated with Analyses 18, 19, in Table 3); Sample 504B-63-4, 90-91 cm	47-49	Blue green clay mineral replacing olivine in red halo (associated with Analyses 8, 9 in Table 4); Sample 504B-37-3, 49-52 cm
27, 28	Greenish orange clay mineral partly replacing the core or an olivine phenocryst (associated with olive green clay mineral and calcium carbonate); Sample 504B-40-1, 37-39 cm		

### Type 1b (dark olive green)

Fe\*/FeO\* + MgO ratio ranges from 0.5 to 0.6, SiO<sub>2</sub> content from 47.6 to 50.4%, and interlayered H<sub>2</sub>O from 11 to 13.3%. Another clay mineral, which is greenish orange, is chemically similar to the dark olive green clay mineral. We observed it in several samples, but are not sure that it has a uniform composition. The Type 1b clay minerals are very close to saponite in composition, although octahedral occupancy (5.46 to 5.70) is too low in some cases.

### Type 1c (olive brown)

This clay mineral is most like the Type 1a clay minerals but has even less SiO<sub>2</sub>. H<sub>2</sub>O content is 11.0 to 12.3%. The mineral is probably another variety of saponite.

### Type 2 (colorless to very pale green)

These clays are very rich in MgO (23.4 to 26.1%) and have SiO<sub>2</sub> contents ranging from 46.7 to 55.8%. H<sub>2</sub>O content is variable (11 to 18%). Because of their optical features, the shipboard scientific team originally identified these clay minerals as talc, but they are too poor in Si and Mg and too rich in Fe, Al, and H<sub>2</sub>O to be talc (see Laverne, this volume.) They are probably saponite or a saponite-talc mixture.

### Type 3 (orange)

There are two orange clay minerals. One is CaO poor (<1%) and MgO rich (21.3 to 24.3%) and has a medium FeO\* content (9.4 to 15.7%). The other is CaO rich (≈15%) and FeO\* rich (20.5 to 22.6%) and con-

tains less MgO (8.1 to 9.5%). It is probably a mixture of clay mineral and Ca-carbonate. Both varieties show a linear correlation between FeO\*/FeO\* + MgO ratio and SiO<sub>2</sub> content. This correlation and the common orange color lead us to consider these clay minerals the same type in spite of their different CaO contents. Structural formulas indicate that a large amount of iron is probably Fe<sup>3+</sup> in tetrahedral sites. Both Type 3 clay minerals may be oxidized saponites, but the Ca-rich variety could be a mixture of oxidized saponite and calcium carbonate.

### Types 4 and 5

The chemical analyses of Types 4 and 5 are on a continuum from lower K<sub>2</sub>O and FeO\* but higher tetrahedral Al contents (Type 4) to higher K<sub>2</sub>O and FeO\* but lower tetrahedral Al contents (Type 5).

Type 4 (dark green) clays are rich in both K<sub>2</sub>O (4.6 to 6.8%) and FeO\* (16.8 to 21.9%). The interlayered H<sub>2</sub>O content is constant at about 8.5%. These clay minerals are found in vesicles and voids down to Sample 504B-38-2, 129-131 cm (563 m BSF), as rare olivine replacements down to Sample 504B-33-1, 69-73 cm (511.5 m BSF), with calcite in Sample 504B-38-1, 28-31 cm (561.8 m BSF), and in veins down to Sample 504B-34-1, 54-56 cm (526 m BSF). They are sometimes associated in olivine replacements with iddingsite or Type 1a or 2 saponite.

Our Analyses 42 and 43 (Table 3) are too rich in MgO to be pure celadonite (see Buckley et al., 1978), and all of the Type 4 clay minerals we analyzed (Analyses 40 to 43) are also too poor in K<sub>2</sub>O to be pure celadonite. Type 4 is thus provisionally identified as a mixture of cela-

Table 3B. Representative microprobe analyses of clay minerals from Hole 504B: chemical composition of minerals.<sup>a</sup>

	Analysis																									
	1	2	3	4	5	6	7	8	9	10	11	12	13	14	15	16	17	18	19	20	21	22	23	24	25	
SiO <sub>2</sub>	50.59	54.21	55.78	50.33	52.31	40.24	42.71	54.44	53.50	51.95	51.60	48.83	48.21	55.21	53.22	54.52	53.91	53.29	55.61	47.80	48.20	48.31	50.27	50.43	48.73	
Al <sub>2</sub> O <sub>3</sub>	3.76	1.63	1.24	1.92	1.97	9.13	7.65	0.06	0.01	0.06	0.19	4.41	3.52	0.83	1.02	0.09	0.04	1.11	1.41	6.86	3.31	3.39	0.28	0.30	3.98	
FeO*	5.59	4.89	5.37	10.20	10.20	8.26	7.69	10.11	10.46	11.19	11.06	9.80	8.67	12.76	13.22	10.33	13.33	10.27	10.67	5.21	19.42	18.80	18.80	17.94	20.27	
MnO	—	0.05	—	—	0.08	—	—	0.03	0.09	0.10	0.03	0.05	—	0.08	0.02	—	—	0.03	0.03	—	0.20	0.23	0.05	—	0.10	
MgO	24.30	25.05	25.78	20.75	22.05	24.22	23.82	22.93	23.19	21.14	21.58	24.51	23.52	21.36	19.81	25.60	22.06	23.47	23.06	23.48	11.33	12.09	17.01	17.13	12.11	
CaO	1.41	0.57	0.43	0.88	0.97	0.83	1.44	0.84	0.91	1.05	0.82	0.90	1.13	0.55	0.74	0.53	0.48	0.92	0.66	1.35	3.14	3.05	1.93	1.74	2.78	
Na <sub>2</sub> O	0.10	0.11	0.09	0.10	0.21	0.15	0.35	0.04	0.09	0.04	0.09	0.14	0.19	0.05	0.11	0.13	0.14	0.10	0.14	0.42	0.33	0.11	0.10	0.15	0.06	
K <sub>2</sub> O	0.18	0.17	0.21	0.33	0.25	0.08	0.11	0.27	0.32	0.12	0.11	0.20	0.29	0.13	0.12	0.09	0.11	0.10	0.21	0.34	0.71	0.32	0.15	0.11	0.22	
TiO <sub>2</sub>	—	0.01	—	0.03	—	—	0.04	—	—	—	—	—	—	—	0.01	—	—	—	0.02	—	—	—	—	—	—	
NiO	0.24	0.20	0.27	0.08	—	0.11	0.08	0.12	0.30	—	0.19	0.06	—	0.25	0.23	0.11	0.19	0.17	0.09	0.13	0.07	0.03	0.37	0.20	—	
Cr <sub>2</sub> O <sub>3</sub>	—	0.02	0.08	—	0.01	—	—	0.12	0.13	0.08	0.19	—	—	—	0.05	0.01	0.04	0.05	—	—	—	—	0.07	0.06	0.10	
Total	86.17	86.91	89.25	84.63	88.03	83.02	83.89	88.97	89.00	84.74	85.85	88.89	85.55	91.21	87.76	91.41	90.29	89.53	91.90	85.61	86.72	86.33	89.05	88.06	88.34	
Si	7.38	7.74	7.77	7.63	7.61	6.28	6.56	7.82	7.73	7.80	7.75	7.08	7.23	7.81	7.79	7.64	7.75	7.63	7.73	7.04	7.59	7.58	7.63	7.69	7.50	
Al	0.62	0.26	0.20	0.34	0.34	1.68	1.38	0.01	—	0.01	0.03	0.75	0.62	0.14	0.18	0.01	0.01	0.19	0.23	0.96	0.41	0.42	0.05	0.05	0.50	
Ti	—	—	—	—	—	—	—	—	—	—	—	—	—	—	—	—	—	—	—	—	—	—	—	—	—	
Z	8.00	8.00	7.97	7.97	7.95	7.96	7.94	7.82	7.73	7.81	7.78	7.83	7.85	7.95	7.97	7.65	7.76	7.82	7.96	8.00	8.00	8.00	7.68	7.74	8.00	
Al	0.03	0.01	—	—	—	—	—	—	—	—	—	—	—	—	—	—	—	—	—	0.23	0.20	0.21	—	—	0.22	
Fe <sup>T</sup>	0.68	0.58	0.62	1.29	1.24	1.07	0.98	1.21	1.26	1.40	1.38	1.18	1.08	1.50	1.61	1.21	1.60	1.23	1.24	0.64	2.55	2.46	2.38	2.28	2.60	
Mn	—	0.01	—	—	0.01	—	—	—	0.01	0.01	—	—	—	0.01	—	—	—	—	—	—	0.03	0.03	0.01	—	0.01	
Ni	0.03	0.02	0.03	0.01	—	0.01	0.01	0.01	0.03	—	0.02	0.01	—	0.03	0.03	0.01	0.02	0.02	0.01	0.01	0.01	0.01	—	0.04	0.02	—
Mg	5.26	5.37	5.35	4.70	4.75	4.92	5.01	4.77	4.70	4.58	4.60	4.80	4.92	4.46	4.35	4.78	4.38	4.75	5.12	2.67	2.85	3.57	3.70	2.80	2.80	
Y	6.00	5.99	6.00	6.00	6.00	6.00	6.00	6.00	6.00	6.00	6.00	6.00	6.00	6.00	5.99	6.00	6.00	6.00	6.00	6.00	5.46	5.55	6.00	6.00	5.63	
Mg	0.06	—	0.04	0.02	0.06	0.75	0.48	0.17	0.33	0.18	0.26	0.53	0.37	0.07	—	0.60	0.38	0.29	0.06	0.04	—	—	0.30	0.22	—	
Ca	0.22	0.09	0.06	0.14	0.15	0.14	0.24	0.13	0.14	0.17	0.13	0.14	0.18	0.08	0.12	0.08	0.07	0.14	0.10	0.21	0.53	0.51	0.31	0.28	0.46	
Na	0.03	0.03	0.02	0.03	0.06	0.05	0.10	0.01	0.03	0.01	0.03	0.04	0.06	0.01	0.03	0.04	0.04	0.03	0.04	0.12	0.10	0.03	0.03	0.04	0.02	
K	0.03	0.03	0.04	0.06	0.05	0.02	0.02	0.05	0.06	0.02	0.02	0.04	0.06	0.02	0.02	0.02	0.02	0.02	0.02	0.04	0.06	0.14	0.06	0.03	0.02	0.04
X	0.34	0.15	0.16	0.23	0.26	0.96	0.84	0.36	0.56	0.38	0.44	0.75	0.67	0.18	0.17	0.74	0.51	0.48	0.24	0.43	0.77	0.60	0.67	0.56	0.52	

<sup>a</sup> FeO\* total iron expressed as FeO. Structural formulas are calculated on the basis of 22 oxygens.

Table 3B. (Continued).

	Analysis																								
	26	27	28	29	30	31	32	33	34	35	36	37	38	39	40	41	42	43	44	45	46	47	48	49	
SiO <sub>2</sub>	47.53	50.82	50.47	47.55	48.01	48.17	55.14	54.99	49.85	48.67	49.12	45.47	36.96	37.95	51.63	51.82	50.04	50.08	46.80	46.87	46.20	33.68	33.54	31.98	
Al <sub>2</sub> O <sub>3</sub>	3.95	0.33	0.35	4.65	4.85	7.26	1.66	1.78	4.02	4.15	2.42	2.08	7.67	8.25	1.57	1.75	4.54	4.42	0.80	1.38	1.24	13.69	13.88	14.97	
FeO*	20.33	16.49	16.78	11.42	11.78	12.85	4.10	3.57	4.21	4.23	9.37	15.69	22.58	20.53	21.92	21.44	16.75	18.30	29.49	28.06	25.87	15.18	15.02	15.06	
MnO	0.07	0.11	0.04	0.08	0.14	—	—	0.03	—	0.05	0.06	—	—	0.02	—	—	—	—	—	0.04	0.14	0.19	0.01	0.21	
MgO	11.31	17.46	17.25	21.84	21.75	21.12	25.64	26.41	24.16	23.38	24.18	21.25	8.07	9.51	8.37	9.04	13.85	12.13	4.75	6.25	8.79	20.54	20.55	22.09	
CaO	2.46	1.97	1.78	1.50	1.64	1.69	0.57	0.59	0.89	1.02	0.89	0.99	14.91	14.95	0.65	0.84	1.34	1.31	0.25	0.51	0.58	1.92	1.92	1.01	
Na <sub>2</sub> O	0.13	0.22	0.25	0.20	0.29	0.82	0.15	0.11	0.25	0.22	0.16	0.09	0.16	0.10	0.13	0.09	0.32	0.34	0.05	0.05	0.01	0.95	0.11	0.15	
K <sub>2</sub> O	0.30	0.31	0.33	0.27	0.34	0.06	0.17	0.15	0.18	0.14	0.20	0.16	0.04	0.02	6.75	6.48	4.60	5.00	8.10	7.08	6.05	0.13	0.05	—	
TiO <sub>2</sub>	—	—	0.03	—	—	0.03	0.01	—	—	—	—	—	0.26	0.26	—	—	—	—	—	—	—	—	0.02	—	
NiO	1.68	0.12	0.17	0.14	—	0.02	0.07	0.22	0.15	0.07	—	—	0.07	—	—	—	—	0.05	0.11	0.13	0.11	0.27	—	—	
Cr <sub>2</sub> O <sub>3</sub>	0.17	—	0.09	—	0.13	—	0.02	0.01	0.02	0.10	0.01	0.04	0.19	0.01	—	—	—	0.05	—	—	—	—	—	0.01	
Total	87.94	87.81	87.54	87.65	88.93	92.02	87.57	87.85	83.78	82.05	86.35	85.76	90.92	91.59	91.02	91.47	91.44	91.67	90.34	90.37	88.98	86.64	85.10	85.48	
Si	7.44	7.72	7.71	7.08	7.06	6.87	7.77	7.72	7.41	7.39	7.31	7.10	6.01	6.03	7.99	7.96	7.46	7.53	7.78	7.68	7.58	5.35	5.38	5.12	
Al	0.56	0.06	0.06	0.81	0.84	1.13	0.23	0.28	0.59	0.61	0.42	0.38	1.47	1.54	0.01	0.04	0.54	0.47	0.16	0.27	0.24	2.56	2.62	2.82	
Ti	—	—	—	—	—	—	—	—	—	—	—	—	0.03	0.03	—	—	—	—	—	—	—	—	—	—	
Z	8.00	7.78	7.77	7.89	7.90	8.00	8.00	8.00	8.00	8.00	7.73	7.48	7.51	7.60	8.00	8.00	8.00	8.00	7.94	7.95	7.82	7.91	8.00	7.94	
Al	0.17	—	—	—	0.09	0.05	0.01	0.11	0.13	—	—	—	—	—	0.28	0.28	0.26	0.31	—	—	—	—	—	—	
Fe <sup>T</sup>	2.65	2.09	2.13	1.42	1.44	1.53	0.48	0.42	0.52	0.54	1.16	2.04	3.06	2.72	2.84	2.75	2.09	2.30	4.09	3.83	3.54	2.01	2.01	2.01	
Mn	0.01	0.01	0.01	0.01	0.02	—	—	—	0.01	0.01	—	—	—	—	—	—	—	—	0.01	0.02	0.03	—	—	0.03	
Ni	0.21	0.01	0.02	0.02	—	0.01	0.02	0.02	0.01	—	—	0.01	—	—	—	—	—	—	—	—	—	0.03	—	—	
Mg	2.66	3.89	3.84	4.55	4.54	4.38	5.42	5.55	5.34	5.31	4.84	3.96	1.97	2.27	1.93	2.07	3.08	2.72	1.18	1.54	2.16	3.93	3.99	3.96	
Y	5.70	6.00	6.00	6.00	6.00	6.00	5.96	6.00	6.00	6.00	6.00	6.00	6.00	5.04	4.99	5.05	5.10	5.43	5.33	5.27	5.38	5.72	6.00	6.00	6.00
Mg	—	0.09	0.11	0.33	0.26	0.11	—	0.01	0.05	0.02	0.64	1.02	—	—	—	—	—	—	—	—	—	0.96	0.95	1.34	
Ca	0.41	0.32	0.29	0.24	0.26	0.26	0.09	0.09	0.14	0.17	0.14	0.17	2.60	2.55	0.11	0.14	0.21	0.21	0.04	0.09	0.10	0.33	0.33	0.17	
Na	0.04	0.06	0.07	0.06	0.08	0.23	0.04	0.03	0.07	0.06	0.05	0.03	0.05	—	0.04	0.03	0.09	0.10	0.02	0.02	—	0.25	0.03	0.05	
K	0.06	0.06	0.06																						

**Chlorite**

Nine occurrences of chlorite are reported by Kurnosov et al. (this volume) in the uppermost portion of the hole (down to Core 34, Section 2; i.e., 527 m BSF). However, we cannot confirm this observation because we only identified chlorite by X-ray diffraction in one vein (in Sample 504B-69-1, 95–99 cm, at about 830 m BSF; i.e., from the very bottom of the hole). The chlorite was associated there with quartz and saponite.

**Mixed-Layer Smectite–Chlorite**

Mixed-layer smectite–chlorite was tentatively identified by X-ray diffraction in the lowermost portion of the hole. It is associated with quartz and calcite in veins in Core 64, Section 1 and Core 66, Section 2, at about 775 and 793 meters BSF, respectively.

**Iddingsite**

Many olivine crystals are altered to smectites and a heterogeneous material that exhibits black, brown, orange, or brownish red color and very low birefringence. A similar material occurs as the major constituent of many veins, particularly in Cores 32 and 34 and, to a lesser extent, in Cores 35 to 37 (i.e., between 507 and 570 m BSF).

The Shipboard Scientific Party of Leg 70 had initially identified these alteration products iron oxyhydroxides. According to microprobe analyses, the chemical composition of this material varies greatly, but it is always either too rich in SiO<sub>2</sub> to be a pure iron hydroxide or too poor in SiO<sub>2</sub> and/or rich in FeO\* to be a pure smectite (see Table 4). We term this material iddingsite where it replaces olivine and iddingsitelike material where it occurs as veins or elsewhere in the rocks. Its compositional field is clearly different from that of clay minerals on the FeO\* versus SiO<sub>2</sub> diagram (Fig. 3).

Microprobe analyses of the iddingsites that replace olivine and optically similar material that fills cracks and vesicles in basalts from Hole 504B are compared in Table 5 with the chemical composition of iddingsites that replace olivine and orthopyroxene and subaerial basalts (Wilshire, 1958). At first the differences between the iddingsites that replace olivine and the similar material that fills vesicles and cracks in Hole 504B seem insignificant. On the other hand, the composition of the orange heterogeneous materials from Hole 504B is slightly different from Wilshire's equivalent, the former having a lower SiO<sub>2</sub> and a higher FeO content than the latter. We believe that most of the orange heterogeneous materials associated with smectite as olivine replacement in Hole 504B basalts are mineralogically and composi-

Table 4. Microprobe analyses of iddingsites from Hole 504B.

a. Mineral color and location		b. Chemical composition of minerals <sup>a</sup>												
		Analysis												
		1	2	3	4	5	6	7	8	9	10	11	12	13
Analyses 1, 2	Iddingsite replacing olivine (associated with Analyses 1, 32, 33, 44, 45, 46 in Table 3); Sample 504B-33-1, 69–73 cm	28.18	26.43	17.11	26.04	24.36	18.65	20.03	28.07	25.10	19.97	21.82	27.04	20.55
Analyses 3, 4	Iddingsite replacing olivine (associated with Analyses 2, 3 in Table 3); Sample 504B-33-1, 69–73 cm	2.64	2.48	1.55	2.42	2.25	2.58	2.74	9.68	8.04	2.34	2.70	2.47	2.12
Analyses 5–7	Iddingsite replacing olivine (associated with Analyses 34, 35 in Table 3); Sample 504B-33-2, 48–52 cm	37.90	40.09	56.36	42.11	49.83	52.99	49.24	30.92	39.74	49.59	46.72	40.94	50.07
Analyses 8, 9	Iddingsite replacing olivine (associated with Analyses 47, 48, 49 in Table 3); Sample 504B-37-3, 49–52 cm	—	—	0.06	—	0.02	0.02	—	0.04	—	0.15	0.06	0.12	—
Analyses 10, 11	Iddingsite at the rim of a vesicle (associated with Analyses 40, 41 in Table 3, at the center); Sample 504B-33-1, 69–73 cm	13.40	13.31	6.24	12.03	5.00	7.01	8.37	4.88	2.57	9.39	9.77	12.74	8.22
Analyses 12, 13	Iddingsite alone in a vein; Sample 504B-33-1, 69–73 cm	1.10	0.93	0.85	0.83	0.77	0.81	0.90	11.95	10.29	0.95	1.04	1.17	1.21
		0.08	0.11	0.18	0.05	0.18	0.13	0.23	0.17	0.20	0.13	0.15	0.20	0.12
		0.19	0.10	0.25	0.19	2.09	0.50	0.33	0.08	0.04	0.15	0.13	0.09	0.21
		0.05	0.05	0.01	0.08	0.01	—	—	—	0.08	0.11	0.04	—	—
		—	0.19	0.14	—	—	—	—	0.04	—	—	0.03	0.25	—
		0.10	0.15	—	0.06	—	—	0.07	0.06	0.17	—	0.07	—	0.19
Total		83.63	83.84	82.75	83.81	84.52	82.70	81.91	85.89	86.21	82.78	82.54	85.04	82.69
Si		5.43	5.18	3.99	5.17	5.10	4.19	4.41	5.17	4.89	4.35	4.63	5.25	4.49
Al		0.60	0.57	0.42	0.57	0.56	0.68	0.71	2.10	1.84	0.60	0.68	0.56	0.55
Ti		0.01	0.01	—	0.01	—	—	—	—	0.01	0.01	—	—	—
Z		6.04	5.76	4.41	5.75	5.66	4.87	5.12	7.27	6.74	4.96	5.31	5.80	5.04
Al		—	—	—	—	—	—	—	—	—	—	—	—	—
Fe <sup>T</sup>		6.08	6.55	10.89	6.97	8.78	9.95	9.03	4.75	6.45	9.03	8.30	6.64	9.14
Mn		—	—	0.01	—	—	—	—	0.01	—	0.03	0.01	0.02	—
Ni		—	0.03	0.03	—	—	—	—	0.01	—	—	—	—	—
Mg		3.87	3.92	2.17	3.58	1.59	2.35	2.76	1.35	0.75	3.05	3.09	3.68	2.68
Y		9.95	10.50	13.10	10.55	10.37	12.30	11.79	6.12	7.20	12.11	11.40	10.34	11.82
Ca		0.23	0.20	0.21	0.18	0.17	0.19	0.21	2.36	2.15	0.22	0.24	0.24	0.28
Na		0.03	0.04	0.08	0.02	0.07	0.06	0.10	0.06	0.08	0.06	0.06	0.08	0.05
K		0.05	0.03	0.07	0.05	0.56	0.14	0.09	0.02	0.01	0.04	0.04	0.02	0.06
X		0.31	0.27	0.36	0.25	0.80	0.39	0.40	2.44	2.24	0.32	0.34	0.34	0.39

<sup>a</sup> FeO\* total iron expressed as FeO. Structural formulas are calculated on the basis of 22 oxygens.

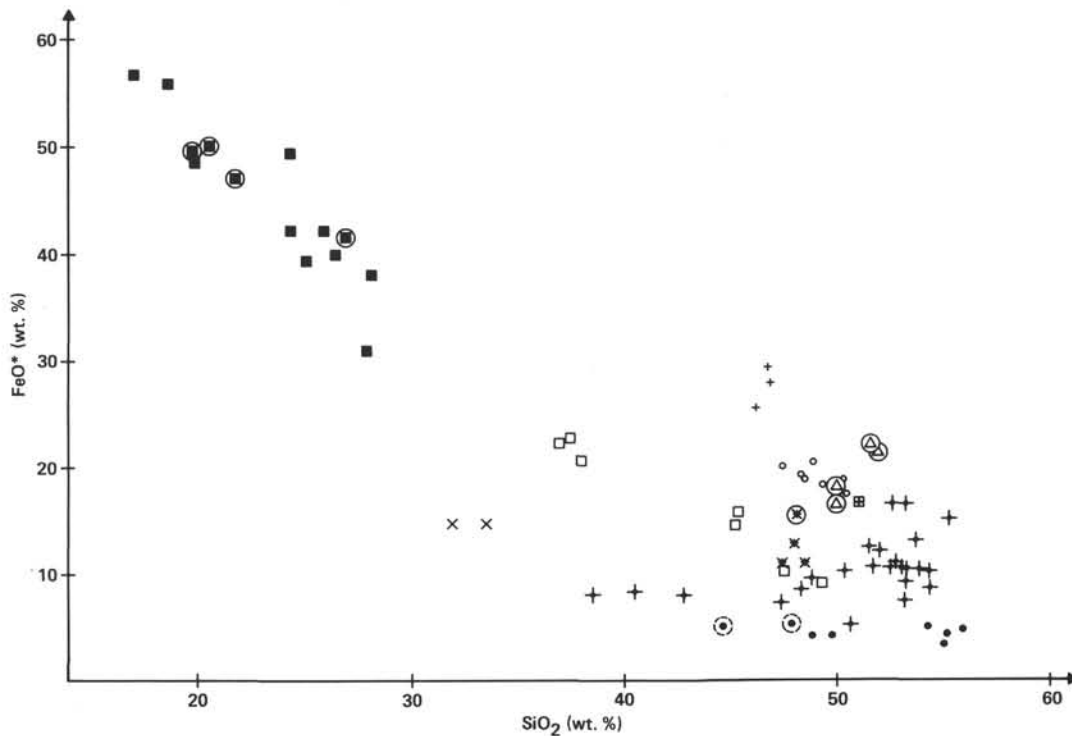


Figure 3. FeO\* versus SiO<sub>2</sub> contents of clay minerals and iddingsites that replace olivine and fill vesicles and voids. Same legend as Figure 2.

Table 5. Composition of iddingsites.

Chemical Composition	Iddingsite after Wilshire (1958)		Iddingsite Replacing Olivine, Hole 504B		Iddingsitelike Material in Vesicles and Veins Hole 504B	
	Average (10 anal.)	Range	Average (10 anal.)	Range	Average (4 anal.)	Range
SiO <sub>2</sub>	37.15	22.08-48.36	23.81	17.11-28.18	22.34	19.97-27.04
TiO <sub>2</sub>	0.13	0.12-0.26	0.02	0-0.08	0.04	0-0.11
Al <sub>2</sub> O <sub>3</sub>	3.44	0-5.09	3.67	1.55-9.68	2.41	2.12-2.70
Fe total <sup>a</sup>	32.28	25.48-62.10	44.16	30.92-56.36	46.83	40.94-50.07
MnO	0.05	0-0.11	0.01	0-0.00	0.08	0-0.15
MgO	6.18	0.60-12.71	8.38	2.57-13.40	10.03	8.22-12.74
CaO	2.12	1.72-3.26	2.93	0.77-11.95	1.09	0.95-1.21
Na <sub>2</sub> O	0.11	0.12-0.13	0.14	0.05-0.23	0.15	0.12-0.20
K <sub>2</sub> O	0.09	0.09-0.10	0.40	0.04-2.09	0.14	0.09-0.21
H <sub>2</sub> O	18.22	~10.00-32.00	16.30	13.89-18.80	16.73	14.96-17.46

<sup>a</sup> As Fe<sub>2</sub>O<sub>3</sub> in Wilshire, 1958; as FeO in this study.

tionally identical to iddingsite, that is, mixtures of various alteration minerals as smectites, goethite, and sometimes calcite, talc, or amorphous silica (Wilshire, 1958). A detailed study would be required to correlate the chemical and optical variability of iddingsite and iddingsite-like material with their conditions of formation.

### Talc

Talc is not commonly found as a pseudomorph after olivine phenocrysts despite optical similarity to some of the clay minerals. We found talc by X-ray diffraction of bulk rock powder samples in six samples from Core 39, Section 2 to Core 70, Section 2 (i.e., from 566 m BSF to the bottom of the hole). Talc was not identified by electron microprobe as a replacement product of olivine (e.g., colorless to very pale green Type 2 clay mineral), indicating that it is probably mixed with a smectite at a

scale smaller than the electron beam diameter (i.e., a few microns). However, talc may be present in the altered basalts elsewhere than in olivine pseudomorphs.

Minor talc occurs in a vein of Sample 504B-37-3, 64-67 cm (593 m BSF) with natrolite, analcime, and trioctahedral smectite (X-ray diffraction identifications). In Sample 504B-52-3, 103-107 cm, we identified talc by electron microprobe in a vein where it separated a trioctahedral smectite from aegirine-augite overgrown on the wall rock clinopyroxene (see Laverne, this volume). In Sample 504B-64-3, 63-68 cm (from 777 m BSF), talc is locally present with quartz in a breccia matrix otherwise made up of trioctahedral smectite (X-ray diffraction identifications).

### Carbonates

Calcite is present in several cores down to the lowest part of Hole 504B drilled during Leg 70. It occurs in three modes:

1) It occurs more often as crack fillings, alone or with trioctahedral smectite, analcime, natrolite, and other Na- and/or Ca-zeolites, anhydrite, iddingsite, quartz, and very rarely melanite. Electron microprobe analyses and X-ray diffraction indicate that it is a Mg-calcite in Sample 504B-37-3, 10-13 cm (Table 6) and pure calcite elsewhere.

2) It sometimes occurs as miarolitic void and vesicle fillings, where it is associated with olive brown smectite (see Fig. 4) or yellow green smectite. Based on microprobe analyses, these occurrences are pure calcium carbonate.

Table 6. Microprobe analyses of calcium carbonates and associated minerals.

a. Mineral color and location												
Analyses 1, 2	Calcite (XRD identification) in vein associated with zeolites and Analyses 4–12 and 15–18 in Table 8; Sample 504B-37-3, 10–13 cm											
Analyses 3, 4	Euhedral calcium-carbonate in vein, associated with melanite; Sample 504B-40-1, 37–39 cm											
Analyses 5–8	Calcium-carbonate/clay mineral mixture replacing olivine (associated with Analyses 27, 28 in Table 3); Sample 504B-40-1, 31–39 cm											
Analyses 9, 10	Calcite at the center of a vesicle (associated with olive brown clay mineral, Analysis 31 in Table 3); Sample 504B-56-1, 2–4 cm											
Analyses 11, 12	Calcite (XRD identification) associated with quartz in a vein; Sample 504B-66-2, 9–13 cm											
b. Chemical composition of minerals <sup>a</sup>												
	Analysis											
	1	2	3	4	5	6	7	8	9	10	11	12
SiO <sub>2</sub>	0.02	0.04	—	—	3.97	0.14	7.22	0.11	0.04	0.07	0.01	0.06
Al <sub>2</sub> O <sub>3</sub>	—	0.03	—	—	0.38	—	0.73	—	—	0.05	0.02	—
FeO*	—	—	—	—	1.19	0.67	3.61	0.45	0.05	—	—	0.15
MnO	—	0.62	—	—	0.39	0.07	0.44	—	0.04	0.14	0.08	—
MgO	2.51	2.76	—	—	3.68	5.25	5.57	4.64	0.01	—	—	—
CaO	55.90	58.00	63.80	64.00	49.72	56.26	43.90	56.01	51.77	51.26	61.15	61.26
Na <sub>2</sub> O	—	0.06	0.06	—	0.03	0.22	0.10	0.06	0.01	0.03	—	0.05
K <sub>2</sub> O	0.06	—	—	—	0.02	—	0.07	—	0.01	0.02	—	—
TiO <sub>2</sub>	—	—	—	0.01	—	—	0.03	—	—	—	—	—
NiO	—	—	—	—	—	0.02	—	—	0.04	—	—	0.02
Cr <sub>2</sub> O <sub>3</sub>	—	—	0.10	0.03	—	—	0.04	0.09	—	—	0.03	0.02
P <sub>2</sub> O <sub>5</sub>	1.08	1.08	0.79	0.67	0.60	0.61	0.64	0.81	0.84	0.84	n.d.	n.d.
Total	59.58	62.59	64.74	64.71	59.99	63.25	63.25	62.24	52.80	52.41	61.29	61.57

<sup>a</sup> FeO\* total iron expressed as FeO.

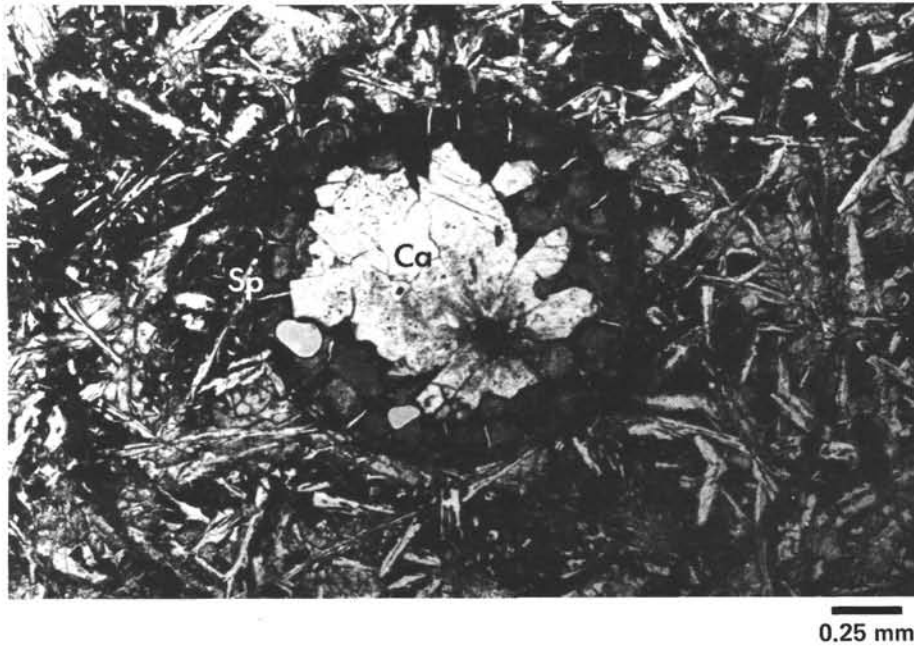


Figure 4. Photomicrograph showing vesicle in Sample 504B-56-1, 2–4 cm from the lower alteration zone filled with olive brown Type 1c saponite (Sp) at the rim and calcite (Ca) at the core. (See Analyses 31 of Table 3, and 9 and 10 of Table 6 for saponite and calcite, respectively.)

3) More rarely, carbonates occur as olivine replacement associated with a greenish brown clay mineral.

Calcite from the upper section of Hole 504B drilled during Leg 69 appears to be more Mg rich than that from the lower part drilled during Leg 70 (see Table 7).

Aragonite is common but never abundant above the 584.5-meter BSF boundary above which red halos are observed. It occurs only once below this depth: as a rela-

tively large prism (10 × 3 mm) with a trioctahedral smectite in Sample 504B-44-2, 97–99 cm (i.e., 607 m BSF).

**Zeolites**

Phillipsite is present down to Core 37, Section 2 (i.e., down to 557 m BSF). It is generally associated with various clay minerals and calcium carbonate in veins

Table 7. MgO content of vein calcites.

Sample (interval in cm)	MgO (%)
504B-9-1, 38-42	~6 <sup>a</sup>
37-3, 10-13	2.5-2.8 <sup>b</sup>
40-1, 37-39	0 <sup>b</sup>
56-1, 2-4	0 <sup>b</sup>
66-2, 9-13	0 <sup>b</sup>

<sup>a</sup> Noack et al. (this volume).<sup>b</sup> This chapter.

crossing altered basalts, glassy pillow rims, and hyaloclastites.

Zeolites other than phillipsite are present in Cores 35, 37, and 38 (from 528 to 570 m BSF). They occur in veins, associated with trioctahedral smectite, apophyllite, anhydrite, calcite, and iddingsite, or as more or less complete replacements of plagioclase microlites and phenocrysts. Zeolites also fill a few vesicles and miarolitic voids.

In veins, zeolite crystals form fibroradial aggregates. The center of such clusters can be made up of analcime ( $\text{NaAlSi}_2\text{O}_6$ ) surrounded by very pale green Type 2 clay mineral (see Fig. 5). Analcime occurs associated with other zeolites, trioctahedral smectite, and calcite in Cores 35, 37, and 38. It forms veins and replaces plagioclase in the wall rocks (see Fig. 4B, Sample 504B-35-1, 68-70 cm). Electron microprobe analyses are given in Table 8. Analcime was also identified by X-ray diffraction in seven samples from Cores 35 (Section 1), 37 (Sec-

tions 1-3), and 38 (Section 1); the last case was examined by Kurnosov et al. (this volume).

Natrolite ( $\text{Na}_2\text{Al}_2\text{Si}_3\text{O}_{10} \cdot 2\text{H}_2\text{O}$ ) was identified by X-ray diffraction in veins from Cores 35 (Sections 1 and 2; see Kurnosov et al., this volume) and 37 (Sections 1-3). It occurs as fibroradial aggregates. Chemical analyses of natrolite with up to 14.9%  $\text{Na}_2\text{O}$  content are reported in Table 8.

The chemical composition of the Ca-, Na-zeolites is extremely variable. Sometimes two adjacent zeolites that are optically similar have different chemical compositions. But most optically similar zeolites have similar chemical compositions. At least three chemically distinct Ca-, Na-zeolites occur in veins from the lower part of Hole 504B (see Table 8). One is a K-rich zeolite ( $5.7 < \text{K}_2\text{O} < 6.2\%$ ), which occurs as large millimeter-sized slabs in a vein of Core 35 (535 m BSF). CaO content ranges from 6.3 to 6.7% and  $\text{Na}_2\text{O}$  from 1.5 to 1.7%.  $\text{H}_2\text{O}$  content is relatively low for a zeolite ( $\approx 10\%$ ). We could not identify this zeolite. The second is a Ca-rich zeolite (10.2 to 10.9%), which contains  $\text{Na}_2\text{O}$  (4.1 to 4.6%), no K, and much  $\text{H}_2\text{O}$  ( $\sim 14\%$ ). It occurs as slabs or fibers in veins (Fig. 6) or in pseudomorphs after feldspars in Core 37 (Fig. 7). It is probably thomsonite ( $\text{NaCa}_2[\text{Al}_5\text{Si}_5]\text{O}_{20} \cdot 6\text{H}_2\text{O}$ ). A similar mineral was analyzed by electron microprobe in Sample 504B-37-3, 18-20 cm by Kurnosov et al. (this volume), who suggested that it was thomsonite.

The third type of zeolite has rather variable composition: CaO contents from 4.6 to 8.7%,  $\text{Na}_2\text{O}$  from 2.5 to 5.9%,  $\text{K}_2\text{O}$  from 0.1 to 1.7%,  $\text{SiO}_2$  from 43 to 48%, and  $\text{H}_2\text{O}$  from 13.5 to 14%. We cannot positively identify

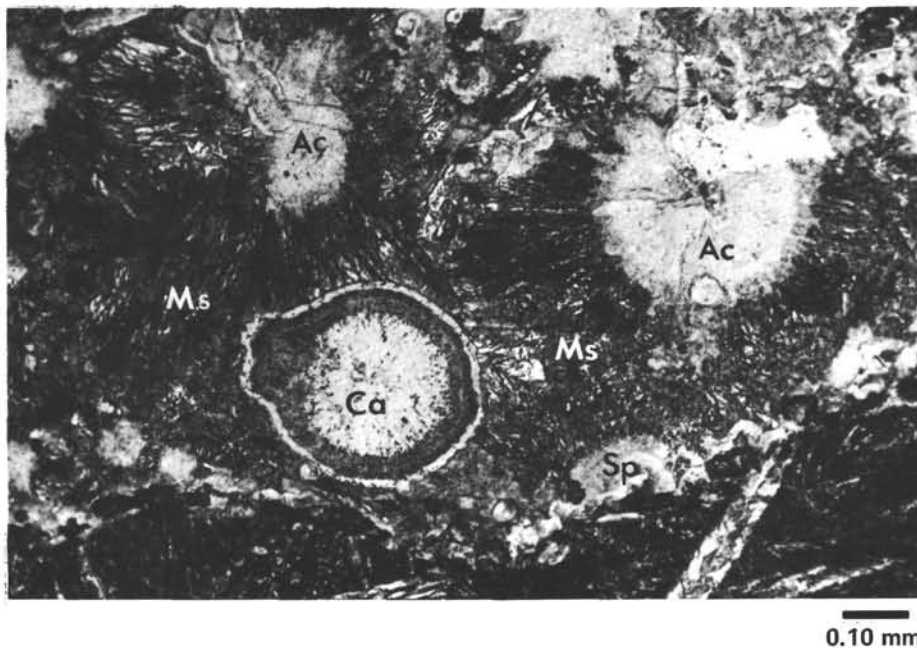


Figure 5. Photomicrograph of a zeolitic vein in Sample 504B-35-1, 68-70 cm, showing analcime (Ac) surrounded by fibroradial mesolite (Ms) and calcite spherule (Ca) surrounded by a double saponite rim (Sp). The host rock bordered by a saponite rim is shown in lower third of the picture. (See Analyses 22 and 23 of Table 8 for mesolite.)

Table 8. Microprobe analyses of zeolites.

a. Mineral color and location.	
Analysis 1	Analcime in vein, at the center of fibroradial aggregates composed by zeolites. Analyses 22-23, this table; Sample 504B-35-1, 68-70 cm
Analysis 2	Analcime in vein; Sample 504B-35-1, 68-70 cm
Analysis 3	Analcime replacing a plagioclase phenocryst; Sample 504B-35-1, 68-70 cm
Analysis 4	Analcime in vein; Sample 504B-37-3, 10-13 cm
Analyses 5-6	Analcime replacing a plagioclase phenocryst; Sample 504B-37-3, 10-13 cm
Analyses 7-12	Fibrous natrolite in vein; Sample 504B-37-3, 10-13 cm
Analyses 13-14	K-rich unidentified large slabs of zeolite in vein; Sample 504B-35-1, 68-70 cm
Analyses 15-16	Probable thomsonite slabs in vein; Sample 504B-37-3, 10-13 cm
Analyses 17-18	Probable thomsonite fibers in vein; Sample 504B-37-3, 10-13 cm
Analysis 19	Probable thomsonite in vein; Sample 504B-37-3, 49-52 cm
Analysis 20	Probable thomsonite-mesolite in vein; Sample 504B-37-3, 49-52 cm
Analysis 21	Probable thomsonite replacing a plagioclase phenocryst; Sample 504B-37-3, 49-52 cm
Analyses 22-23	Probable mesolite fibroradial aggregates in vein; Sample 504B-35-1, 68-70 cm

b. Chemical composition of minerals <sup>a</sup>																							
	Analysis																						
	1	2	3	4	5	6	7	8	9	10	11	12	13	14	15	16	17	18	19	20	21	22	23
SiO <sub>2</sub>	56.47	57.53	54.59	55.87	56.15	55.87	47.06	47.14	45.28	44.03	45.30	46.87	50.54	49.58	41.26	41.09	41.32	41.82	41.97	46.58	41.83	47.99	42.95
Al <sub>2</sub> O <sub>3</sub>	21.24	21.24	24.51	23.29	23.81	24.07	27.13	27.46	27.96	28.45	27.55	27.26	25.51	25.11	28.96	29.24	28.99	29.82	30.30	28.14	29.99	26.57	27.97
FeO*	—	0.05	0.05	—	0.08	—	—	—	—	—	—	—	—	—	—	0.06	0.01	—	0.05	0.07	—	0.10	0.04
MnO	—	0.01	—	—	0.01	—	—	0.04	—	0.07	0.01	—	—	0.01	—	—	0.04	—	—	—	—	—	0.05
MgO	—	0.01	0.02	—	—	—	—	—	—	—	—	—	—	—	—	—	—	—	—	—	—	—	—
CaO	0.09	0.03	0.15	0.03	0.04	—	1.52	1.68	3.35	5.41	4.19	1.64	6.25	6.68	10.94	10.23	10.57	10.22	10.21	7.78	9.88	4.57	8.69
Na <sub>2</sub> O	9.65	9.67	12.03	11.27	11.91	11.50	14.87	14.03	12.96	11.12	12.24	14.32	1.45	1.71	4.14	4.55	4.39	4.40	4.37	4.30	3.95	5.91	2.49
K <sub>2</sub> O	—	—	0.02	0.05	—	0.03	—	—	—	0.02	—	—	5.70	6.23	0.05	0.03	0.02	—	—	—	—	0.08	1.69
TiO <sub>2</sub>	0.03	—	—	—	0.03	—	—	0.01	—	—	0.02	0.01	—	—	—	—	—	—	—	0.02	—	—	—
NiO	0.04	0.04	—	0.03	0.07	0.05	—	—	0.19	—	—	—	—	0.04	—	—	—	—	0.14	—	—	0.09	—
Cr <sub>2</sub> O <sub>3</sub>	—	0.05	—	0.01	—	—	—	—	—	0.07	—	—	—	—	0.03	—	0.09	—	—	0.06	0.09	—	—
P <sub>2</sub> O <sub>5</sub>	0.04	—	—	—	—	—	n.d.	n.d.	n.d.	n.d.	n.d.	n.d.	0.12	0.09	0.09	0.18	0.16	0.14	0.13	0.08	0.19	0.01	0.12
Total	87.57	88.64	91.38	90.55	92.09	91.52	90.59	90.35	89.75	89.16	89.31	90.10	89.57	89.45	85.53	85.38	85.69	86.54	87.11	87.04	85.85	85.31	84.00
Si	2.47	2.48	2.32	2.39	2.37	2.36	23.81	23.82	23.18	22.71	23.27	23.79	25.56	25.33	22.04	21.96	22.04	22.01	21.93	23.93	22.09	24.96	23.14
Al	1.09	1.08	1.23	1.17	1.18	1.18	16.18	16.36	16.87	17.30	16.68	16.31	15.21	15.12	18.24	18.42	18.23	18.50	18.66	17.04	18.67	16.29	17.76
Fe <sup>T</sup>	—	—	—	—	—	—	—	—	—	—	—	—	—	—	—	0.03	0.03	—	—	0.02	0.03	—	0.02
Mn	—	—	—	—	—	—	—	—	0.02	—	0.03	—	—	—	—	—	—	0.02	—	—	—	—	0.03
Mg	—	—	—	—	—	—	—	—	—	—	—	—	—	—	—	—	—	—	—	—	—	—	—
Ca	—	—	—	—	—	—	0.82	0.91	1.84	2.99	2.31	0.89	3.39	3.66	6.26	5.86	6.04	5.76	5.72	4.28	5.59	2.55	5.02
Na	0.82	0.81	0.99	0.92	0.97	0.97	14.59	13.75	12.86	11.12	12.19	14.10	1.42	1.69	4.29	4.71	4.54	4.49	4.43	4.28	4.04	5.96	2.60
K	—	—	—	—	—	—	—	—	—	—	0.01	—	—	3.68	4.06	0.03	0.02	0.01	—	—	—	0.05	1.16
Ti	—	—	—	—	—	—	—	—	—	—	—	—	—	—	—	—	—	—	—	—	—	—	—
Ni	—	—	—	—	—	—	—	—	—	0.08	—	—	—	—	0.02	—	—	—	0.06	—	—	0.04	—
Cr	—	—	—	—	—	—	—	—	—	—	0.03	—	—	—	—	0.01	—	0.04	—	0.02	0.04	—	—
P	—	—	—	—	—	—	n.d.	n.d.	n.d.	n.d.	n.d.	n.d.	0.05	0.04	0.04	0.08	0.07	0.06	0.06	0.03	0.08	—	0.05
Total	4.38	4.37	4.54	4.48	4.52	4.51	55.40	54.87	54.82	54.19	54.47	55.10	49.31	49.93	50.94	51.08	51.00	50.89	50.85	49.63	50.47	49.90	49.78

<sup>a</sup> FeO\* total iron expressed as FeO. Structural formulas are calculated on the basis of 7 oxygens for analcime and 80 oxygens for other zeolites.

this zeolite, which could be a mesolite (Na<sub>2</sub>Ca<sub>2</sub>[Al<sub>6</sub>Si<sub>9</sub>]O<sub>30</sub> • 8H<sub>2</sub>O). It occurs as semispherules in veins from Cores 35 and 37. More detailed X-ray diffraction studies are required to properly identify the various zeolites present in Hole 504B.

**Iron Sulfides**

Pyrite is frequently found in association with trioctahedral smectite in veins from the section of Hole 504B below the 584.5-meter BSF boundary above which red halos are observed. Shipboard descriptions of the cores clearly indicate that the frequency and size of the pyrite crystals, if not their abundance, increase with depth. Secondary pyrite is rare above this boundary: it occurs only in Cores 3 and 13 (Noack et al., this volume) and in Sample 504B-47-2, 130-140 cm (Kurnosov et al., this volume).

Marcasite has been found only in Sample 504B-36-3, 37-39 cm, where it occurs in a 5-mm-wide zone of the inner dark gray core adjacent to a red halo.

**Anhydrite**

Hole 504B basalts contain the first anhydrite (CaSO<sub>4</sub>) reported from oceanic basalts (Alt et al., this volume).

Anhydrite was identified by X-ray diffraction in several veins at 581 meters BSF and lower; it occurs almost to the bottom of the hole drilled during Leg 70. It is present in Samples 504B-43-2, 28-30 cm; 504B-48-3, 14-18 cm and 43-47 cm; 504B-53-1, 3-5 cm; 504B-68-1, 12-14 cm; and 504B-69-1, 95-99 cm, where it is always accompanied by trioctahedral smectite. In Sample 504B-48-3, 14-18 cm, anhydrite occurs as large (up to 5-mm-long) euhedral prisms embedded in a platy gyrolite matrix near the central portion of a vein with salbands of quartz and trioctahedral smectite (X-ray diffraction identifications; see Fig. 8). In Sample 504B-40-3, 130-135 cm, anhydrite occurs in a vug of a dolerite with a trioctahedral smectite and two generations of calcite (X-ray diffraction identifications). Anhydrite was also found by X-ray diffraction in veins in Samples 504B-61-2, 145-148 cm; 504B-64-1, 65-68 cm; 504B-66-2, 0-5 cm; and 504B-68-1, 81-87 cm, where it was generally accompanied by quartz (Kurnosov et al., this volume).

**Quartz**

Quartz appears in Core 48, Section 3 (656 m BSF) and often thereafter down to the bottom of the hole. It occurs in veins as single crystals (up to 2 mm) or as small

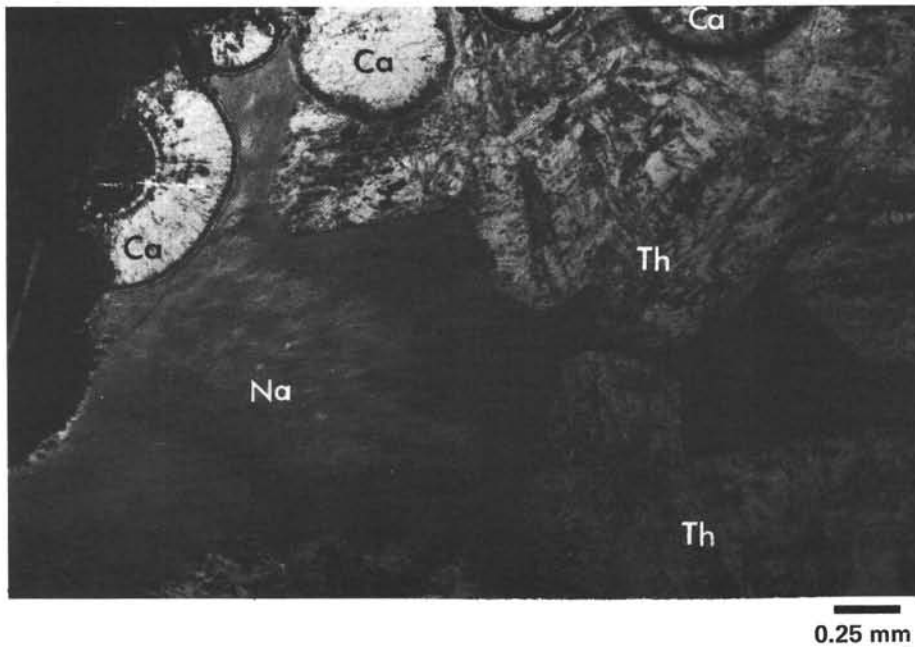


Figure 6. Photomicrograph of a zeolitic vein in Sample 504B-37-3, 10-13 cm, showing Mg-calcite spherules (Ca) surrounded by fibrous natrolite aggregates (Na) and blocky thomsonite (Th). The host rock bordered by a saponite rim is shown in the upper left corner. (See Analyses 7 to 12, and 15 to 18 of Table 8 for natrolite and thomsonite, respectively.)

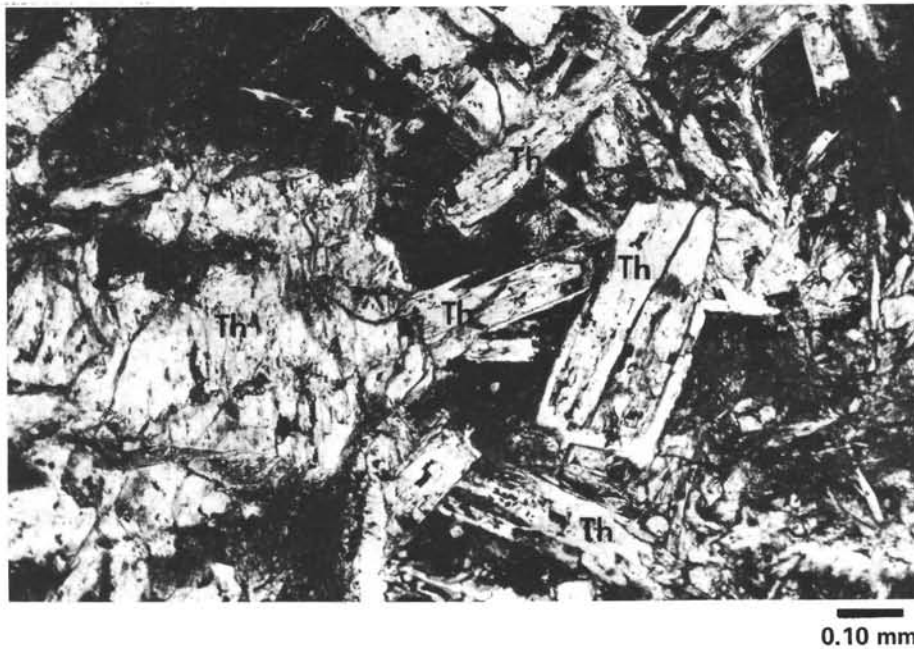


Figure 7. Photomicrograph of host rock adjacent to a zeolitic vein in Sample 504B-37-3, 49-52 cm. The plagioclase phenocrysts and microlites are replaced by thomsonite (Th). (See Analysis 21 of Table 8.)

crystal aggregates. Quartz was identified optically in Cores 49, 54, 56, 62, 64, 65, 66, and 69. The presence of quartz was confirmed by X-ray diffraction analysis in Cores 49, 55, 56, 64, 66, 69, and 70. It is sometimes associated with trioctahedral smectite, gyrolite, and anhy-

drite in Core 48, with talc and trioctahedral smectite in a breccia matrix in Sample 504B-64-3, 63-68 cm, with pyrite in Cores 64 and 69, with trioctahedral smectite and probable chlorite in Core 69, and with trioctahedral smectite, probable interlayered smectite and chlorite,

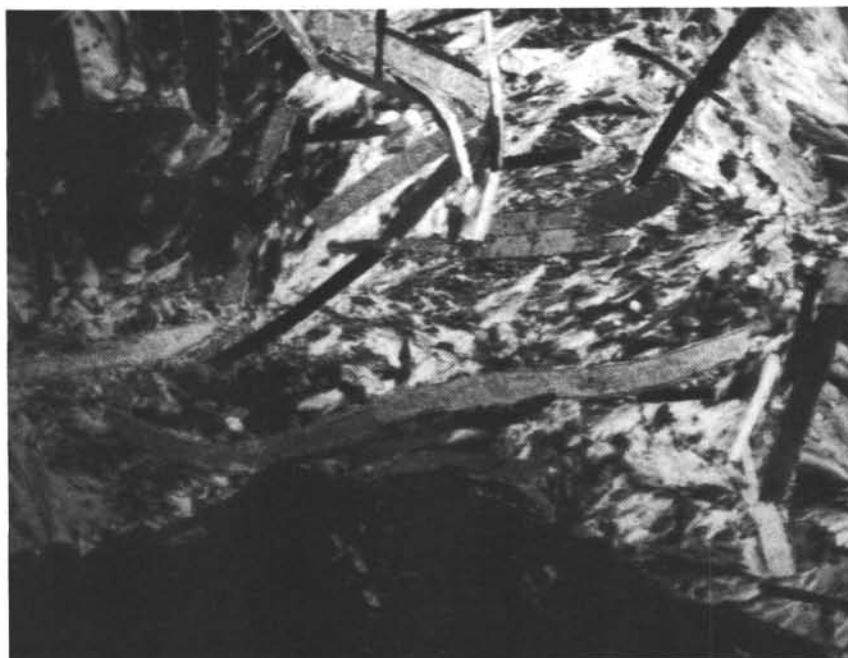


Figure 8. Photomicrograph of the anhydrite-bearing vein in Sample 504B-48-3, 14–18 cm. The large bladed anhydrite crystals (up to 5 mm in length) are embedded in sheaflike aggregates of gyrolite fibers. The host rock in the lower part of the photograph is lined with a smectite border overgrown with clear quartz prisms.

and calcite in Cores 64 and 66. Kurnosov et al. (this volume) identified quartz by X-ray diffraction in veins in Cores 64 and 66, where it accompanies anhydrite.

#### Apophyllite

Apophyllite ( $\text{KCa}_4\text{Si}_8\text{O}_{20}[\text{F},\text{OH}]\cdot 8\text{H}_2\text{O}$ ) was identified by X-ray diffraction in a vein of Sample 504B-37-1, 76–80 cm (from 541 m BSF). It is associated with analcime, natrolite, and thomsonite and encloses a trioctahedral smectite and fibroradial aggregates of calcite (all X-ray diffraction identifications except thomsonite, which was identified optically). Apophyllite was also found in Sample 504B-61-1, 55–60 cm (Kurnosov et al., this volume).

#### Gyrolite

Gyrolite ( $\text{Ca}_2\text{Si}_3\text{O}_7[\text{OH}]_2\cdot \text{H}_2\text{O}$ ) was identified by X-ray diffraction in a vein of Sample 504B-48-3, 14–18 cm, where it is associated with anhydrite, quartz, and trioctahedral smectite. It may be present in a powdered bulk rock sample of Sample 504B-37-1, 94–96 cm with trioctahedral smectite and in Sample 504B-38-1, 7–15 cm (see Kurnosov et al., this volume).

#### Melanite

Crystals of euhedral melanite ( $\text{Ca}_3\text{Fe}_9\text{Ti}_2[\text{SiO}_4]_3$ ), a titanian garnet, occur in a vein of a single sample (Sample 504B-40-1, 37–39 cm; 572.5 m BSF). They are associated with a Ca-carbonate, aegirine-augite, and a Fe-rich saponite (see Laverne, this volume).

#### Aegirine-Augite

Aegirine-augite occurs as reaction rims on clinopyroxene crystals bordering Ca-carbonate and Fe-sapon-

ite veins in three samples (Samples 504B-40-1, 37–39 cm; 504B-52-3, 103–107 cm; and 504B-58-1, 9–13 cm; 573, 669, and 720 m BSF, respectively; see Laverne, this volume).

#### Fassaite

Fassaite (Al-rich, Na-poor clinopyroxene) was found just at the vein wall of a single sample (Sample 504B-52-3, 13–16 cm, 668 m BSF; Laverne, unpublished data).

#### K-Feldspar

Secondary K-feldspar (X-ray diffraction identification) was observed only once, as an incipient replacement product of igneous plagioclase, in Sample 504B-34-2, 16–20 cm (528 m BSF). See Pertsev and Boronikhin, this volume.

### ALTERATION ZONATION

Two main types of color zonation related to alteration occur along surfaces once exposed to seawater in Hole 504B basalts: red halos are often accompanied by dark gray outer bands above 584 meters BSF, and pale grayish green discoloration occurs adjacent to the zeolitic veins between 549.5 and 553 meters BSF.

Red or reddish brown halos up to 5 cm in width, usually accompanied by outer dark gray bands, occur parallel to many cracks and veins or at the perimeter of breccia zones down to 584.5 meters BSF (i.e., in Sample 504B-40-3, 130–135 cm). Below this critical depth no zonation is apparent, and altered basalts display a uniform or mottled dark gray color. Red halos become progressively less abundant, thinner, and paler (more orange brown than red or reddish brown) with increasing depth.

The red halos derive their color from the presence of iddingsite and Fe-hydroxides, which are the most abundant secondary products replacing olivine. These secondary products stain otherwise apparently fresh primary silicates and fill cracks and voids. Red halos generally display a sharp boundary with the dark gray inner portion of the rock and a diffuse transition to the outer dark gray band. Dichotomous, double, and tailing-out red halos are observed.

A wide variety of alteration mineral parageneses occurs in the various alteration zonations studied so far, but similar secondary minerals or mineral associations in similar alteration zones recur. We describe three samples that are representative of different types of alteration zonation that display red halos. The zonation sequences are designated A to C to facilitate comparison.

In Sample 504B-13-4, 38–43 cm (zonation Sequence A) there are three alteration zones as one proceeds from the interior of the sample toward the once exposed surface. Zone A1 is an inner dark gray portion of rock where a pale olive green clay mineral (probably a saponite) replaces olivine and fills primary voids. Zone A2 is a red halo 5 mm thick, where dark brown, almost opaque iddingsite replaces olivine and iddingsitelike material fills pore spaces. Bright red stains are extremely abundant in cracks through all the primary silicates. The boundary between Zones A1 and A2 is very sharp (there is no iddingsite or red stain in Zone A1), whereas the transition between Zones A2 and A3 is progressive (red stains decrease and become lighter in color). Zone A3 is an outer dark gray band 10 mm thick. Near Zone A2, both iddingsite (plus iddingsitelike material) and pale olive green clay mineral replace olivine and fill pore spaces. Then, farther away from the red halo, only the pale olive green clay mineral (saponite?) replaces olivine, and the primary voids are filled by a bright green clay mineral, probably a celadonite–nontronite.

Sample 504B-16-2, 80–93 cm (zonation Sequence B) also exhibits three alteration zones. Zone B1 is a 10-mm-thick dark gray band where a bright green clay mineral (probably celadonite–nontronite) both fills primary voids and replaces olivine. It coexists with dark brown iddingsite, which occurs along cracks through the olivine pseudomorphs and at their periphery.

Zone B2 is a 4-mm-thick red halo. It is also characterized by an abundance of red stains in primary silicates and by dark brown, almost opaque iddingsite pseudomorphs after olivine. A few light olive brown (saponite?) olivine pseudomorphs are also observed. The transitions between the red halos and both Zones B1 and B3 are gradational.

Zone B3 is another 10-mm-thick dark gray zone where, at first, both brown iddingsite and light olive brown or orange brown clay minerals replace olivine. Farther away from the red halo, the bright green clay mineral fills the primary voids, whereas the light olive brown clay mineral (saponite?) replaces the olivine.

In Zonation Sequence B, the position of the various zones with respect to an exposed surface could not be inferred from the hand specimen because no crack or vein was visible. However, a comparison with zonation Se-

quences A and C leads us to suggest that the dark gray zone (Zone B3) corresponds to the outer dark gray bands of Zones A3 and C3 (see below). On the other hand, the dark gray zone (Zone B1) does not have an equivalent in the other cases studied. Further, Sample 504B-16-2 (80–93 cm) provides the only example (so far as we know) of the presence of celadonite–nontronite on both sides of a red halo.

Sample 504B-34-1, 7–19 cm (zonation Sequence C) provides the most interesting red halos (see Fig. 9) because this 12-cm-long core section apparently exhibits two red halos, each accompanied by an outer dark gray band on both sides of a dark gray rhomb-shaped inner portion. Another longitudinal cross section of the core shows that the two red halos belong to one and the same alteration zone, which is shaped in cross section like a textbook diagram of a geosyncline. The upper dark gray band is adjacent to the smectite vein along which the core broke off. In hand specimen, the olivine phenocrysts in the red halos are bright red, whereas they display a black color in both the dark gray inner portion and the outer bands.

Zone C1, the inner dark gray portion, essentially contains pale olive brown clay minerals (probably saponite) as primary void fillings and partial replacement of olivine crystals. Olivine relics are quite abundant. The boundaries with both the lower and upper red halos are very sharp.

Zone C2, the upper halo, is about 15 mm thick, about twice as thick as the lower one. The lower halo is actually a doublet formed by a first 20-mm-thick halo outwardly ranging from brownish red to brownish gray followed by a second 5-mm-thick bright red halo quickly grading into a 7-mm-thick adjacent dark gray outer band. The boundaries between red halos and outer dark gray bands are transitional but abrupt. The red halos are characterized by the abundance of red stains in the otherwise apparently unaltered primary silicates and by dark brown iddingsite as the main olivine replacement product. However, in this sample, a light olive brown clay mineral (saponite?) is also present in the olivine pseudomorphs and vesicle fillings. It is particularly obvious when it replaces the largest olivine phenocrysts, whereas in the small olivine pseudomorphs the light olive brown clay mineral is stained brown and masked by iron hydroxides, the combination of the two secondary products forming the iddingsite.

Zone C3, the dark gray outer bands adjacent to both the lower and upper red halos, range in thickness from 8 to 2 mm, respectively. The upper dark gray band could not be studied readily with the microscope because it was almost completely lost during the preparation of the thin sections. However, the lower dark gray band has bright green to yellowish green, rarely orange or bluish green, clay mineral(s) filling primary voids. Olivine is replaced by a complex association of dark brown iddingsite(?) and a light brown to almost colorless clay mineral.

These descriptions represent only three examples among a large collection, but they illustrate the range of secondary mineral parageneses. Much more work will be required before the picture becomes clear.

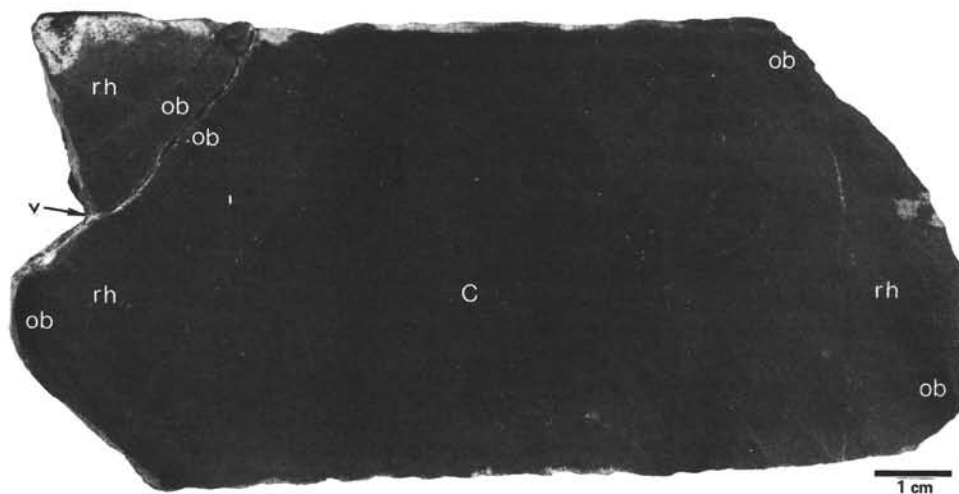


Figure 9. Photograph of slabbed core from the upper alteration zone (Sample 504B-34-1, 7–19 cm) displaying a dark gray core (C), apparently two red halos (rh), and two dark gray outer bands (ob) (only the upper one appears in the photograph). Notice open vein (v) along the upper margin of the sample. See text for detailed description.

The second type of alteration zonation is much more restricted. Relatively thick (2–3-cm) zeolitic veins occur from Core 35, Section 1 to Core 38, Section 2 (i.e., from 528.5 to 563 m BSF), but wall rock discoloration only occurs adjacent to veins in Core 37, Sections 1 to 3 (i.e., between 549.5 and 553 m BSF). In a dozen samples from this roughly 3.5-meter-long core interval, the color of the wall rock adjacent to the zeolitic veins changes from a dark gray to a pale grayish green near the veins. The discoloration affects irregularly shaped zones of rock up to 1 cm away from the vein. The boundary between discolored and dark gray rock is very diffuse. The color change of the wall rock is due to its intense alteration by the solutions from which the vein minerals precipitated. The discolored wall rocks offer the only instances of significant plagioclase replacement observed in the portion of Hole 504B drilled during Legs 69 and 70. Not only are the primary voids filled with secondary minerals, but most of the igneous minerals are replaced by some of the same alteration minerals that form the veins. For example, analcime, apophyllite, thomsonite, and natrolite are found as pseudomorphs after plagioclase in the wall rock adjacent to a vein in Sample 504B-37-1, 19–22 cm, which is essentially made up of the same secondary minerals (besides a trioctahedral smectite). Where calcite is a major component of the vein, it is also found in the wall rock, but almost always as a replacement product of olivine along with various clay minerals, as in Sample 504B-37-1, 76–80 cm. These mineralogical observations are confirmed by bulk rock geochemistry, including oxygen isotope analyses.

#### REPLACEMENT OF MAGMATIC MINERALS

The three major magmatic silicates, (i.e., olivine, plagioclase and clinopyroxene) are variously affected by alteration. The alteration of primary opaque minerals has not yet been studied in detail. Cr-spinel, which occurs in some cores, is not altered, but titanomagnetites are variably altered, depending on their grain size and occurrence in the cores. As in other oceanic basalts,

olivine is always the first primary mineral, not including titanomagnetite, to be altered.

#### Replacement of Olivine

Except in the uppermost portion of the hole (down to Core 8, i.e., 320 m BSF [Noack et al., this volume]), where olivine relics are often observed, and in Lithostratigraphic Unit 27 (Core 39, Section 2 to Core 41; i.e., from 572 to 589 m BSF), olivine is generally completely replaced by alteration products. Olivine relics also occur in Core 35, Section 2; Core 62, Section 1; and Core 63, Section 4. The maximum depth at which fresh olivine occurs is 773 meters BSF (Core 63, Section 4). One of the most striking features of the basalts from Hole 504B is the large variety of olivine replacement products. Ten types are described below.

#### Colorless to Very Pale Green Clay Mineral (Type 2) + Iddingsite

The first type of association is common down to Core 35 (from the basement/sediment interface to 536 m BSF). It generally occurs in the red halos. In Sample 504B-33-1, 69–73 cm, it coexists with the association K, Fe-rich Type 5 clay mineral + saponite (Type 2) + iddingsite (described further below).

The colorless to very pale green clay mineral (Type 2) areas corresponding to old olivine crystals generally seem to be optically continuous (apparently single crystals). The cleavage direction and continuity of this clay are not affected by cracks. Black to reddish brown iddingsite fills cracks and surrounds the former olivine phenocrysts (Fig. 10). It is interesting that the darker (more Fe-rich) the iddingsite, the lighter in color (more Fe-poor) the clay mineral (see Tables 3 and 4).

#### Pale Green Clay Mineral (Type 1a)

Pale green clays replace olivine in the same rocks as the association described above (from the basement/sediment interface to 536 m BSF), but whereas the Type 2 clay minerals and iddingsite occur in the red halos, the

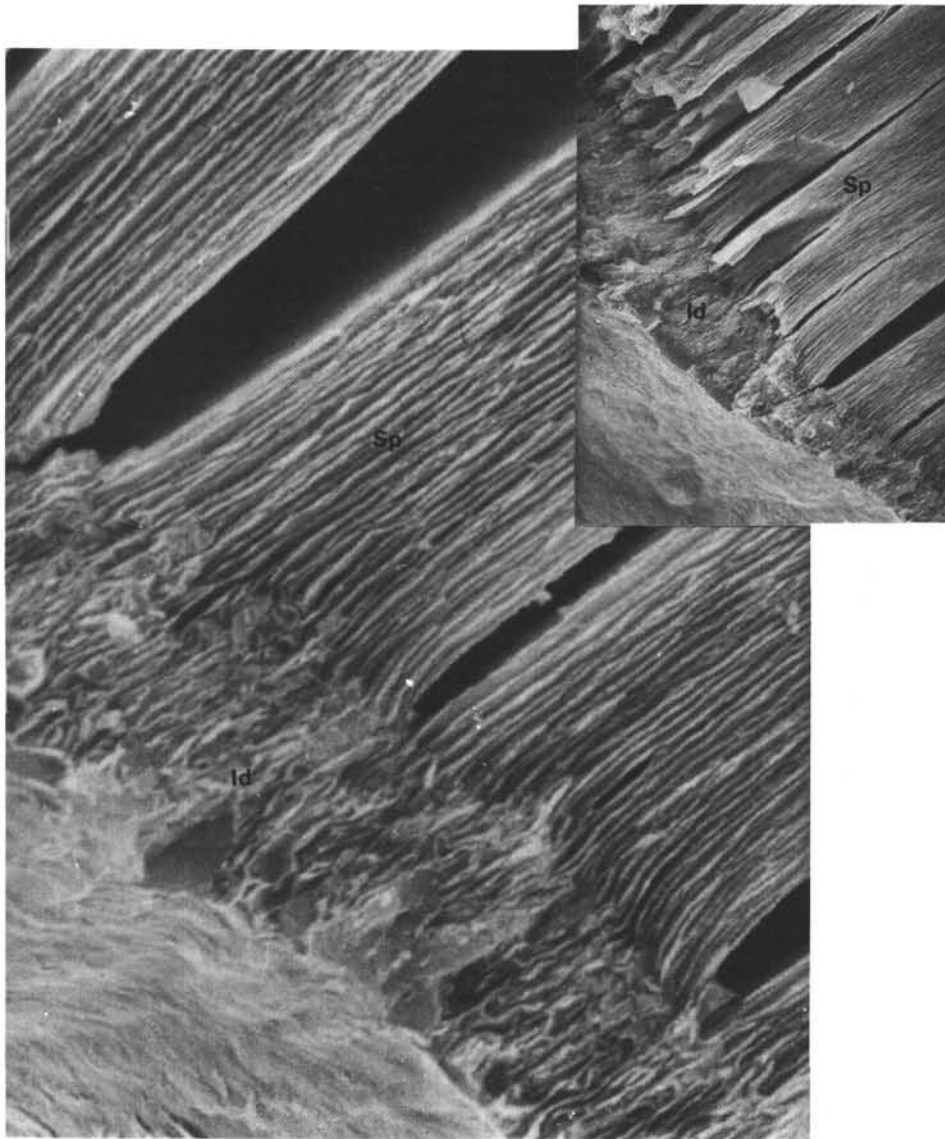


Figure 10. Scanning electron microscope photograph showing an olivine phenocryst completely replaced by an iddingsite rim (Id) (i.e., a mixture of iron hydroxide and saponite) and pale green Type 2 saponite (Sp). Sample 504B-33-1, 69–79 cm, from the upper alteration zone; magnification of originals, 8000 and 80,000 $\times$ . Both photographs are reduced to 62% of originals.

pale green clay occurs only in the adjacent more central portions of the samples. The contact between the oxidized halos and the less oxidized inner portion of the samples is typically so sharp that it can cross a single olivine phenocryst, which thus exhibits both types of replacement. As previously noted, the pale green clay minerals (Type 1a) are richer in Fe than the colorless clay minerals (Type 2) (Table 3). The presence in the same sample of both types of olivine replacement can be summarized as follows. In the first type, olivine  $\rightarrow$  Mg, Fe-rich saponite. In the second type, olivine  $\rightarrow$  Mg-rich but Fe-poor saponite + Mg-poor but Fe-rich iddingsite. Thus, the apparent effect of the brown Fe-rich veins on the adjacent rock is to concentrate iron in the iddingsites at the periphery of and along the cracks through olivine crystal pseudomorphs.

### Orange Clay Mineral (Type 3)

This type of olivine replacement is common in Cores 33, 37, and 38 (from 517 to 569 m BSF). It is not present below Core 38, Section 2 (i.e., below 569 m BSF). It is located in the red halos, where it coexists with, but is less abundant than, the two first types of olivine replacement.

In Sample 504B-33-1, 69–73 cm, a very particular type of olivine replacement occurs: a 2-mm-diameter olivine phenocryst is completely replaced by a granular orange clay mineral which exhibits the typical iddingsite brown color at the crystal rim and along cracks but becomes progressively lighter in color toward the core (Fig. 11). The various colors correspond to the different Fe and Si contents of the clay mineral (Table 3).

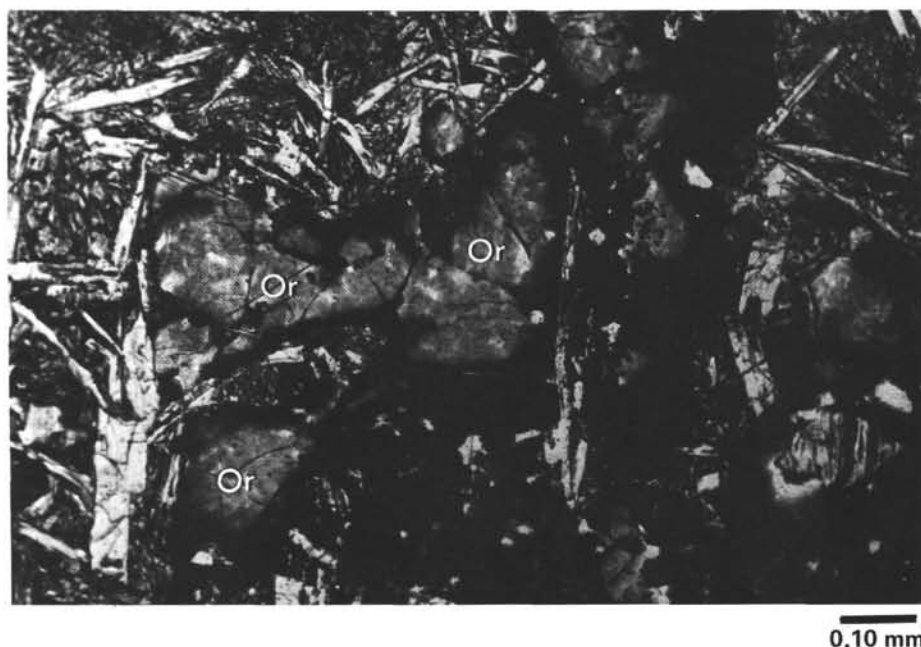


Figure 11. Photomicrograph showing olivine phenocryst replaced by orange Type 3 smectite (Or) in Sample 504B-33-1, 69–73 cm, from the upper alteration zone. (See Analyses 36 and 37 of Table 3.)

Still another type of orange smectite occurs in Sample 504B-38-2, 192–131 cm. Its very high CaO content (14 to 15%) indicates that it is not a pure clay mineral (Table 3) but probably an oxidized saponite–calcium carbonate mixture.

#### Dark Green Clay Mineral (Type 4)

Olivine phenocrysts from the uppermost 200 meters of the hole are often replaced by dark green clay minerals (Type 4) that we tentatively identify as celadonite–nontronite mixtures. These clay minerals are sometimes accompanied by iddingsite or saponite (Types 1a or 2), and more rarely by calcite.

#### Bright Green Clay Mineral (Type 5) + Colorless Smectite (Type 2) + Iddingsite + Pale Green Smectite (Type 1a)

We observed this type of replacement only once, in the upper part of the studied section (in Sample 504B-33-1, 69–73 cm, at 517 m BSF). Among the numerous olivine phenocrysts that are completely altered, only two are replaced by this material. They are both located in a reddish brown halo around a brown orange vein which has an iddingsitelike composition. The boundaries of the old olivine phenocryst are outlined by iddingsite, which also penetrates the crystal along cracks. Bright green and colorless clay minerals are distributed in an apparently random manner nearby (see Fig. 12). The boundaries between the three secondary products are always very sharp. The pale green smectite occurs as very small grain aggregates.

Chemical analyses of the 3 clay minerals and the iddingsite are presented in Tables 3 and 4. Both microscopic and electron scanning microphotographs illustrate the relationships among these (Plate 1). The bright green

K-rich clay, probably a celadonite, forms rims around colorless saponite cores, suggesting that colorless saponite crystallized after the green celadonite. The contacts among Fe, K-rich and Mg-rich clay minerals and iddingsite are very sharp on X-ray scanning of K, Mg, and Fe.

Several points are particularly interesting in this type of olivine replacement, but the most unusual is the association of the green K, Fe-rich clay mineral (celadonite) in the same two olivine pseudomorphs with a K and Fe-poor, Mg-rich clay mineral (saponite), the contact between these two materials being very sharp.

We propose the following two-stage alteration sequence: (1) partial alteration of olivine to celadonite and iddingsite; (2) replacement of the remaining olivine relics by saponite.

#### Blue-Green Clay Mineral (Type 6) + Ca-rich Iddingsite

This type of olivine replacement occurs only in two samples (Sample 504B-35-1, 126–130 cm and 504B-37-3, 49–52 cm; at 536 and 530 m BSF). The associated iddingsite seems to be very heterogeneous and granular, and it is abnormally rich in CaO (10 to 12%). This high CaO content (see Analyses 8 and 9 in Table 4) could be explained by the formation in nearby veins of Ca-zeolites, calcite, and hydrated Ca silicates (apophyllite and gyrolite) during the circulation of Ca-rich fluids. The blue green clay mineral is the only pseudomorph with a Si content lower than that of the olivine it replaces (see Analyses 47 to 49 in Table 3).

#### Olive Brown Clay Mineral (Type 1c)

Olive brown clay minerals partially or completely replace olivine only from Cores 39 to 59 and are most

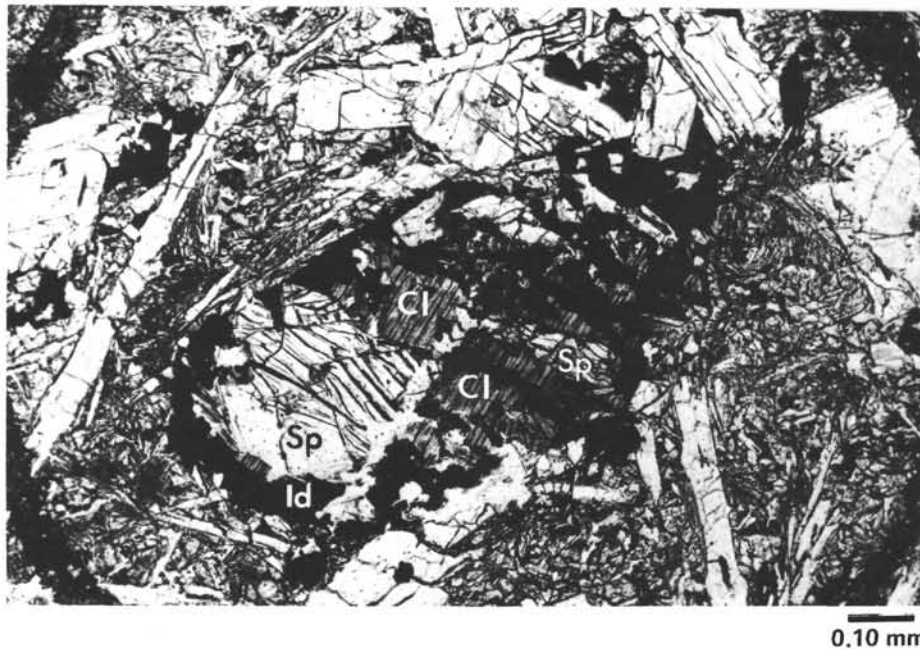


Figure 12. Olivine phenocryst in Sample 504B-33-1, 69–73 cm (from the upper alteration zone) replaced by colorless Type 2 saponite (Sp) and bright green Type 5 celadonite (Cl) at the center and iddingsite (Id) at rim. Same sample as in Figure 10. (See Analyses 1–3, 32, 33, and 44–46 of Table 3 for saponite and celadonite, and Analyses 1 and 4 of Table 4 for iddingsite.)

abundant in Cores 52 to 56 (from 571 to 741 m BSF). In the case of partial replacement of olivine, these olive brown clay minerals surround relics of fresh olivine. This replacement chemically corresponds to an increase in Si, Ca, and Al and, to a lesser extent, a decrease of K, Na, Fe and Mg.

#### Medium Olive Green Clay Mineral (Type 1a) ± Opaques

This type of replacement is frequent below Core 38 (from 571 m BSF to the bottom of the hole). Fresh olivine relics are surrounded and separated from each other by Type 1a clay minerals. The transformation of olivine to Type 1a clay mineral produces Si, Ca, Na, and K gains and Mg and Fe losses.

#### Dark Olive Green Clay Mineral (Type 1b) + Medium or Pale Olive Green Clay Mineral (Type 1a) + Opaque Needles

Although present in Cores 40, 41, 43, 50 and 52, this association is particularly developed in Cores 57 to 63. (Its overall range is from 574 to 773 m BSF.) In the central part of original olivine phenocrysts, patches of dark olive green saponite (Type 1b) or fresh olivine are separated and surrounded by medium or pale olive green saponite (Type 1a). Opaque minerals are scattered through the phenocrysts or are grouped in the pale olive green clay mineral patches; in the latter case very thin opaque needles (0.02 mm long, 0.001 mm in diameter), orange in reflected light, form a trellislike network.

The dark olive green Type 1b saponite is richer in Ca, Fe, and (to a lesser extent) Al, and poorer in Mg than the pale olive green Type 1a saponite. Dark olive green Type 1b saponite is richer in Ca, Si, Fe, and Al and poorer in Mg than the olivine it replaces. The chemical

composition of the different mineral phases (olivine, dark olive green, and pale olive green saponites) is given in Table 3 and illustrated by scanning microphotographs in Plates 2 and 3. The opaque needles contain up to 73% Ni and are Fe rich. The clay mineral is slightly richer in Ni than the olivine it replaces. The Ni contents of the other types of olivine replacement products do not vary significantly from that of the former olivine.

This type of alteration of olivine phenocrysts seems to occur in two steps: (1) the crystal rims are altered to a pale green saponite; (2) the cores are altered to a slightly different dark green saponite. The microphenocrysts are all altered to a clay mineral of a color and composition intermediate between those of Types 1a and 1b.

The only X-ray microdiffraction on a dark olive saponite pseudomorph after an olivine phenocryst in Sample 504B-63-4, 76–82 cm showed a 060 *d* spacing at 1.527 Å, indicating a trioctahedral spacing.

#### Greenish Brown Clay Mineral + Ca-Carbonates

This type of replacement occurs in only one sample (Sample 504B-40-1, 37–39 cm, at 574 m BSF), where a Ca-carbonate vein occurs with melanite (Ca, Ti garnet) crystals (see Laverne, this volume). In the wall rock of this vein, olivine crystals are only partly replaced by a heterogeneous dark green material (see Plate 4) that looks like a clay mineral but is too rich in CaO (44 to 56%) and poor in SiO<sub>2</sub> (0 to 0.7%) to be a smectite (Table 3). As previously noted, the greenish brown smectite has about equal amounts of FeO\* and MgO (17%) and contains some CaO (1.78 to 1.97%; see Analyses 27 and 28, respectively, Table 3).

Two other types of olivine replacement occur in some samples, but the compositions of the replacement products have not been determined. They are (1) Ca-car-

bonate alone in Sample 504B-38-1, 28–31 cm; and (2) olive brown Type 1c clay mineral + carbonate in Sample 504B-52-1, 100–105 cm.

### Replacement of Plagioclase

Plagioclase is often replaced in the lower portion of the hole by colorless or pale green clay minerals and in the wall rock of the zeolitic veins by secondary products that are a very pale green smectite (Table 2), thomsonite (Table 8) or analcime (Table 8). A relationship exists between the nature of a vein adjacent to an altered plagioclase crystal and the composition of the alteration products of the plagioclase.

### Replacement by Colorless (Type 2) to Very Pale Green (Type 1a) Smectite

Plagioclase replacement by Type 1a saponite occurs frequently in the lower part of the hole. Plagioclase crystals directly in contact with or close to veins that are filled by colorless to very pale green saponite are often partly or completely replaced by the same mineral. This alteration progresses along cleavage planes and small cracks of the plagioclase crystals. The smectite is an iron saponite and has a chemical composition that ranges between Types 2 and 1a (Table 3). Plagioclase is replaced by very pale green saponite only, even when the adjacent vein is composed of orange iddingsite or K, Fe-rich bright green celadonite.

### Replacement by Zeolite

Plagioclase replacement by zeolites occurs in Core 35, Section 1 and Cores 37, 38, and 39 (from 528 to 569 m BSF) in a 1.5-mm-wide zone on both sides of the zeolitic veins. It is heterogeneous with respect to Si, Ca, and Al. The replacement of plagioclase by zeolite reflects the composition of the adjacent vein. When the latter is made up of thomsonite, analcime, or both zeolites, the plagioclase that occurs in adjacent rock is replaced by thomsonite (Fig. 7), analcime, or both zeolites, respectively. The microprobe analysis of a zeolite replacing a plagioclase phenocryst is reported in Table 8.

### Replacement of Pyroxene

Clinopyroxene is always completely fresh throughout the hole, except in Samples 504B-40-1, 37–39 cm; 504B-52-3, 103–107 cm; and 504B-58-1, 9–13 cm (from 573, 669, and 720 m BSF, respectively), where aegirine-augite reaction rims are observed on pyroxenes of the wall rocks of Ca-carbonate, Fe-saponite and, occasionally, talc veins (Laverne, this volume).

## VEINS

The mineralogy of veins is quite variable. A detailed description of the various mineral parageneses in veins from Hole 504B is beyond the scope of this initial report, but we shall describe the most common vein mineral associations. Alteration of host rocks adjacent to veins is related to the mineralogy of the veins, and both are related to depth.

### Veins above 584.5 m BSF

In the portion of the hole where red halos occur, most veins are less than 0.5 mm thick. They are usually made up of various combinations of iddingsitelike material (see analysis, Table 4), dark green Type 4 clay mineral (probably celadonite-nontronite; see analysis, Table 3), and pale green or olive brown Type 1 and 2 saponite (according to microprobe analyses and X-ray diffraction). Wherever all three alteration products coexist in a vein, iddingsitelike material or celadonite-nontronite occur at the vein walls, the saponite always at its center. An iddingsitelike vein may intersect and finally merge with a zeolite + saponite vein, indicating that the two types of veins formed during different stages (see next paragraph). The predominance of one alteration mineral over the others in a vein crossing alteration zones seems to be related to the location of the vein, or portion of the vein, with respect to alteration zonation. For instance, iddingsitelike material prevails or is the only vein component in portions of veins that crosscut or are adjacent to red halos. Celadonite-nontronite (dark green Type 4 clay mineral) or saponite (pale green Type 1, or olive brown Type 2) are more abundant in veins located in the outer or inner dark gray zones, respectively.

Minor amounts of aragonite, calcite, and phillipsite often occur, along with the clay minerals, in veins in the upper portion of Hole 504B. Phillipsite generally follows the clay minerals coating the vein walls and often precedes the carbonates; but the opposite case is also observed, as in Sample 504B-37-1, 19–22 cm.

### Zeolitic Veins

Zeolitic veins that range in thickness from 1 to 10 mm occur in Core 35 from 534.5 to 543.5 m BSF and in Cores 37 and 38 (i.e., from 552.5 to 570.5 m BSF). No zeolitic veins were found in Core 36. The veins consist primarily of various zeolites and apophyllite, with relatively minor pale green to olive green Type 1a and/or 2 saponite (according to X-ray diffraction and electron microprobe analysis). Minor calcite and rare iddingsitelike material also occur, even in veins in samples that do not exhibit red halos.

We identified by optics, X-ray diffraction, and/or electron microprobe analyses the following zeolites: analcime, natrolite, thomsonite, and possible mesolite. Apophyllite is also present. The most common mineral sequence in zeolitic veins is as follows, from the walls to the center of the vein: saponite, zeolites and apophyllite, and calcite. Iddingsitelike material seems to have crystallized before or just after the clay mineral, that is, early in the sequence. In some cases the zeolites appear to belong to another vein that formed later than and eventually merged with the vein containing the iddingsitelike material (as in Samples 504B-37-3, 49–52 cm and 504B-38-2, 48–50 cm). In Sample 504B-35-1, 126–130 cm, a zeolitic vein without iddingsitelike material occurs crossing a red halo rich in iddingsitelike material. All of these observations suggest that the iddingsitelike material and,

hence, the red halos formed before and independently of the zeolitic veins.

In a few veins, analcime appears to be the first mineral to have crystallized on vein walls; in others, analcime or a zeolite are intergrown with calcite and seem to have formed at the same time or to have continued crystallizing with the carbonate.

A thin vein with heulandite and chabazite was found (X-ray diffraction identifications) in Sample 504B-49-1, 69–70 cm (from 657 m BSF).

#### **Veins below 584.5 m BSF**

From 584.5 m BSF to the bottom of the hole, the most common veins are made up primarily of pale green to olive green saponite (Types 1 and/or 2). The saponite is often accompanied by variable amounts of pyrite, minor calcite, quartz, and rare talc. The amount of pyrite in the veins appears to increase with downhole depth. One large aragonite crystal was found in a saponitic vein in Sample 504B-44-2, 97–99 cm. All of these veins are thin, their thickness generally ranging from 0.05 to 3 mm, except for one that ranged from 3 to 6 mm.

Two other types of veins occur below 584.5 m BSF. Both are characterized by the presence of unusual minerals. The first special group comprises four veins up to more than 5 mm in thickness in which anhydrite is present in addition to the olive green saponite common to all veins below 584.5 m BSF. Such anhydrite-bearing veins were found in Samples 504B-43-2, 28–30 cm; 504B-48-3, 14–18 cm (which also contained abundant gyrolite and minor quartz); 504B-68-1, 12–14 cm; and 504B-69-1, 95–99 cm. Crystallization appears to have proceeded from the wall to the center of the vein, with crystallization of saponite, eventual quartz, and anhydrite intergrown with gyrolite.

The second group of special veins comprises the several veins that contain aegirine–augite at the vein walls. These veins are described in detail by Laverne (this volume). They occur in Sample 504B-40-1, 37–39 cm, where the aegirine–augite appears with melanite (a titanian andradite) and abundant Ca–carbonate; 504B-52-3, 103–107 cm, where it appears with talc; and 504B-58-1, 9–13 cm, where it appears with pyrite. All three veins are less than 1 mm thick and contain a dark green clay mineral with a chemical composition that electron microprobe analysis indicates to be probably a mixture or mixed-layer mineral. The crystallization sequence appears to be (1) aegirine–augite as a reaction rim on the wall rock clinopyroxene, (2) eventual melanite, (3) the green clay mineral, and (4) either Ca–carbonate or pyrite.

#### **PRIMARY VOID FILLINGS**

The fillings of vesicles and miarolitic voids are often zoned, and their mineralogical composition is complex.

The mineralogical composition of void fillings appears to be related to the alteration zonation of the host basalt and, hence, to depth. Iddingsitlike material and the dark green celadonite–nontronite (Type 4) occur frequently in void fillings between Cores 32 and 38, but they do not occur below Core 38, Section 2 (i.e., below 564 m BSF). On the other hand, the dark olive green

(Type 1b) and olive brown (Type 1c) saponite is very common in voids below 564 m BSF.

The most common mineral paragenesis observed in void fillings above 564 m BSF is as follows: iddingsitlike material forms the rim of the filling next to the void walls (see Table 4 for chemical composition). Next to the iddingsitlike material in the void is a dark green celadonite–nontronite (Type 4; see chemical composition in Table 3). A pale green to colorless, probably Type 1a or 2 saponite, forms the core of the filling. Calcium carbonates are rarely present at the center of the void fillings, and the dark green and/or colorless clay minerals are sometimes missing.

The zoning suggests that alteration occurred in two stages. In the first, an iddingsitlike material (probably a mixture of iron hydroxide and saponite) first precipitated in the void walls. This was followed by formation of the dark green celadonite–nontronite; olivine phenocrysts were partly replaced by iddingsite only.

In the altered wall rocks of the zeolitic veins in Core 37, Sections 1 and 2, various zeolites also make up the veins and replace wall rock plagioclase. They occur at the center of a few void fillings. In this zone, they seem to have formed during the first stage of alteration.

During the second stage, a Mg-rich, Fe, K-poor saponite filled the central parts of the vesicles and miarolitic voids and replaced olivine. A similar alteration sequence was observed in young pillow basalts drilled during Legs 54 and 70 (see Honnorez, 1981; Laverne and Vivier, in press). In Hole 504B, in a given sample, the dark green (Stage 2) clay mineral (Type 4) often occurs in void fillings only, providing the principal textural evidence that it formed later than other clay minerals. The other types of clay minerals also replace olivine phenocrysts as well as fill voids, indicating that they formed earlier.

Rather than supposing that alteration occurred in two stages, however, one can assume that the green nontronite precipitated first on the void walls and that it was followed by the colorless saponite. Later still, the portion of the green nontronite closest to the wall was transformed to iddingsitlike material by the addition of iron hydroxide. This may have occurred as a result of centripetal migration (diffusion) of oxidizing, Fe-rich solutions.

Below 564 meters BSF the most common void filling is made up of dark olive green (Type 1b) or olive brown (Type 1c) clay minerals, both probably saponites. Rarely, the saponites are close to the walls, with calcite appearing at the center.

The clay minerals in vesicles from the lowest part of the hole (i.e., from Cores 40 to 69) could be regular mixed-layer trioctahedral smectite–chlorite, but further detailed X-ray diffraction work is required to confirm this. A large (at least 10-mm-diameter) vug in Sample 504B-40-3, 130–135 cm is filled, from walls to center, by a trioctahedral green smectite, anhydrite, and calcite.

#### **THE SUCCESSION OF ALTERATION PROCESSES**

We have identified three zones of alteration in Hole 504B according to the downhole distribution of altera-

tion minerals and bulk altered rock chemistries (see below): an upper alteration zone from the sediment/base-ment interface down to 584.5 m BSF (i.e., down to Core 40, Section 3, inclusive), a lower alteration zone from 584.5 m BSF to the bottom of the hole at 835.5 m BSF, and a third alteration zone, the zeolitic zone, which overlaps the other two but is restricted primarily to the upper one between 534.5 and 570.5 meters BSF. (A single zeolitic vein occurs at 657 m BSF.)

The rocks from both the upper and lower alteration zones appear to have been altered by a succession of various processes, one of which could have simultaneously generated saponite throughout the hole.

The rocks from the upper alteration zone are characterized by the abundance of red halos occurring between dark gray cores and thin outer dark gray bands. The red color of the halos results from the replacement of olivine by iddingsite and the formation in veins and nearby portions of the rock of iddingsitelike material (i.e., a mixture of iron hydroxides and saponite). These minerals are accompanied by a minor amount of orange, Fe-rich (Type 3) clay mineral. The upper alteration zone is also characterized by the presence of celadonite and celadonite–nontronite (Type 4 and 5 clay minerals), which mainly precipitated in primary voids in the outer gray bands, and by phillipsite, aragonite, and minor calcite in veins crossing all of the color zones. Light-colored (Type 1a and 2) saponite has pervasively replaced olivine in all three of the color zones of the upper alteration zone. Saponite followed iddingsite and iddingsitelike material, but the relationship between celadonite–nontronite and saponite is unknown.

The basalts that form the upper alteration zone reflect the superimposed effects of successive alteration processes at low temperature. In the absence of evidence of replacement among alteration products, we assume that the spatial distribution of secondary minerals corresponds to their depositional sequence through time. Our description of the alteration sequence is provisional, however, and will have to be confirmed or invalidated by more detailed studies.

The first alteration process appears to be responsible for the common replacement of olivine crystals by iddingsite, the more rare filling of cracks and vesicles by iddingsitelike material and the crystallization even more rarely of orange clay minerals (Type 3). The alteration process results in the formation of the red halos characteristic of the upper alteration zone. Iddingsite and iddingsitelike material often are associated with clay minerals in the olivine pseudomorphs and void fillings, respectively, where they generally occupy an outer position, whereas saponite (Type 2 clay minerals) or more rarely the unidentified blue green clay mineral (Type 6) occupies a more central position. In the only observed case where celadonite (Type 5 clay mineral) accompanies iddingsite and saponite in an olivine pseudomorph in a red halo, iddingsite also occupies the peripheral position. Whenever iddingsitelike material is present in the outer dark gray bands (i.e., close to the outer limit of red halos), it is again in a peripheral position with respect to either saponite (Type 2), celadonite–nontronite

(Type 4), or celadonite (Type 5) in olivine pseudomorphs or vesicle fillings, respectively.

One must therefore conclude that iddingsite and iddingsitelike material crystallized first and were followed by saponite in the red halos and by either saponite, celadonite, or celadonite–nontronite in the dark gray outer bands. Hence, iddingsite and iddingsitelike vein fillings are ascribed to the first alteration stage of the upper alteration zone, whereas the other secondary minerals formed during later stages of alteration of this zone.

Farther away from the red halos, in the portions of the dark gray bands closest to the previously exposed surfaces, iddingsite is absent and olivine is often replaced by a light-colored clay mineral, probably a saponite, whereas the voids are filled by celadonite–nontronite (Type 5 clay mineral). The dark gray inner cores of the samples that display red halos have no iddingsitelike material (except crack fillings rooted in the red halos) and rarely contain nontronite–celadonite. The major alteration product is a saponite (Type 1a and 2 clay minerals).

Saponite appears to have pervasively invaded all of the rocks of the upper alteration zone regardless of their color zonation. On the other hand, celadonite–nontronite is mainly restricted to outer dark gray bands (i.e., to the color zones closest to the previously exposed surfaces). At this point in our study, it is very difficult to decide whether saponite crystallized before or after celadonite or celadonite–nontronite.

Previous studies of dredged and cored basalts (Honnorez, 1981 and unpublished data; Alt and Honnorez, in press; Laverne and Vivier, in press) have shown that celadonite–nontronite is the first secondary product to precipitate in the primary voids of zero age young submarine basalts, where it forms black halos parallel to exposed surfaces and cracks. It is soon followed by iron hydroxide and finally by saponite (at about 0.8 m.y. of age). On the other hand, no primary phase is affected until the crust is more than 1 m.y. old. Therefore, one cannot actually speak of “alteration” of basalts in the black halos. Alt and Honnorez (1981, in press) propose that both the nontronite–celadonite and Fe–hydroxides precipitated in the basalts when the very low-temperature reducing to anoxic hydrothermal solutions that carry Si and Fe mix with cold, oxygenated seawater and impregnate the uppermost basalts before their burial by a sediment cover. A similar clay mineral and iron oxides were found at various submarine locations interpreted as sites of recent or present day hydrothermal activity at or near the axis of spreading centers such as the Mid-Atlantic Ridge (FAMOUS [Franco-American Mid-Ocean Undersea Study] area Transform Fault A, Hoffert et al., 1978), the Red Sea (Bischoff, 1972), the Gulf of Aden (Cann et al., 1977), or the hydrothermal mounds south of the Galapagos Spreading Center (Honnorez, Von Herzen, et al., 1981). Black halos, celadonite–nontronite, and iron hydroxides are followed in older rocks by saponite, which replaces olivine phenocryst and fills up the primary spaces in the basalts beyond the black halos (Böhlke et al., 1980; Laverne and Vivier, in press). Therefore, our opinion is that celadonite and celadonite–

nontronite also crystallized before saponite in the rocks from the upper alteration zone of Hole 504B. However, we have no confirming evidence for this.

Finally, phillipsite and calcium carbonates (mainly aragonite with some Mg-calcite) are the last secondary minerals to have precipitated in the upper alteration zone. They are almost exclusively restricted to veins.

The lower alteration zone is deprived of any color zonation and is characterized by the presence of pyrite and saponite, which are progressively more abundant with depth. Pyrite occurs mainly in veins, with quartz and saponite (Type 1a and 1b) and calcite. The lower alteration zone also is characterized by an abundance of Type 1b saponite and opaque minerals, which replace olivine, and by the occurrence of mixtures or possibly irregular mixed-layer saponite-chlorite; more careful study is necessary to identify the latter minerals properly. The lower alteration zone is also characterized by the absence of iddingsite, iddingsitelike material, celadonite, celadonite-nontronite, phillipsite, and aragonite (only one occurrence reported at 607 m BSF). No potassic mineral was observed below 584.5 m BSF, indicating that only small amounts of seawater percolated down to the lower alteration zone. This is in good agreement with the low  $^{87}\text{Sr}/^{86}\text{Sr}$  ratios measured in bulk rocks from the same portion of the hole (Barrett, this volume).

In the lower alteration zone, the light green, Fe-poor saponite (Type 1a) evidently formed first, replacing the rims of olivine phenocrysts, whereas the dark green, Fe-rich saponite (Type 1b) later replaced the cores of these crystals. Similarly, the walls of the vesicles and cracks are lined with the same two types of saponite followed by calcite, quartz, and pyrite.

We note that the replacement of olivine by Type 1a saponite above was already common in dark gray cores of hand specimens from the upper alteration zone displaying color zonation (down to 536 m BSF). The main difference between the olivine pseudomorphs in the upper and lower alteration zones replaced by Type 1a saponite consists of a slight color difference in the clay mineral, which is pale green in the upper zone, whereas it is either pale green, or more often medium olive green, below Core 38, Section 1 (i.e., 571 m BSF and along the entire lower alteration zone). Moreover, Type 1a saponite generally is the only replacement product of olivine in the upper alteration zone, whereas it is almost always accompanied by Type 1b saponite in the olivine pseudomorphs of the lower alteration zone. This observation would support the working hypothesis that after a first alteration stage during which iddingsite and iddingsitelike material (i.e., mixtures of iron hydroxide and saponite) formed in the upper alteration zone only (possibly followed by the precipitation of celadonite-nontronite or celadonite during a second stage), saponite was the only clay mineral to precipitate through the entire section of the ocean crust drilled at Hole 504B.

The boundary between the upper and lower alteration zones is transitional, with celadonite-nontronite disappearing first at 548 meters BSF, then phillipsite at 557 meters BSF, and finally the red halos (+ iddingsite and iddingsitelike material) at 584.5 meters. One occurrence

of aragonite was observed below this boundary, whereas pyrite was observed twice above it. The transitional character of the boundary between upper and lower alteration zones is confirmed by the bulk rock chemistry of the freshest basalts samples (see also Hubberten et al., this volume).

The zeolitic zone is represented by veins superimposed on what we have described as the upper alteration zone, but which corresponds to the transition zone just mentioned, as evident in the bulk-rock chemistry. The veins contain minerals that are not otherwise found elsewhere in Hole 504B. The zeolitic zone veins occurring in the upper alteration zone are made up of saponites (Type 1a and/or 2) followed by various zeolites (analclime, natrolite, thomsonite, possibly mesolite, and an unidentified K-rich zeolite), apophyllite, and calcite, in order of precipitation from the walls to the center of the vein. The host rocks on both sides of the veins are discolored to a pale green because of the pervasive replacement of olivine and plagioclase by some of the same minerals as those forming the veins. In the lower alteration zone, there is one thin vein containing heulandite, chabazite, and saponite. We estimate, on the basis of petrographic observations, that zeolitic alteration was superimposed in a narrow interval in the upper alteration zone and in a much narrower interval in the lower alteration zone; that is, the vein minerals such as the zeolites (excluding phillipsite) and saponites (Types 1a and/or 2) precipitated in cracks later than the alteration products characterizing the two principal alteration zones.

Several special veins consisting mainly of Type 1a saponite were found in both the upper and lower alteration zones, but we did not find any evidence for assigning them to either of the principal alteration zones. Some of these veins were thin, with saponite nearest the walls and then quartz and anhydrite, with gyrolite or calcite at the center. Rarer veins were made up of saponite and calcium carbonate (probably calcite) and/or melanite and/or talc. The abundance of calcic minerals in all these veins as well as in the adjacent host rocks indicates that the hydrothermal solutions circulating along the cracks during this event were rich in calcium. Depending on the evolution of the solution chemistry, Ca-carbonates (high  $f_{\text{CO}_2}$ , but low  $a_{\text{Si}}$ ) or Ca-rich zeolites (high  $a_{\text{Si}}$ , low  $f_{\text{CO}_2}$ ) or other Ca-silicates such as gyrolite ( $\text{Ca}_2\text{Si}_3\text{O}_7[\text{OH}]_2 \cdot \text{H}_2\text{O}$ ) or apophyllite ( $\text{KC}_4\text{Si}_8\text{O}_{20}[\text{F}, \text{OH}] \cdot 8\text{H}_2\text{O}$ ), or anhydrite (high  $a_{\text{SO}_4}$  and low  $a_{\text{Si}}$  and  $f_{\text{CO}_2}$ ) would precipitate. The formation of these minerals was also probably facilitated by the increase in pH and the depletion in Mg and Al due to the precipitation of the salband saponite. The oxygen isotope analyses of the saponite from these veins, which we report in a later section, indicate that they probably precipitated between 60 and 110°C, depending on what  $\delta^{18}\text{O}$  value is assumed for seawater.

Olivine is the only primary mineral that is pervasively altered in the rocks of the upper alteration zone. Plagioclases and pyroxenes are usually fresh. On the other hand, in addition to olivine, which is always altered, plagioclase is often replaced by saponite in the lower alteration zone. Both olivine and plagioclase are perva-

sively replaced by various zeolites and smectites in the host rocks adjacent to the veins representing the zeolitic zone superimposed on the upper alteration zone. Clinopyroxene is only altered to aegirine-augite in the salbands of the veins containing saponite, Ca-carbonate, and/or melanite, and/or talc in the rocks of the lower alteration zone.

### BULK ROCK GEOCHEMISTRY

Changes in bulk rock chemistry that occurred as a result of the various seawater-basalt interactions were assessed by performing chemical analyses on 177 samples from Hole 504B. Twenty pairs or triplets of subsamples were isolated from large rock samples displaying color zonation (see section on alteration zonation). The bulk rock chemical compositions of the freshest looking (i.e., most uniformly dark gray) samples and subsamples from the inner portions of zoned samples (Hubberten et al., this volume) were compared with those of adjacent samples from nearby core fragments, subsamples of adjacent outer bands, and samples that are visibly altered and display colors ranging from red to green to dark gray.

The major advantage of studying the chemical changes due to alteration in Hole 504B instead of other DSDP holes stems from the relative compositional homogeneity of the tholeiites encountered. The tholeiites are homogeneous throughout the hole except in Lithologic Units 5 (Core 18 to Core 19, Section 2) and 36 (Core 54 to Core 57, Section 1) (Autio and Rhodes, this volume; Etoubleau et al., this volume; Hubberten et al., this volume).

Major elements were analyzed by the following techniques. Si, Ti, Al, Fe, Mn, Mg, Ca, K, Na, and P were determined by X-ray fluorescence analyses on fused glass beads of lithium metaborate (rock-to-flux ratio, 1:4) using a Philips PW 1450 computerized spectrometer and Philips "alphas" program. CO<sub>2</sub> and S were determined by colorimetric titration. H<sub>2</sub>O<sup>+</sup> was measured by Karl Fischer titration after the thermal decomposition of rock. Ferrous iron was measured by manganometric titration. The analytical data are presented in Table 9, and the bulk rock chemical analyses recalculated on a volatile-free basis are presented in Table 10.

Compared with the 43 electron microprobe analyses of fresh glasses from Hole 504B (Natland et al., this volume; see continuous lines in Figs. 13 and 14), all of the samples from the hole are altered, even those considered fresh by Hubberten et al. (this volume; see dotted lines in Figs. 13 and 14). Moreover, Figure 14 indicates that the oxidation ratio of all bulk rock samples (i.e., Fe<sup>3+</sup>/Fe<sup>T</sup>) are higher than the value characteristic of unaltered oceanic tholeiites (0.15). Other criteria used by various authors to distinguish altered oceanic basalts (see references in Honnorez, 1981), such as K<sub>2</sub>O and H<sub>2</sub>O<sup>+</sup> contents, do not always appear to be useful in the case of the Hole 504B basalts. Figures 13 and 15 perfectly illustrate this fact: the K<sub>2</sub>O content of most samples straddle the average fresh glass value below 584.5 meters BSF, even though these samples have Fe<sup>3+</sup>/Fe<sup>T</sup> ratios ranging

from 0.21 to 0.50 and H<sub>2</sub>O<sup>+</sup> contents between 0.61 and 2.51%, indicating that they experienced oxidative hydration.

When the H<sub>2</sub>O<sup>+</sup> contents of all the samples analyzed are plotted against Fe<sup>3+</sup>/Fe<sup>T</sup> (see Fig. 16), it is clear that most points representative of the upper and lower alteration zone rocks overlap. The samples with the highest water contents have only average values of Fe<sup>3+</sup>/Fe<sup>T</sup>, and they are equally distributed between the two zones. However, part of this overlap between the oxidation ratios could be ascribed to the postdrilling oxidation of saponite in the rocks from the lower alteration zone as demonstrated by Andrews et al. (this volume), because saponite is the major secondary mineral present in this portion of the hole. If this is true, the rocks from the lower alteration zone would be characterized by lower values of Fe<sup>3+</sup>/Fe<sup>T</sup> than rocks from the upper alteration zone. Indeed, the samples from the lower alteration zone have a tendency toward both low H<sub>2</sub>O<sup>+</sup> contents and low values of Fe<sup>3+</sup>/Fe<sup>T</sup>, whereas the samples from the upper alteration zone have the opposite relations. These contrasts correspond to the mineralogical distinction between the upper alteration zone, which is characterized by the presence of red halos (goethite with saponite) formed under oxic conditions, and the lower alteration zone, which is characterized by the abundance of pyrite forming under anoxic or suboxic conditions.

Nevertheless, unquestionable differences exist among the chemical trends of the samples belonging to the three alteration zones encountered in Hole 504B. Compared with the fresh glass average, the basalts from the upper alteration zone have slightly lower MgO and higher K<sub>2</sub>O contents, although other major oxides of the samples from the upper alteration zone have no trends. Subsamples from the red halos (squares in Figs. 13 and 14) are always distinctly enriched in K<sub>2</sub>O, and to a lesser extent FeO\*, compared with the adjacent dark gray inner counterparts (Fig. 13 and 14, squares and circles, respectively). Simultaneously, their H<sub>2</sub>O<sup>+</sup> content and Fe<sup>3+</sup>/Fe<sup>T</sup> values increase, whereas their SiO<sub>2</sub> content slightly decreases. The major element enrichment and the silica depletion correspond to the common replacement of olivine phenocrysts in the red halos by iddingsite (i.e., saponite-goethite mixtures) as opposed to saponite alone in the dark gray cores, or saponite and celadonite in the dark gray outer bands. No normalization of the chemical analyses to a relatively insoluble element such as Ti is required, because the TiO<sub>2</sub> content of almost all of the analyzed samples remains practically constant (see Table 10).

As mentioned earlier, the basalts from the lower alteration zone are characterized by a lack of K<sub>2</sub>O enrichment (only Samples 504B-48-1, 95-100 cm and 504B-42-1, 116-120 cm, have 0.16 and 0.11% K<sub>2</sub>O versus the 0.03% average of fresh glass; see Fig. 16). However, they display a definite trend toward MgO enrichment and a concomitant CaO and possibly Al<sub>2</sub>O<sub>3</sub> depletion, even though many samples are still very close to fresh glass average values in MgO and CaO contents. The other major element contents are unchanged in the lower alteration zone.

The changes in  $K_2O$  and  $MgO$  contents observed in the lower and upper alteration zones, respectively, are explained by the secondary mineral parageneses observed in these portions of the hole. The altered rocks from the upper alteration zone (i.e., above 584.5 m BSF) commonly contain potassic secondary minerals such as celadonite (Type 5 clay mineral), celadonite–nontronite mixture (Type 4 clay mineral), phillipsite, and (rarely) K-feldspar, which explain the altered rocks' tendency to be enriched in potassium. On the other hand, the rocks from the lower alteration zone (i.e., those below 584.5 m BSF) lack all of these secondary minerals but contain talc, increasing amounts of saponite with depth, and (toward the bottom of the hole) mixed-layer or mixtures of chlorite and saponite. These minerals produce the observed trend of progressively increasing  $MgO$  with depth.

Hubberten (this volume) and Hubberten et al. (this volume) demonstrate that the basalts from the portion of the hole higher than 544 meters BSF have lower sulfur contents than those from below this depth. According to these authors, the sulfur depletion would be due to a complete oxidation of the primary sulfides and the removal of sulfur as  $SO_4$  from samples analyzed from the upper portion of the hole, whereas sulfur remains in the lower portion of the hole as secondary pyrite as a result of the suboxic to anoxic conditions. On the other hand, the thallium content is higher in basalts from above 544 meters BSF than in those from below this limit (J. Erzinger, unpublished, in Hubberten et al., this volume) because  $Tl^{3+}$  is insoluble when it oxidizes and forms  $Tl(OH)_3$  under the oxic conditions prevailing in the upper portion of the hole. Thallium is soluble and therefore removed from the lower basalts because of the suboxic to anoxic conditions characterizing the alteration in the lower portion of the hole.

Hubberten (this volume) and Hubberten et al. (this volume) divided Hole 504B into upper and lower portions on the basis of bulk rock S and Tl contents. Their boundary is about 40 meters higher than the depth we call the limit between the upper and lower alteration zones. We do not know whether this 40-meter discrepancy is due to a sampling bias in one or more sets of data (this chapter, Hubberten [this volume], Hubberten et al. [this volume], and Noack et al. [this volume]) or whether it corresponds to a transition zone in which the more sensitive chemical elements such as S and Tl are already reacting to a change in alteration conditions and other, less sensitive elements and the secondary mineralogy are not. We favor the concept of a transition zone; some samples from below our 584.5-meter BSF limit (e.g., Samples 504B-42-1, 116–120 cm and 504B-48-1, 95–100 cm) have  $K_2O$  contents higher than the fresh glass average, some samples from above Hubberten's boundary at 544 meters BSF (e.g., Samples 504B-8-4, 120–123 cm and 504B-28-5, 14–17 cm) have high sulfur contents, and 28 samples from below this boundary have sulfur contents lower than the average for fresh basalts. Similarly, pyrite and marcasite were found above our 584.5-meter BSF limit (e.g., in Sample 504B-36-3,

27–39 cm), and iron oxides and even faint reddish halos were found below this limit (e.g., in Sample 504B-42-1, 116–126 cm, which has a higher  $K_2O$  content than fresh glass). A transition zone, if it exists, would span a few tens of meters and exhibit the mineralogical and chemical characteristics of both zones either simultaneously or, more likely, in alternation.

Finally, the zeolitic zone is clearly characterized in Figures 13 and 14 by significant increases in the  $MgO$ ,  $CaO$ , and, in one case,  $K_2O$  contents of the green host rocks (triangles in Figs. 13 and 14) adjacent to the veins. We have noted that the igneous minerals of these green salband rocks are pervasively replaced by the same minerals as those that form the veins, that is, mainly saponite (hence the  $MgO$  enrichments), calcic zeolites or gyrolite (hence, the  $CaO$  enrichments), analcime, and apophyllite (hence, the  $K_2O$  enrichments). These mineralogical changes are accompanied by increases in  $H_2O^+$  and  $CO_2$  contents and depletions in  $Al_2O_3$  and, in one case, in  $TiO_2$  (from 0.91 to 0.70% in the green salband of Sample 504B-37-1, 76–80 cm). None of the other major elements seems to be affected by the alteration that generated the zeolitic veins.

The differences between the chemical trends of the upper and lower alteration zones, and therefore the alteration mineralogy of the corresponding rocks, can be explained in terms of reaction temperatures, effective water–rock ratios, and the compositions of the altering solutions. The  $K_2O$  enrichments, increased  $^{87}Sr/^{86}Sr$  ratios, high thallium contents, and depletions in silica and sulfur of the upper alteration zone basalts (which are characterized by the presence of red halos, i.e., Fe oxides) indicate the effects of large volumes of oxygenated seawater reacting with the oceanic crust at low temperatures.

On the other hand, the trend toward  $MgO$  enrichment and concomitant depletions in  $CaO$  and possibly  $Al_2O_3$  of the basalts from the lower alteration zone as well as their low  $^{87}Sr/^{86}Sr$  ratios, low thallium contents, and the abundance in pyrite and absence of red halos (Fe-oxides) could be interpreted either as the result of alteration at low water–rock ratios under suboxic to anoxic conditions or as reactions between basalts and evolved seawater solutions, that is, solutions derived from seawater that subsequently lost the chemical characteristics of unaltered seawater because of reactions with the ocean crust. The lack of potassium enrichment, and the thallium depletion, the increased  $MgO$  contents, and the decreased  $CaO$  contents of the lower alteration zone basalts could as well be explained as the result of basalt–seawater interaction at high temperature, that is, at least  $150^\circ C$  (Seyfried and Bischoff, 1979), although the temperature effects may have been obscured by the low water–rock ratios. However, the oxygen isotope analyses of the isolated secondary minerals from these rocks (see following section) indicate that they formed at temperatures ranging from  $60$  to  $110^\circ$ , depending on the  $\delta^{18}O$  value ascribed to the solution. This temperature range almost exactly corresponds to the present

Table 9. Bulk rock chemical analyses.

Component	Gray Core	Red Halo	Gray Core	Red Halo	Red Halo <sup>a</sup>	Gray Core	Red Halo <sup>b</sup>	Red Halo <sup>c</sup>	Gray Core	Red Halo	Gray Core	Red Halo
Sample Interval (cm) Piece	504B-33-1 (12-14) 182	504B-33-1 (31-37) 185	504B-33-1 (77-80) 192	504B-33-1 (77-80) 192	504B-33-1 (77-80) 192	504B-34-1 (7-19) 219	504B-34-1 (7-19) 219	504B-34-1 (7-19) 219	504B-36-3 (22-24) 318	504B-36-3 (22-24) 318	504B-36-3 (37-39) 320	504B-36-3 (37-39) 320
SiO <sub>2</sub>	49.50	49.80	48.90	49.40	49.40	49.30	49.60	49.60	49.90	49.0	50.00	49.50
TiO <sub>2</sub>	0.91	0.91	0.89	0.92	0.90	0.90	0.94	0.94	0.97	0.88	0.87	0.88
Al <sub>2</sub> O <sub>3</sub>	16.00	15.90	15.80	15.90	16.10	15.70	15.40	15.60	15.50	15.80	15.60	15.50
Fe <sub>2</sub> O <sub>3</sub>	3.32	2.91	3.49	2.70	3.56	3.79	3.18	3.73	3.58	3.17	4.36	4.62
FeO	5.74	5.81	5.76	5.68	5.40	5.50	5.77	5.43	5.39	5.64	5.84	5.98
MnO	0.16	0.14	0.16	0.15	0.16	0.15	0.15	0.16	0.16	0.16	0.18	0.19
MgO	8.58	8.37	8.55	8.44	8.35	8.36	8.56	8.37	8.49	8.32	7.89	8.32
CaO	13.00	13.10	13.00	13.20	13.20	13.00	12.80	12.90	13.10	13.00	13.00	13.00
Na <sub>2</sub> O	2.13	2.47	2.37	2.27	2.43	2.43	2.34	2.45	2.41	2.45	2.29	2.37
K <sub>2</sub> O	0.11	0.02	0.04	0.02	0.05	0.10	0.03	0.08	0.08	0.01	0.12	0.02
P <sub>2</sub> O <sub>5</sub>	0.08	0.07	0.07	0.07	0.07	0.07	0.07	0.07	0.08	0.05	0.06	0.05
H <sub>2</sub> O <sup>+</sup>	0.86	0.75	0.95	0.72	0.78	0.86	0.79	0.85	0.85	0.53	0.71	0.51
CO <sub>2</sub>	0.11	0.13	0.26	0.24	0.19	0.29	0.20	0.19	0.34	0.09	0.75	0.11
Total	100.49	100.38	100.24	99.71	100.59	100.45	99.83	100.37	100.55	100.00	100.67	100.17
Fe <sup>3+</sup> +Fe <sup>T</sup>	0.34	0.31	0.35	0.30	0.37	0.38	0.33	0.38	0.37	0.34	0.40	0.32
FeO*	8.77	8.47	9.00	8.21	8.63	8.94	8.74	8.84	8.66	8.54	9.84	8.87

<sup>a</sup> Farther from core.<sup>b</sup> Upper portion.<sup>c</sup> Lower portion.<sup>d</sup> Farther from zeolitic vein.<sup>e</sup> Adjacent to zeolitic vein.

Table 9. (Continued).

Sample Interval (cm) Piece	504B-42-2 (24-28) 661	504B-42-2 (59-61) 667	504B-43-1 (63-65) 679	504B-43-2 (44-46) 697	504B-43-2 (44-46) 697	504B-48-1 (95-100) 870	504B-48-3 (20-23) 894	504B-48-3 (23-25) 895	504B-49-2 (94-96) 947	504B-49-2 (101-103) 947	504B-54-1 (139-42) 1062	504B-54-1 (48-63) 1063	504B-59-1 (57-63) 1252
SiO <sub>2</sub>	49.30	49.20	49.60	49.40	49.30	49.30	50.30	49.80	49.40	49.60	49.70	49.10	49.40
TiO <sub>2</sub>	0.90	0.85	0.88	0.87	0.87	0.99	0.99	0.99	0.84	0.89	1.36	1.32	0.98
Al <sub>2</sub> O <sub>3</sub>	16.00	15.70	15.30	15.60	15.20	14.50	15.00	15.00	16.20	16.10	15.30	14.90	15.40
Fe <sub>2</sub> O <sub>3</sub>	3.17	3.25	2.80	3.09	3.28	4.02	3.42	3.18	2.94	3.64	3.22	4.24	3.10
FeO	5.75	5.74	6.84	6.27	6.31	6.86	6.26	7.04	5.84	5.25	5.58	5.29	6.15
MnO	0.17	0.15	0.15	0.16	0.16	0.15	0.20	0.18	0.16	0.16	0.18	0.17	0.18
MgO	8.21	8.54	8.51	8.45	8.87	8.85	8.50	8.43	8.22	8.30	8.15	8.39	8.36
CaO	13.10	13.00	12.90	13.10	12.70	10.40	12.70	12.80	13.30	13.10	12.40	12.10	12.90
Na <sub>2</sub> O	2.42	2.18	2.25	2.15	2.25	2.07	2.47	2.21	3.34	2.77	2.53	2.62	2.22
K <sub>2</sub> O	0.04	0.02	0.01	0.02	0.02	0.16	0.05	0.02	0.03	0.06	0.04	0.04	0.02
P <sub>2</sub> O <sub>5</sub>	0.05	0.06	0.06	0.06	0.05	0.06	0.07	0.07	0.06	0.06	0.15	0.16	0.07
H <sub>2</sub> O <sup>+</sup>	0.85	1.06	0.75	0.81	1.03	2.51	0.66	0.61	0.61	0.65	0.86	0.90	0.82
CO <sub>2</sub>	0.13	0.14	0.08	0.11	0.14	0.17	0.19	0.11	0.13	0.22	0.17	0.81	0.14
Total	100.09	99.89	100.13	100.09	100.18	100.04	100.81	100.44	100.07	100.80	99.64	100.04	99.74
Fe <sup>3+</sup> +Fe <sup>T</sup>	0.33	0.34	0.27	0.31	0.32	0.34	0.33	0.29	0.31	0.34	0.34	0.42	0.31
FeO*	8.68	8.78	9.43	9.13	9.35	10.77	9.34	9.93	8.54	9.05	9.05	8.61	9.37

range of temperatures in Hole 504B: 59°C (measured at the sediment/basement interface) and 125°C (inferred at the bottom of the hole) (Becker et al., this volume).

### OXYGEN ISOTOPE GEOCHEMISTRY

Table 11 presents the  $\delta^{18}\text{O}$  values in isolated secondary minerals that were identified by X-ray diffraction.

The partition coefficients of analcime are unknown, but what we know of smectites requires the trioctahedral smectites (saponite) from the lower part of Hole 504B to have formed at relatively high temperatures (90–110°C), if a 0‰ value is assumed for seawater (Yeh and Savin, 1977). The formation temperature of the smectite would be 60°C if one assumes the –4‰ value of the overlying sediment pore waters (Mottl, Lawrence et al., 1980).

Forty bulk rock oxygen isotope analyses are reported in Table 12 and plotted versus depth in Figure 14. Seventeen values by Barrett and Friedrichsen (this volume) are also shown in Figure 14. The  $\delta^{18}\text{O}$  values obtained by Barrett and Friedrichsen range from 6.4 to 7.8‰ for the upper 260 meters of the hole, that is, down to 534.5 meters BSF; from 6.2 to 6.4‰ in the interval from 534.5

to 594.5 meters BSF; and from 5.8 to 6.2‰ below 594.5 meters BSF. On the other hand, our 40 measurements range from 6.1 to 12.7‰ without any downhole trend. Moreover, three of the samples corresponding to host rocks adjacent to zeolitic veins display  $\delta^{18}\text{O}$  values from 9.2 to 12.7‰. Such unusually large enrichments in  $^{18}\text{O}$  of young basalts agree with the petrographic observation concerning these samples that igneous plagioclase and olivine pseudomorphs are replaced by some of the same minerals that form the veins (see Table 8). Finally, one sample from the uppermost portion of the hole (Sample 504B-21-2, 54–59 cm) also has a high  $\delta^{18}\text{O}$  value (12.0‰) even though it is not adjacent to one of the zeolitic veins.

### CONCLUSIONS

Hole 504B, which was drilled into the 5.9 m.y. old crust of the southern flank of the Costa Rica Rise, tapped a hydrothermal system at its conductive or near-conductive stage (Langseth et al., this volume; Becker et al., this volume). All of the samples studied, whether in thin section, by X-ray diffraction, electron microprobe, or

Table 9. (Continued).

504B-36-3 (83-85) 324	Light Gray <sup>d</sup>	Light Green <sup>e</sup>	Light Gray <sup>d</sup>	Light Green <sup>e</sup>	504B-37-2 (94-96) 377	504B-39-2 (62-64) 488	504B-39-3 (123-125) 495	Light Gray <sup>d</sup>	Light Green <sup>e</sup>	504B-40-4 (73-75) 567	504B-42-1 (9-11) 642	504B-42-1 (116-120) 656
	504B-37-1 (76-80) 352	504B-37-1 (94-96) 355	504B-40-3 (130-135) 558									
50.10	49.50	48.50	48.30	46.70	49.10	49.60	49.30	48.50	47.40	49.10	49.20	48.90
0.92	0.90	0.65	0.92	0.93	0.88	0.87	0.81	0.76	0.62	0.77	0.91	0.88
15.20	15.00	8.50	14.30	10.70	15.20	16.10	16.30	17.90	17.20	16.50	15.70	15.00
2.46	3.11	3.99	3.35	4.38	2.56	2.66	2.20	3.02	3.52	1.94	3.13	4.19
7.24	6.31	4.03	6.14	6.09	6.36	6.47	6.49	5.02	3.83	6.52	5.74	5.88
0.16	0.17	0.11	0.16	0.16	0.16	0.15	0.15	0.21	0.18	0.14	0.17	0.18
8.40	8.31	9.39	8.66	9.17	8.10	8.04	8.44	7.42	8.70	9.09	8.54	9.32
12.80	12.80	13.20	12.70	14.20	13.80	13.20	13.20	13.70	14.00	13.20	12.80	12.00
2.11	2.44	2.56	2.65	2.83	2.27	2.37	2.05	2.14	2.27	1.96	2.40	2.32
0.01	0.16	1.60	0.21	0.23	0.23	0.01	0.02	0.01	0.12	0.01	0.04	0.11
0.06	0.05	0.05	0.05	0.07	0.06	0.07	0.06	0.04	0.04	0.05	0.06	0.05
0.51	0.76	6.01	2.54	4.58	0.61	0.61	0.91	0.82	1.47	0.77	1.12	1.44
0.10	0.89	1.96	0.49	0.81	0.46	0.10	0.08	0.28	0.96	0.08	0.11	0.18
100.07	100.40	100.55	100.47	100.85	99.79	100.25	100.01	99.82	100.31	100.07	99.92	100.45
0.23	0.31	0.47	0.33	0.39	0.27	0.27	0.23	0.35	0.45	0.21	0.33	0.34
9.50	9.22	8.23	9.39	10.51	8.77	8.90	8.55	7.84	7.15	8.33	8.67	9.75

Table 9. (Continued).

504B-60-1 (9-14) 1255	504B-61-2 (12-15) 1299	504B-61-2 (33-38) 1302	504B-62-1 (105-109) 1327	504B-62-1 (112-118) 1328	504B-62-2 (5-8) 1332	504B-62-2 (13-18) 1333	504B-64-3 (63-68) 1447	504B-64-3 (93-98) 1451	504B-70-1 (36-41) 1562	504B-70-2 (0-3) 1563	504B-70-2 (12-16) 1564
49.90	49.80	49.60	48.90	48.50	49.50	49.90	49.30	49.70	49.80	49.20	49.30
0.98	1.01	0.98	1.04	1.00	1.01	0.98	0.99	0.90	0.88	0.90	0.90
14.50	15.30	15.00	15.80	14.80	14.80	14.60	14.70	15.30	15.10	15.40	15.30
3.39	3.84	4.41	4.20	4.65	4.24	4.35	5.75	2.91	3.77	3.41	3.01
6.00	6.35	5.35	5.94	5.08	5.39	5.19	5.07	6.79	5.31	5.85	6.29
0.14	0.18	0.17	0.18	0.17	0.17	0.18	0.13	0.17	0.17	0.18	0.17
9.41	7.79	8.62	7.03	9.55	8.93	8.97	9.02	8.29	9.46	8.73	8.90
12.20	13.10	12.50	13.60	11.60	12.10	11.80	11.40	12.80	12.70	12.80	12.80
2.32	2.06	2.19	2.17	2.04	2.03	1.99	2.18	2.11	2.12	2.12	2.12
0.04	0.01	0.01	0.02	0.02	0.01	0.02	0.01	0.01	0.01	0.01	0.01
0.07	0.08	0.07	0.08	0.08	0.09	0.07	0.06	0.07	0.05	0.06	0.06
1.12	1.08	1.36	1.02	1.63	1.34	1.27	1.33	0.62	1.36	1.00	0.89
0.39	0.12	0.33	0.12	0.53	0.22	1.37	0.23	0.13	0.27	0.14	0.09
100.46	99.72	100.59	100.10	100.65	99.83	100.69	100.17	99.80	100.00	99.80	99.84
0.34	0.32	0.43	0.39	0.45	0.41	0.43	0.50	0.28	0.42	0.39	0.30
9.15	9.96	9.42	9.81	9.50	9.36	9.28	10.39	9.50	9.26	8.85	9.09

X-ray fluorescence, are altered. They contain secondary minerals both as olivine replacements and as fillings of primary voids, cracks, and vesicles. Saponite is ubiquitous in the samples studied. All of the analyzed samples have higher  $H_2O^+$  contents and  $Fe^{3+}/Fe^T$  values than fresh oceanic tholeiites. However, part of this higher bulk rock  $Fe^{3+}/Fe^T$  value may be due to the post-drilling oxidation of saponite (Andrews et al., this volume).

Three more or less overlapping alteration zones were encountered along the 561-meter length of the basement hole. At the sediment/basement interface the measured temperature is 59°C; at the bottom of the hole the temperature is inferred to be 125°C. The upper alteration zone is characterized by red halos because of the abundance of iddingsite pseudomorphs after olivine. The halos comprise dark gray inner portions and outer bands, the latter being generally adjacent to veins or other formerly exposed surfaces. Bulk rock analyses show that the red halos have higher  $H_2O^+$  and  $K_2O$  contents and  $Fe^{3+}/Fe^T$  values, but lower  $SiO_2$  contents, than the adjacent inner dark gray rocks. No other major-element

changes are noticed. The part of the dark gray outer bands adjacent to the red halos often contains mixtures of iddingsite and celadonite or celadonite-nontronite. Farther away from the red halos, the dark gray outer bands contain only celadonite or celadonite-nontronite and saponite. The dark gray rocks from the upper alteration zone (excluding the outer bands adjacent to red halos) usually do not contain iddingsite, but various types of saponites are common both as void fillings and as olivine pseudomorphs. Igneous plagioclase and clinopyroxene are almost always unaltered. Veins in the upper alteration zone are made up of saponites and celadonite-nontronite, with occasional iddingsite, phillipsite, aragonite, or calcite. Dark gray rocks from the upper alteration zone are often richer in  $H_2O^+$ ,  $K_2O$ , and thallium, and have higher values of  $Fe^{3+}/Fe^T$  and  $^{87}Sr/^{86}Sr$ , than their counterparts from the lower alteration zone. They also appear to be depleted in sulfur and silica. These changes in bulk rock composition correspond to the abundance of potassic secondary minerals and of olivine replacements by iddingsite (i.e., goethite-saponite mixtures) or various saponites, as well as the

Table 10. Bulk rock chemical analyses recalculated on a volatile-free basis.

Component	Gray Core	Red Halo	Gray Core	Red Halo	Red Halo <sup>a</sup>	Gray Core	Red Halo <sup>b</sup>	Red Halo <sup>c</sup>	Gray Core	Red Halo	Gray Core	Red Halo	
Sample Interval (cm) Piece	504B-33-1 (12-14) 182	504B-33-1 (31-37) 185	504B-33-1 (77-80) 192	504B-33-1 (77-80) 192	504B-33-1 (77-80) 192	504B-34-1 (7-19) 219	504B-34-1 (7-19) 219	504B-34-1 (7-19) 219	504B-36-3 (22-24) 318	504B-36-3 (22-24) 318	504B-36-3 (37-39) 320	504B-36-3 (37-39) 320	
SiO <sub>2</sub>	49.73	50.05	49.43	49.99	49.59	49.64	50.18	49.93	49.92	50.21	49.39	50.23	49.80
TiO <sub>2</sub>	0.91	0.91	0.90	0.93	0.90	0.90	0.95	0.95	0.98	0.88	0.88	0.96	0.88
Al <sub>2</sub> O <sub>3</sub>	16.07	15.98	15.97	16.29	16.16	15.81	15.58	15.70	15.60	15.90	15.72	15.57	14.99
Fe <sub>2</sub> O <sub>3</sub>	3.34	2.92	3.53	2.73	3.57	3.82	3.22	3.75	3.60	3.19	4.39	3.18	4.65
FeO	5.77	5.84	5.82	5.75	5.42	5.54	5.84	5.47	5.42	5.67	5.89	6.01	5.95
MnO	0.16	0.14	0.16	0.16	0.16	0.15	0.15	0.16	0.16	0.16	0.18	0.17	0.19
MgO	8.62	8.41	8.64	8.54	8.38	8.42	8.66	8.43	8.54	8.37	7.95	8.36	7.99
CaO	13.06	13.16	13.14	13.36	13.25	13.09	12.95	12.99	13.18	13.08	13.10	13.06	13.08
Na <sub>2</sub> O	2.14	2.48	2.39	2.30	2.44	2.45	2.37	2.47	2.42	2.46	2.31	2.38	2.32
K <sub>2</sub> O	0.11	0.02	0.04	0.02	0.05	0.10	0.03	0.08	0.08	0.01	0.12	0.02	0.04
P <sub>2</sub> O <sub>5</sub>	0.08	0.07	0.07	0.07	0.07	0.07	0.07	0.07	0.08	0.05	0.06	0.06	0.05
Total	99.99	99.98	100.09	100.14	99.99	99.99	100.00	100.00	99.98	99.98	99.99	100.00	99.99
Fe <sup>3+</sup> /Fe <sup>T</sup>	0.34	0.31	0.35	0.30	0.37	0.38	0.33	0.38	0.37	0.34	0.40	0.32	0.41
FeO*	8.77	8.47	9.00	8.21	8.63	8.98	8.74	8.84	8.66	8.54	9.84	8.87	10.13

<sup>a</sup> Farther from core.<sup>b</sup> Upper portion.<sup>c</sup> Lower portion.

Table 10. (Continued).

Sample Interval (cm) Piece	504B-42-2 (59-61) 667	504B-43-1 (63-65) 679	504B-44-3 (44-46) 697 697	504B-48-1 (95-100) 870	504B-48-3 (20-23) 894	504B-48-3 (23-25) 895	504B-49-2 (94-96) 947	504B-49-2 (101-103) 947	504B-54-1 (39-42) 1062	504B-54-1 (48-63) 1063	504B-59-1 (51-63) 1252	504B-60-1 (9-14) 1255	504B-61-2 (12-15) 1299
SiO <sub>2</sub>	49.90	49.90	49.80	49.80	50.60	50.3	49.90	49.70	49.90	50.40	49.90	50.40	49.50
TiO <sub>2</sub>	0.86	0.89	0.88	0.88	1.02	0.99	0.99	0.85	0.98	1.38	1.34	0.99	1.03
Al <sub>2</sub> O <sub>3</sub>	15.90	15.40	15.70	15.40	14.90	15.00	16.30	14.50	15.50	15.20	15.60	14.70	15.50
Fe <sub>2</sub> O <sub>3</sub>	3.29	2.82	3.12	3.31	4.13	3.42	2.96	3.39	3.27	4.31	3.14	3.43	3.90
FeO	5.82	6.89	6.32	6.37	7.05	6.26	5.88	6.00	5.67	5.38	6.23	6.06	6.45
MnO	0.15	0.15	0.16	0.16	0.15	0.20	0.18	0.16	0.14	0.18	0.17	0.18	0.18
MgO	8.65	8.57	8.52	8.96	9.09	8.50	8.45	8.28	9.41	8.26	8.53	8.46	7.91
CaO	13.20	13.00	13.20	12.80	10.70	12.70	13.40	12.20	12.60	12.30	13.10	12.30	13.30
Na <sub>2</sub> O	2.21	2.27	2.18	2.27	2.13	2.47	2.22	2.36	2.32	2.57	2.66	2.25	2.09
K <sub>2</sub> O	0.02	0.01	0.02	0.02	0.16	0.05	0.02	0.03	0.04	0.04	0.04	0.04	0.01
P <sub>2</sub> O <sub>5</sub>	0.06	0.06	0.06	0.05	0.06	0.07	0.06	0.07	0.15	0.16	0.07	0.07	0.08
Total	100.06	99.96	99.96	100.02	99.9	99.96	99.88	99.98	98.95	100.02	99.99	100.04	99.98
Fe <sup>3+</sup> /Fe <sup>T</sup>	0.34	0.27	0.31	0.32	0.34	0.33	0.29	0.31	0.34	0.34	0.42	0.31	0.34
FeO*	8.78	9.43	9.13	9.35	10.77	9.34	9.93	8.54	9.05	8.61	9.26	9.15	9.96

oxidation of primary sulfides. We interpret the upper alteration zone to be the result of low-temperature alteration by large amounts of seawater percolating through the upper ocean crust.

The lower alteration zone is characterized by the lack of color zonation (the rocks have a uniform or mottled dark gray color), a downward-increasing abundance of pyrite and very pale green to dark olive green saponites, and the presence of talc, quartz, and calcite. Fe-oxides, celadonite, celadonite-nontronite mixtures, aragonite, and phillipsite are generally absent. Chlorite also occurs toward the bottom of the hole. Olivine phenocrysts are replaced by fairly light-colored olive green saponite, and plagioclase and clinopyroxene are essentially unaltered. The numerous veins in the lower alteration zone are generally made up of saponite and pyrite, with minor amounts of calcite, talc, and quartz. The rocks from the lower alteration zone have a slight tendency to lower H<sub>2</sub>O<sup>+</sup> contents and Fe<sup>3+</sup>/Fe<sup>T</sup> values than the rocks from the upper alteration zone, but the dark gray basalts from both zones have essentially overlapping ranges of values for H<sub>2</sub>O<sup>+</sup> content and Fe<sup>3+</sup>/Fe<sup>T</sup>. The lower alteration zone basalts are enriched in K<sub>2</sub>O with respect to the fresh glasses, but much less so than the rocks from the upper alteration zone. However, they display a definite downhole enrichment in MgO and depletion in

CaO and possibly Al<sub>2</sub>O<sub>3</sub>. Nevertheless, most samples from the lower alteration zone have contents of these three major oxides close to those of fresh glass. They also usually have higher sulfur but lower thallium contents than the dark gray rocks from the upper alteration zone. Finally, their <sup>87</sup>Sr/<sup>86</sup>Sr value is similar to that of the average East Pacific Rise basalts. The alteration in the lower alteration zone appears to result from suboxic to anoxic reactions between oceanic basalts and small amounts of solutions that may be at higher temperatures than those prevalent in the upper alteration zone. The presence of chlorite toward the bottom of the hole is evidence of the higher temperatures. However, the low water-rock ratio, which is inferred from the lack of increase in K<sub>2</sub>O contents and <sup>87</sup>Sr/<sup>86</sup>Sr values, obscures the effects of higher temperatures. Therefore, some of the chemical changes observed in the rocks from the lower alteration zone could have resulted from reactions of oceanic basalts with evolved seawater, that is, the solution derived from seawater after the seawater reacted with the oceanic crust.

The upper and lower alteration zones overlap each other by a few tens of meters, essentially between 544 and 584.5 meters BSF (the latter depth corresponding to the deepest recovered red halo). In this transition zone alternating bulk rock samples display the chemical char-

Table 10. (Continued).

504B-36-3 (83-85) 324	Gray Core	Green Halo	Gray Core	Green Halo	504B-37-2 (94-96) 377	504B-39-2 (62-64) 488	504B-39-3 (123-125) 495	Gray Core	Red Halo	504B-40-4 (73-75) 567	504B-42-1 (9-11) 642	504B-42-1 (116-120) 656	504B-42-2 (24-28) 661
	504B-37-1 (76-80) 352	504B-37-1 (94-96) 355	504B-40-3 (130-135) 558										
50.37	50.13	52.39	49.57	48.92	49.74	49.83	49.79	49.10	48.40	49.50	49.90	49.50	49.70
0.92	0.91	0.70	0.94	0.97	0.89	0.87	0.82	0.77	0.63	0.78	0.92	0.89	0.91
15.28	15.19	9.18	14.67	11.21	15.40	16.20	16.50	18.10	17.60	16.60	15.90	15.20	16.10
2.47	3.15	4.31	3.43	4.59	2.59	2.67	2.22	3.06	3.60	1.96	3.17	4.24	3.20
7.28	6.39	4.35	6.30	6.38	6.44	6.50	6.55	5.09	3.91	6.57	5.82	5.95	5.80
0.16	0.17	0.12	0.16	0.17	0.16	0.15	0.15	0.21	0.18	0.14	0.17	0.18	0.17
8.45	8.41	10.14	8.89	9.61	8.20	8.08	8.52	7.52	8.89	9.16	8.65	9.43	8.28
12.87	12.96	14.26	13.03	14.87	13.48	13.30	13.33	13.90	14.30	13.30	13.00	12.10	13.20
2.12	2.47	2.76	2.72	2.96	2.30	2.38	2.07	2.17	2.32	1.98	2.43	2.35	2.44
0.01	0.16	1.73	0.21	0.24	0.23	0.01	0.02	0.01	0.12	0.01	0.04	0.11	0.04
0.06	0.05	0.05	0.05	0.07	0.06	0.07	0.06	0.04	0.04	0.05	0.06	0.05	0.05
99.99	99.99	99.99	99.97	99.99	99.99	100.06	100.03	99.97	99.99	100.05	100.06	100.00	99.89
0.23	0.31	0.47	0.33	0.39	0.27	0.27	0.23	0.35	0.45	0.21	0.33	0.39	0.33
9.50	9.22	8.23	9.39	10.51	8.77	8.90	8.55	7.84	7.15	8.33	8.67	9.75	8.68

Table 10. (Continued).

504B-61-2 (33-38) 1302	504B-62-1 (105-109) 1327	504B-62-1 (112-118) 1328	504B-62-2 (5-8) 1332	504B-62-2 (13-18) 1333	504B-64-2 (63-68) 1447	504B-64-2 (93-98) 1451	504B-70-1 (36-41) 1562	504B-70-2 (0-3) 1563	504B-70-2 (12-16) 1564
50.20	49.40	49.70	50.40	50.90	50.00	50.20	49.60	49.90	49.87
0.99	1.05	1.03	1.03	1.00	1.00	0.91	0.89	1.34	0.91
15.20	16.00	15.20	15.10	14.90	14.90	15.40	15.40	15.20	15.48
4.46	4.24	4.77	4.31	4.44	5.83	2.94	3.83	4.31	3.04
5.41	6.00	5.21	5.48	5.29	5.14	6.86	5.40	5.38	6.36
0.17	0.18	0.17	0.17	0.19	0.13	0.17	0.17	0.17	0.17
8.72	7.10	9.80	9.09	9.15	9.15	8.37	9.62	8.53	9.00
12.60	13.70	11.90	12.30	12.00	11.60	12.90	12.90	12.30	12.95
2.21	2.19	2.09	2.07	2.03	2.21	2.13	2.16	2.66	2.14
0.01	0.02	0.02	0.01	0.02	0.01	0.01	0.01	0.04	0.01
0.07	0.08	0.08	0.09	0.07	0.06	0.07	0.05	0.16	0.06
100.04	99.96	99.97	100.05	99.99	100.03	99.96	100.03	99.99	99.99
0.43	0.39	0.45	0.41	0.43	0.50	0.28	0.39	0.42	0.30
9.42	9.89	9.50	9.36	9.28	10.39	9.50	8.85	9.26	9.09

acteristics of either zone. The characteristics of both the upper and lower alteration zones are found in different samples from the transition zone, and no samples have intermediate properties. For instance, their  $H_2O^+$  contents and  $Fe^{3+}/Fe^T$  values completely overlap.

The zeolite veins forming the zeolitic zone occur primarily between 528.5 and 563 meters BSF. Hence, the zeolitic zone essentially coincides with the lower part of the upper alteration zone, but one could consider it to be included in the transition between the upper and lower alteration zones. The zeolitic veins are made up, from the vein walls to the center, of saponite followed by various Ca- and/or Na-zeolites (including analcime, natrolite, thomsonite, and possibly mesolite), apophyllite, and calcite. We assigned saponite-heulandite-chabazite veins observed at 657 meters BSF to the zeolitic zone because, like other veins in the zeolitic zone, it is formed of zeolites that do not occur anywhere else in the hole. From 549.5 to 553 meters BSF, the host rock adjacent to the zeolitic veins exhibits a light purplish to green color due to the pervasive replacement of olivine, plagioclase, and clinopyroxene by some of the same minerals that form the veins. These intensive replacements of the igneous minerals in the green salbands resulted in significant increases in the bulk rock  $K_2O$ ,  $MgO$ ,  $CaO$ ,  $CO_2$ , and  $H_2O^+$  contents,  $\delta^{18}O$  and  $Fe^{3+}/Fe^T$  ratios, whereas

they were depleted in  $Al_2O_3$  and, in one case,  $TiO_2$ . The abundance of calcic minerals in these veins and the adjacent host rocks indicates that the solution circulating along the open fissures had high Ca activity. The types of calcium-bearing minerals, carbonates, silicates, or sulfate that precipitated depended on the solution chemistry: high  $f_{CO_2}$  but low Si activity would favor carbonate formation; conversely, high Si activity and low  $f_{CO_2}$  would favor the precipitation of zeolite, gyrolite, or anhydrite (if K were also present). Finally, anhydrite would form when the solutions were rich in  $SO_4$  but poor in silica and  $CO_2$ . The oxygen isotope analyses of the mineral from these veins indicate that they probably formed at 60 or 110°C, depending on the  $O^{18}$  value assumed for the solutions. This range of probable temperatures during alteration closely corresponds to temperatures measured at the top of the basement and bottom of Hole 504B, that is, 59 and 125°C.

In both the upper and lower alteration zones, there are several veins containing saponite next to walls and quartz + anhydrite + gyrolite ± calcite in the centers. There are also rare veins of saponite, calcium carbonate (calcite?), and/or melanite and/or talc. In these veins the wall rock clinopyroxene is fringed along the vein with aegirine-augite or fassaite. We found no evidence to assign them to the zeolitic zone except that they also

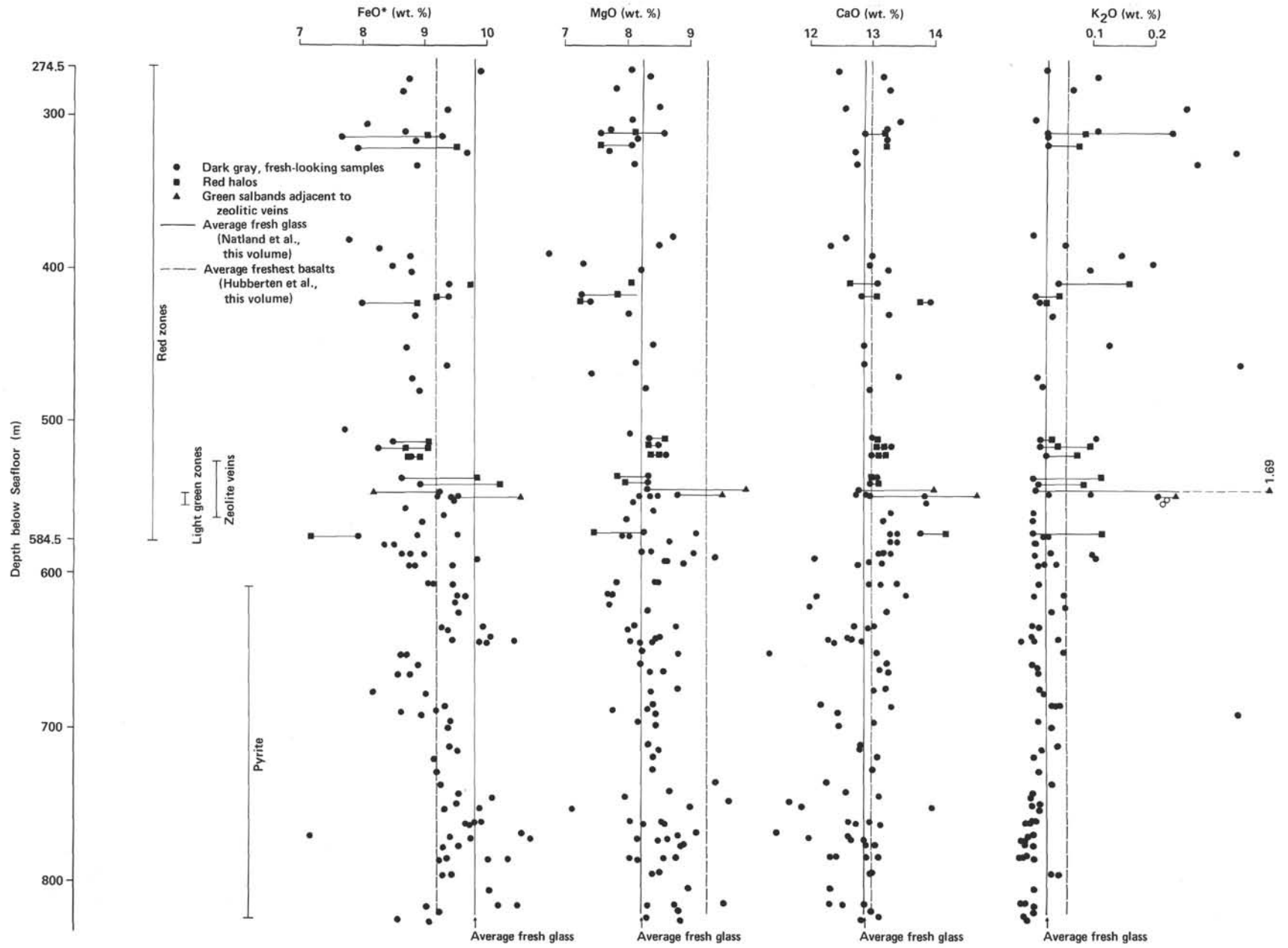


Figure 13. Downhole variations of bulk rock chemical composition with respect to FeO total, MgO, CaO, and K<sub>2</sub>O contents compared to distribution of the upper alteration zone (red zones), lower alteration zone (pyrite), and the zeolitic zone (zeolitic veins and light green zones).

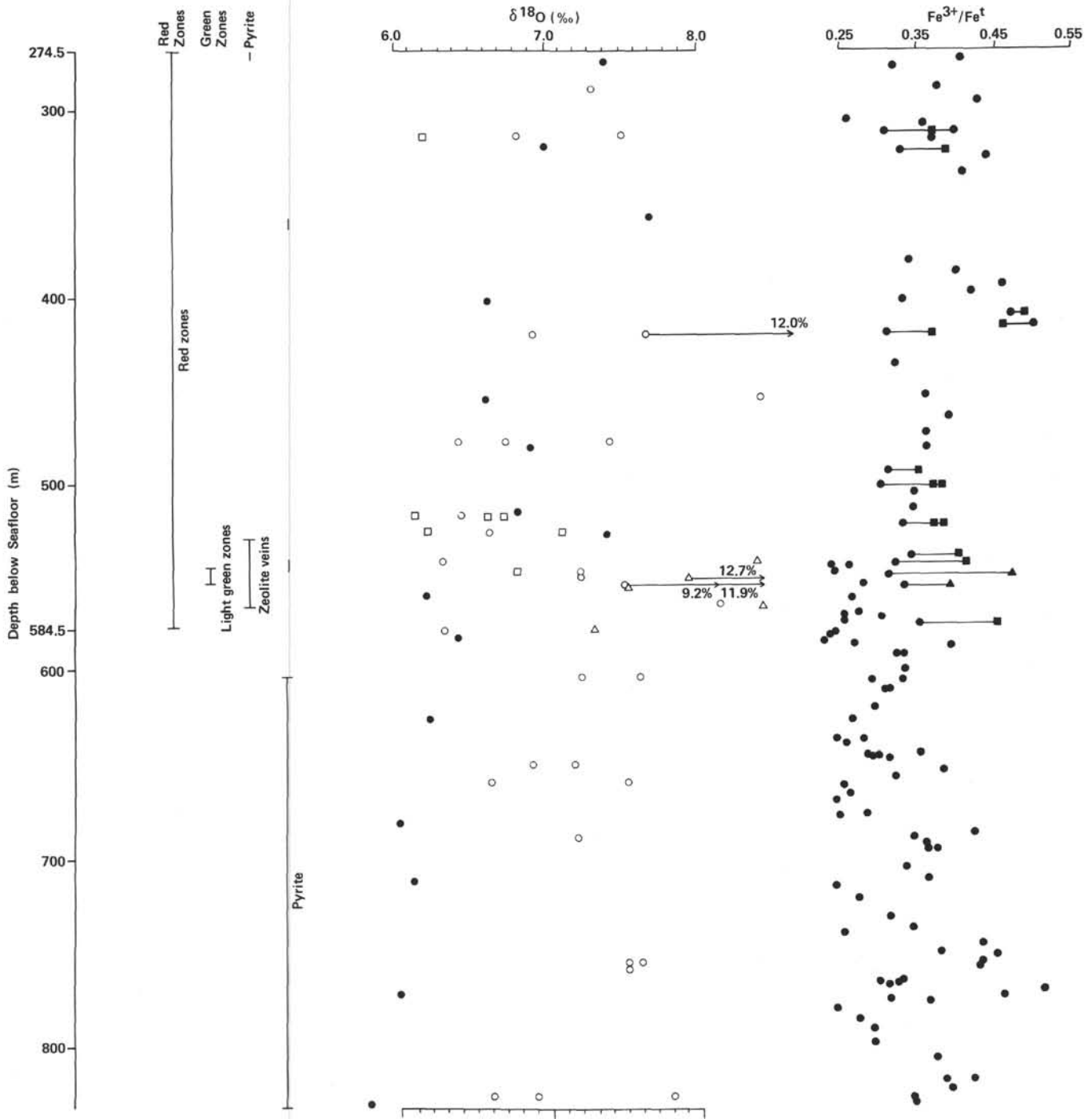


Figure 14. Downhole variations of bulk rock oxygen isotope geochemistry (open circles are  $\delta^{18}\text{O}$  measured in our samples, full circles  $\delta^{18}\text{O}$  values from Barrett and Friedrichsen, this volume) and bulk rock oxidation ratio,  $\text{Fe}^{3+}/\text{Fe}^{\text{T}}$  (legend as in Fig. 13).

all contain calcium-rich minerals, either carbonates, silicates, or sulfate.

From petrographic evidence, it appears that iddingsite, iddingsitelike material, and the orange Type 3 clay minerals formed first in the red halos of the upper alteration zone, where they were followed by a pale green, Fe-poor saponite (Type 2). The same saponite formed simultaneously in the dark gray inner portions of samples with halos and in unzoned samples from the upper alter-

ation zone. A similar Fe-poor saponite (Type 1a) replaced the rims of olivine phenocrysts in the uniformly colored rocks from the lower alteration zone, where it was followed by another, slightly different-looking and Fe-rich (Type 1b) saponite. Again, the first mineral (after occasional iddingsitelike material) to have precipitated on the vein walls from the upper and lower alteration zones and the zeolitic zone is also a green saponite (Type 1a, 1b, or very rarely 1c). It seems, therefore, that after

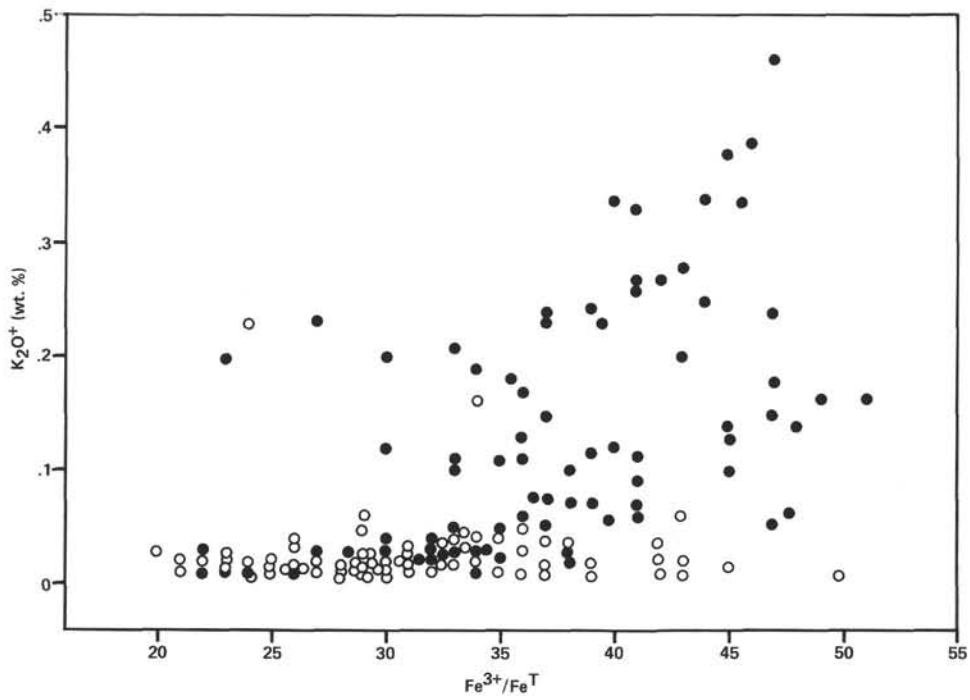


Figure 15. K<sub>2</sub>O<sup>+</sup> content versus Fe<sup>3+</sup>/Fe<sup>T</sup> of bulk rocks. Black and white circles correspond to samples from above and below 584.5 m BSF, respectively.

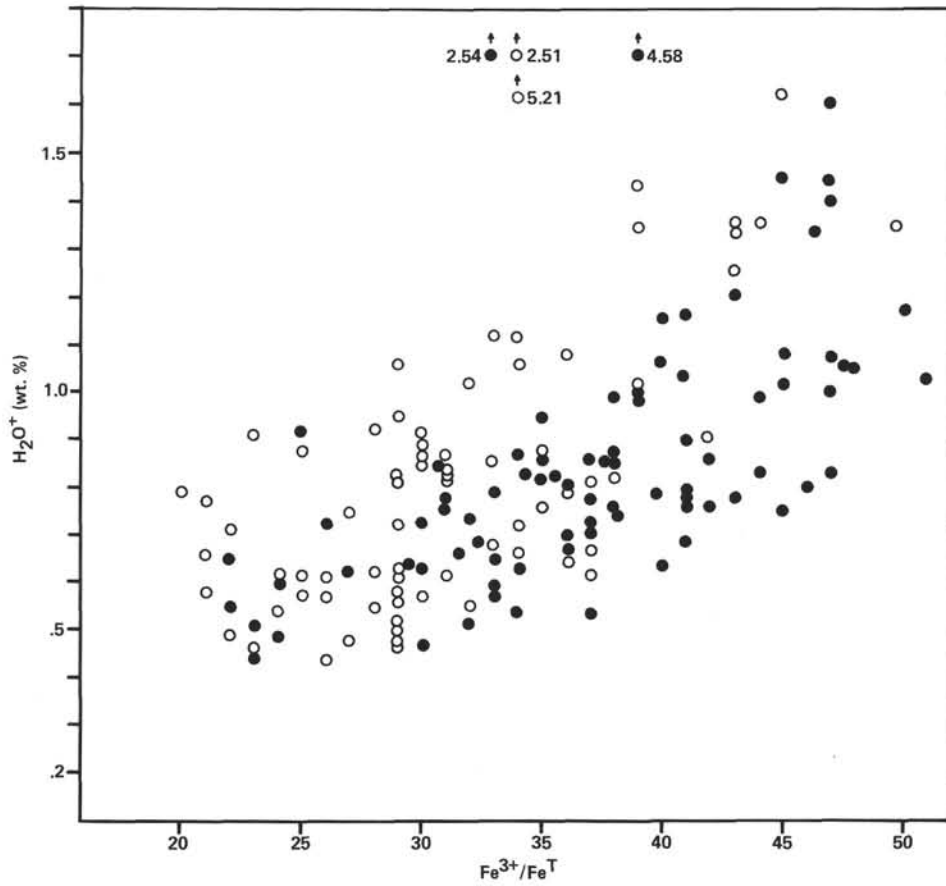


Figure 16. H<sub>2</sub>O<sup>+</sup> content versus Fe<sup>3+</sup>/Fe<sup>T</sup> of bulk rocks. Same legend as in Figure 15.

Table 11.  $\delta^{18}\text{O}$  values in isolated mineral samples.

Sample	$\delta^{18}\text{O}$ (‰) <sup>a</sup>
Sample 504B-37-1, 76–80 cm	
Analcime	17.8
Trismectite	11.2
Salband	12.7
Sample 504B-37-1, 94–96 cm	
Analcime	18.2
Trismectite	13.4
Salband	11.9
Sample 504B-48-3, 14–18 cm	
Trismectite	13.2

<sup>a</sup> K. Muehlenbachs, analyst.

iddingsite more or less completely replaced the olivine phenocrysts and iddingsitelike material precipitated in a few voids and cracks and, hence, formed the red halos of the upper alteration zone, saponites exhibiting various intensities of green and with various Fe-contents precipitated in all of the rocks of Hole 504B. In the dark gray outer bands of the upper alteration zone, saponite would have formed simultaneously with celadonite or a celadonite–nontronite mixture, but no evidence was found to indicate whether saponite crystallized before or after the celadonite. Finally, aragonite (or calcite) + phillipsite were the last secondary minerals to crystallize, mainly as crack fillings, in the upper alteration zone, and calcite or quartz + pyrite precipitated last in the veins and pyrite in the basalts of the lower alteration zone. Petrographic evidence indicates that the vein zeolites and associated minerals of the zeolitic zone formed later than the secondary minerals of the upper alteration zone. Similarly, the thin vein with heulandite and chabazite formed later than those of the lower alteration zone.

One could imagine a simple but purely hypothetical model. Early after the emplacement of the basalts on the seafloor, the outer black bands formed along the exposed surfaces of the rock fragments as a result of the precipitation of celadonite and iron oxide from low temperature hydrothermal solutions; then cold, oxygenated seawater percolated down through the uppermost ocean crust and reacted with the basalts. During this seawater-dominated alteration at low temperature, iddingsite replaced the olivine phenocrysts, and iddingsitelike material lined the veins and vugs nearby. As a consequence, the red halos appeared down to 584.5 meters BSF. Thereafter, only evolved solutions, that is, seawater depleted in oxygen, potassium, and radiogenic strontium, reacted with the basalts located deeper than 584.5 meters BSF or with the portion of the upper basalts beyond the red halos. This later alteration process was rock dominated (low water–rock ratios), and it took place under suboxic to anoxic conditions. The reaction temperature was probably higher at greater depths. Finally (possibly quite recently), hydrothermal solutions circulated along newly formed fissures, where the Ca- and/or Na-zeolites, calcite, and gyrolite of the zeolitic zone precipitated. The fact that the alteration temperatures inferred from isolated secondary minerals coincide with the tem-

Table 12.  $\delta^{18}\text{O}$  data.

Sample Number (interval in cm)	Mineral Color, Location	$\delta^{18}\text{O}$ (‰) <sup>a</sup>
504B-5-2, 15–20	Gray	7.3
8-2, 45–52	Gray core	6.8
8-2, 45–52	Red halo	6.2
8-2, 45–52	Yellow rim	7.5
21-2, 54–59	Yellow rim	12.0
21-2, 54–59	Red halo	6.9
25-1, 34–38	Gray	8.4
28-4, ?	Gray	7.4
28-5, 14–17	Gray	6.4
33-1, 31–37	Gray core	6.9
33-1, 31–37	Red halo	6.6
33-1, 77–80	Gray core	6.4
33-1, 77–80	Red halo	6.7
33-1, 77–80	Red halo, farther away from core	6.1
34-1, 7–19	Gray core	6.6
34-1, 7–19	Upper red halo	7.1
34-1, 7–19	Lower red halo	6.2
36-3, 22–24	Gray core	7.2
36-3, 22–24	Red halo	6.8
36-3, 37–39	Gray core	6.8
36-3, 37–39	Red halo	6.8
37-1, 76–80	Light gray, farther away zeolitic vein	7.2
37-1, 76–80	Light green, adjacent to zeolitic vein	12.7
37-1, 94–96	Light gray, farther away from zeolitic vein	9.2
37-1, 94–96	Light green, adjacent to zeolitic vein	11.9
40-3, 130–135	Light gray, farther away from zeolitic vein	6.3
40-3, 130–135	Light green, adjacent to zeolitic vein	7.3
43-2, 44–46	Dark gray	7.2
43-2, 44–46	Dark gray	7.6
48-3, 14–18	Dark gray, adjacent to anhydrite + 3 smectite veins	7.2
48-3, 23–25	Dark gray	6.9
49-2, 101–103	Dark gray	6.6
49-2, 101–103	Dark gray	7.5
54-1, 39–42	Dark gray	7.2
62-1,	Dark gray	7.5
62-1, 112–118	Dark gray	7.6
62-2, 5–8	Dark gray	7.5
70-1, 36–41	Dark gray	6.9
70-2, 0–3	Dark gray	6.6
70-2, 12–16	Dark gray	7.8

<sup>a</sup> K. Muehlenbachs, analyst.

peratures measured at the top of the basement and at the bottom of the hole does not imply that the alteration processes are still operating in Hole 504B. One must keep in mind that similar solutions could have formed deeper than the lower alteration zone, in the greenschist facies domain, for example, and migrated upward into the upper crust. These then could have percolated horizontally as part of a large horizontal cell, forming the restricted occurrences of zeolites in Hole 504B.

## ACKNOWLEDGMENTS

We thank Jeffrey Alt for help with the mineral identifications by X-ray diffraction.

C. L. thanks Ferard Bocquier, Henri Bougault, and Gérard Vivier for having provided the use of their laboratories. She also thanks

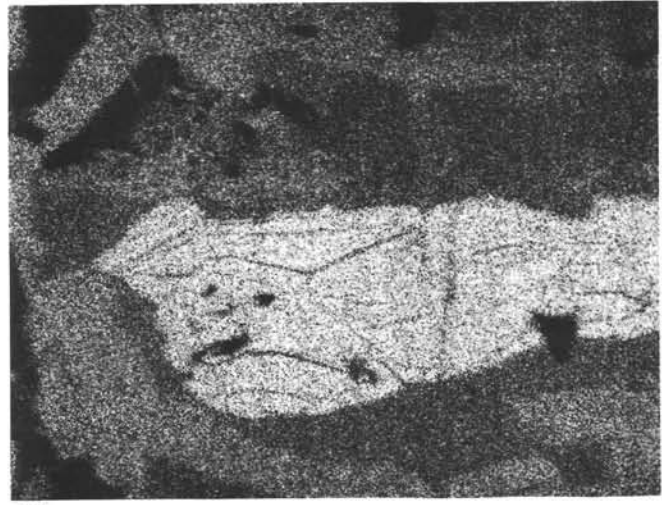
Marcel Bohn for his help during the electron microprobe analyses carried out at CNEXO, Brest (France).

This research was supported by U.S.A. N.S.F. Grant OCE-8117698 to J. H. and a F.R.G. D.F.G. grant to H. H. and R. E. as well as contributions from Rosenstiel School of Marine and Atmospheric Science, University of Miami.

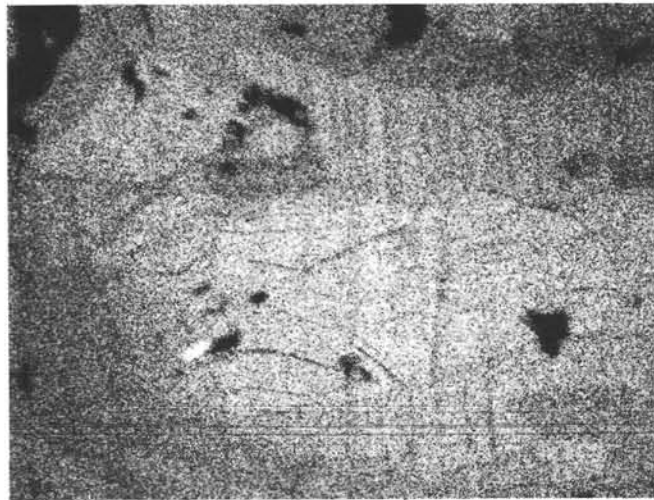
Jeffrey Alt and James Natland reviewed the manuscript. The comments of Peter Rona are also appreciated.

#### REFERENCES

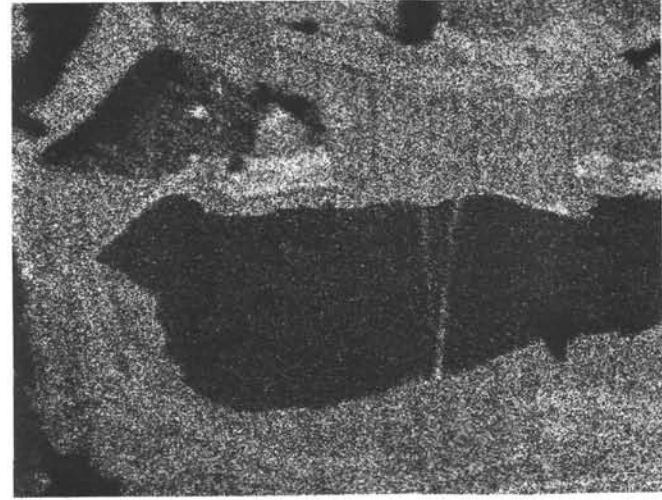
- Alt, J. C., in press. Alteration of the upper oceanic crust: DSDP Site 417. II. Bulk rock chemical and oxygen isotopic effects. *J. Geophys. Res.*
- Alt, J. C., and Honnorez, J., 1981. A model for the aging of the upper oceanic layer 2 at low temperature. GSA Annual Meeting, Cincinnati. (Abstract)
- , in press. Alteration of the upper oceanic crust: DSDP Site 417. I. Petrographic and mineralogic studies. *J. Geophys. Res.*
- Andrews, A. J., 1980. Saponite and celadonite in layer 2 basalts, DSDP Leg 37. *Contrib. Mineral. Petrol.*, 73:323-340.
- Bass, M. N., 1976. Secondary minerals in oceanic basalts with special reference to Leg 34, DSDP. In Yeats, R. S., Hart, S. R., et al., *Init. Repts. DSDP*, 34: Washington (U.S. Govt. Printing Office), 393-431.
- Bischoff, J. L., 1972. A ferroan nontronite from the Red Sea geothermal system. *Clay and Clay Mineral.*, 20:217-223.
- Böhlke, J. K., Honnorez, J., and Honnorez-Guerstein, B.-M., 1980. Alteration of basalts from Site 396B, DSDP: Petrographic and mineralogic studies. *Contrib. Mineral. Petrol.*, 73:341-364.
- Buckley, H. A., Bevan, J. C., Brown, K. M., Johnson, L. R., and Farmer, V. C., 1978. Glauconite and celadonite: two separate mineral species. *Mineral. Mag.*, 42:373-382.
- Cann, J. R., Winter, C. K., and Pritchard, R. G., 1977. A hydrothermal deposit from the floor of the Gulf of Aden. *Mineral. Mag.*, 41:173-199.
- Hoffert, M., Perseil, A., Hekinian, R., Choukroune, P., Needham, H. P., Francheteau, J., and LePichon, X., 1978. Hydrothermal deposits sampled by diving saucer in Transform Fault "A" near 37°N on the Mid-Atlantic Ridge FAMOUS area. *Oceanologica Acta*, 1:73-86.
- Honnorez, J., 1981. The aging of the oceanic crust at low temperature. In Emiliani, C. (Ed.), *The Sea* (Vol. 7): New York (John Wiley and Sons), 525-587.
- Honnorez, J., Von Herzen, R. P., and Leg 70 Scientific Party, 1981. Hydrothermal mounds and young ocean crust of the Galapagos: preliminary deep sea drilling results, Leg 70. *Geol. Soc. Am. Bull.*, 92:457-472.
- Laverne, C., and Vivier, G., in press. Petrographical and chemical study of basement from the Galapagos Spreading Center, Leg 70. In Honnorez, J., Von Herzen, R. P., et al., *Init. Repts. DSDP*, 70: Washington (U.S. Govt. Printing Office).
- Mottl, M. J., Bender, M. L., Lawrence, J. R., Anderson, R. N., Hart, S. R., and Shipboard Scientific Party, 1980. Hot formation waters sampled from basement in the oceanic crust, IPOD Hole 504B. *Eos*, 61:995. (Abstract)
- Seyfried, W. E., and Bischoff, J. L., 1979. Low temperature alteration by seawater: an experimental study at 70°C and 150°C. *Geochim. Cosmochim. Acta*, 43:1937-1947.
- Seyfried, W. E., Shanks, W. C., and Dibble, W. E., 1978. Clay mineral formation in DSDP Leg 34 basalts. *Earth Planet. Sci. Lett.*, 41: 265-276.
- Wilshire, H. G., 1958. Alteration of olivine and orthopyroxene in basic lavas and shallow intrusions. *Am. Mineralogist*, 43:120-147.
- Yeh, H-W., and Savin, S. W., 1977. Mechanism of burial metamorphism of argillaceous sediments: 3. O-isotope evidence. *Geol. Soc. Am. Bull.*, 88:1321-1330



Mg



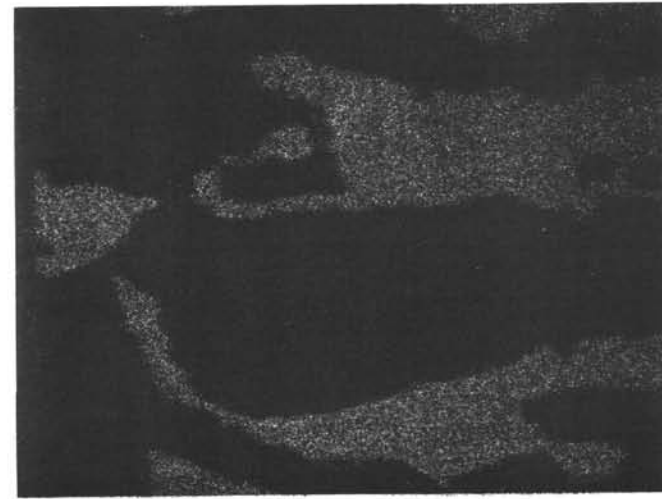
Si



Fe

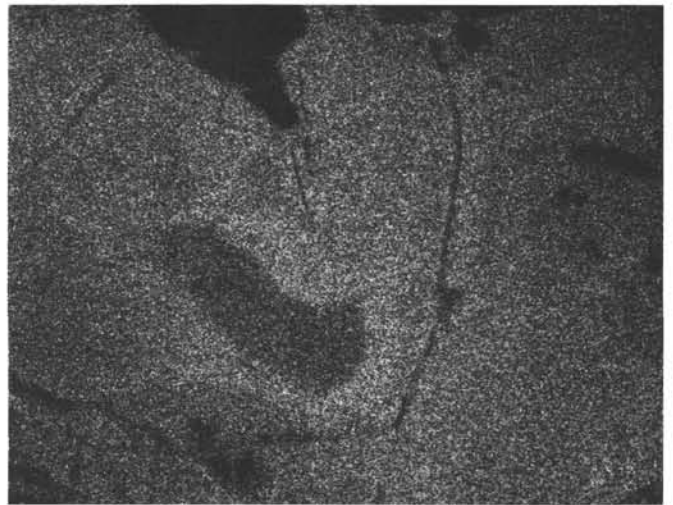
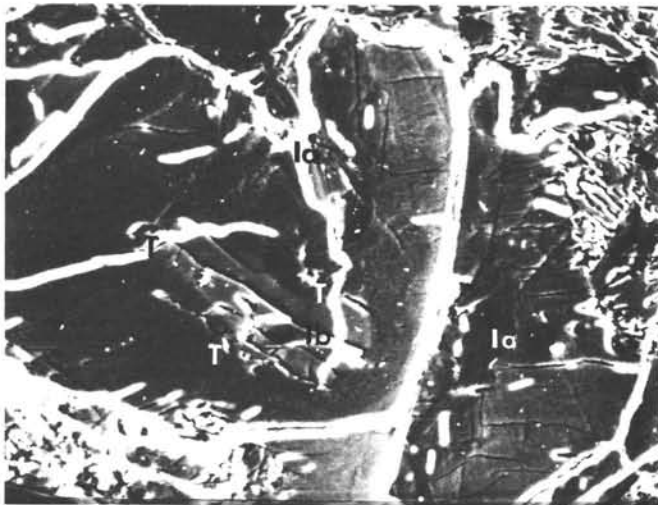


Al

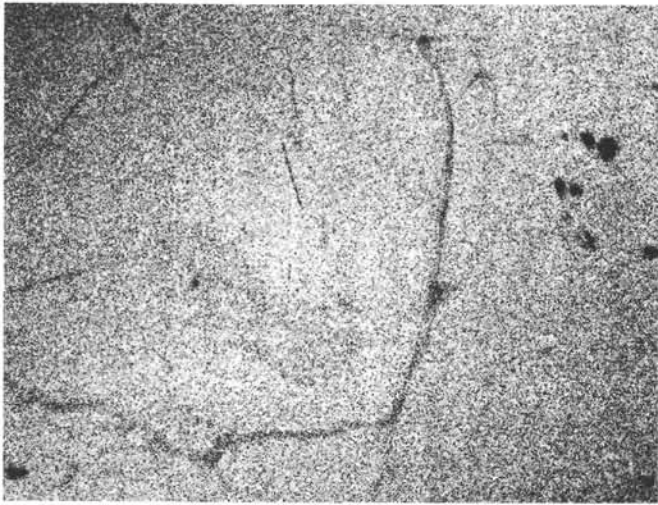


K

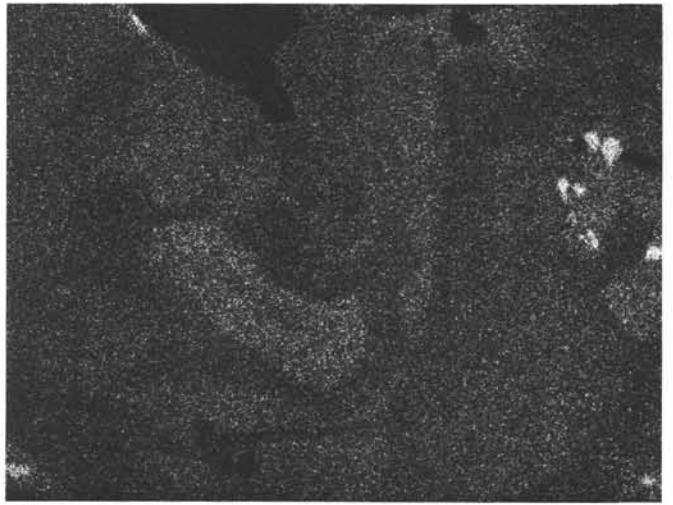
Plate 1. X-ray scanning photographs of olivine replacement products in Sample 504B-33-1, 69–73 cm (from about 517 m BSF). 2, colorless Type 2 saponite; 5, bright green Type 5 celadonite; Id, iddingsite; Pl, probably plagioclase. Magnification 400 $\times$ .



Mg



Si



Fe

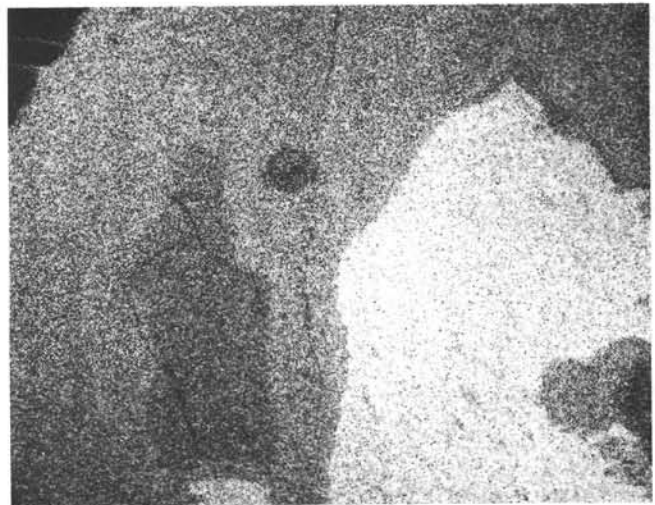
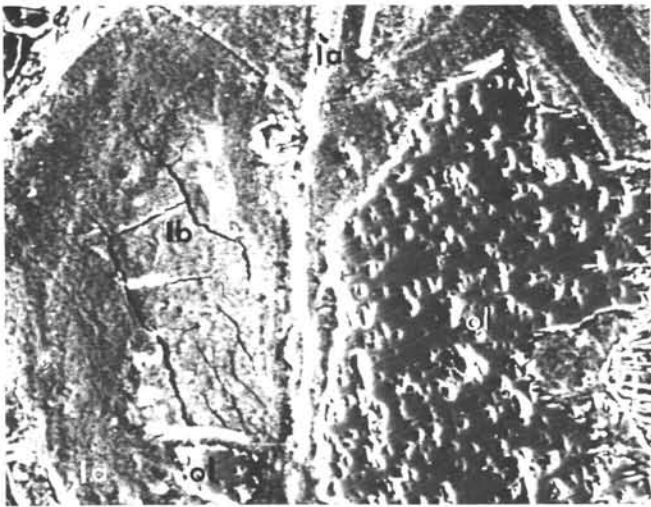


Al

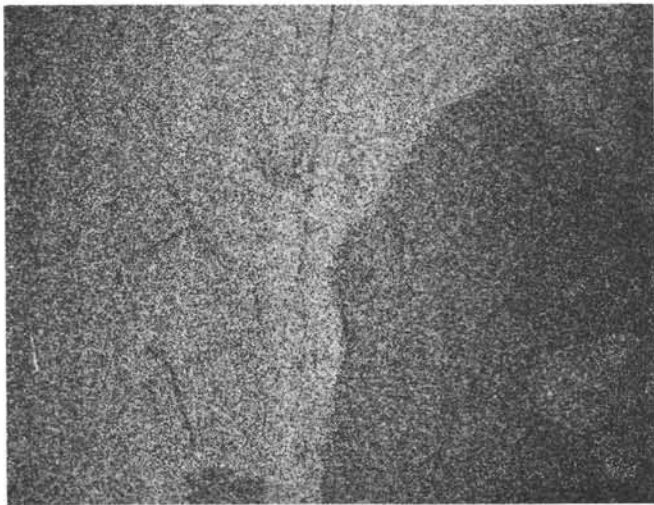


Ca

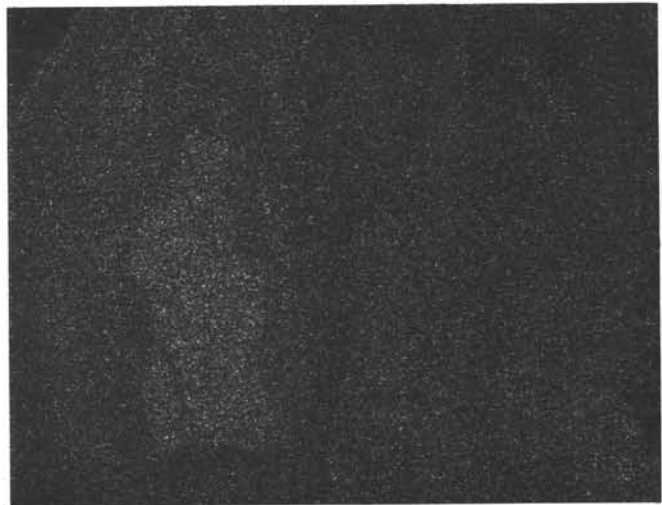
Plate 2. X-ray scanning photographs of olivine replacement products in Sample 504B-63-4, 7-10 cm (from about 772 m BSF). 1a, pale olive green Type 1a saponite; 1b, dark olive green Type 1b saponite; T, saponite transitional between Types 1a and 1b. Magnification 400 $\times$ .



Mg



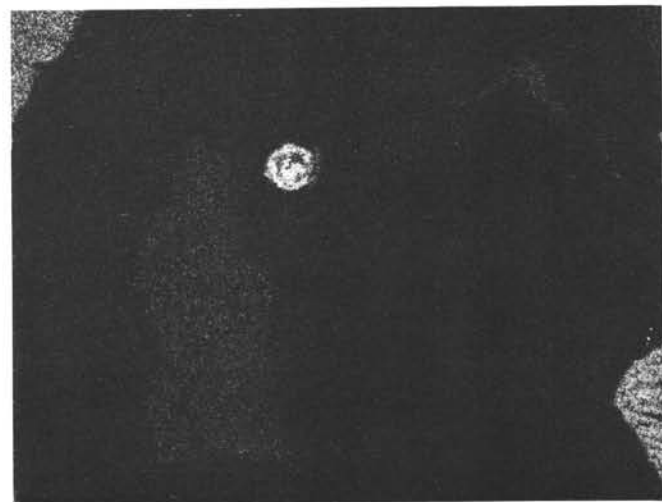
Si



Fe

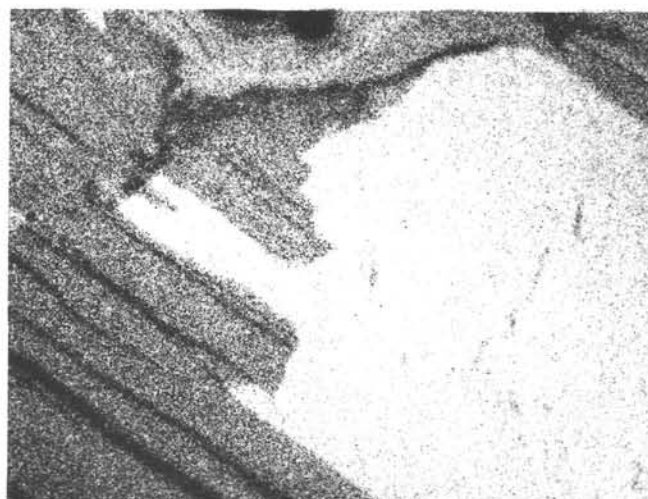
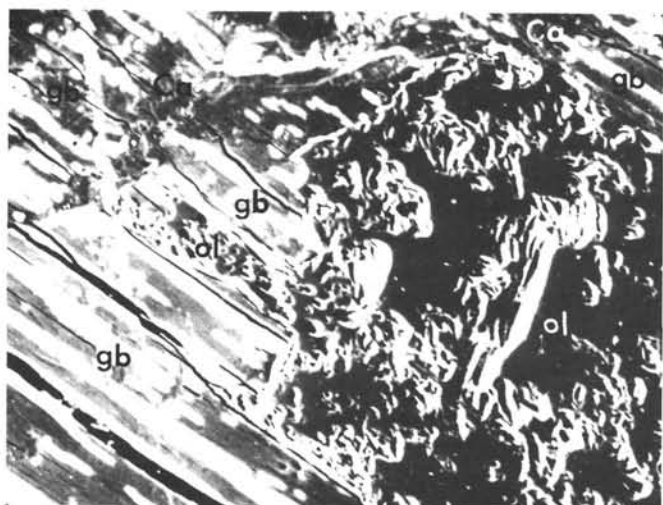


Al

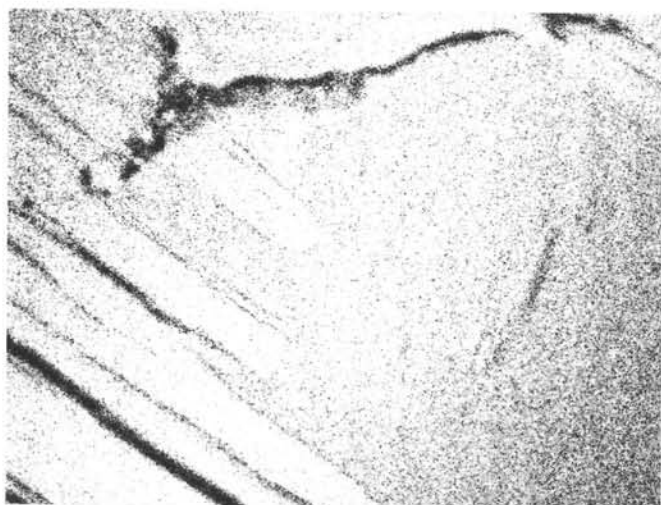


Ca

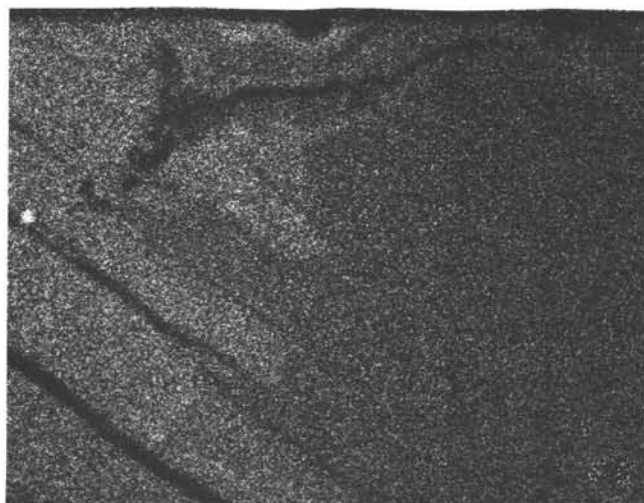
Plate 3. X-ray scanning photographs of olivine replacement products in Sample 504B-63-4, 60-61 cm (from about 772 m BSF). 1a, pale olive green Type 1a saponite; 1b, dark olive green Type 1b saponite; ol, olivine. Magnification  $\times 400$ .



Mg



Si



Fe



Al



Ca

Plate 4. X-ray scanning photographs of olivine replacement products in Sample 504B-40-1, 37-39 cm (from about 580 m BSF). gb, greenish brown smectite; ol, olivine; Ca, Mg-rich calcium carbonate. Magnification, 400 $\times$ .